

**Study on epoxy resin with dynamic covalent bonding for
environmentally friendly structural materials**

Hsing-Ying Tsai

February 2021

Study on epoxy resin with dynamic covalent bonding for
environmentally friendly structural materials

Hsing-Ying Tsai

Doctoral program in Materials Science and Engineering

Submitted to the Graduate School of
Pure and Applied Sciences
in Partial Fulfillment of the Requirements
for the Degree of Doctoral of Philosophy in
Engineering

at the

University of Tsukuba

CONTENT

<u>CONTENT</u>	I
<u>LIST OF TABLES</u>	IV
<u>LIST OF FIGURES</u>	V
<u>LIST OF ABBREVAITONS AND SYMBOLS</u>	VIII
<u>LIST OF PUBLICATIONS PRESENTED</u>	IX
CHAPTER I GENERAL INTRODUCTION	1
CHAPTER II BACKGROUND AND LITERATURE REVIEW	4
2.1 INTRODUCTION TO THERMOSETTING RESIN SCIENCE	4
2.1.1 <i>Structure formation of thermosets</i>	5
2.1.1.1 Chain-growth polymerization.....	5
2.1.1.2 Step-growth polymerization.....	5
2.1.1.3 Mixed polymerization	6
2.1.1.4 Controlled polymerization	6
2.1.2 <i>Processing of thermosets</i>	6
2.1.3 <i>Properties and characteristics of epoxy resin</i>	7
2.1.3.1 Thermal properties.....	7
2.1.3.2 Mechanical properties.....	9
2.1.3.3 Adhesion properties	10
2.1.4 <i>Application of epoxy resin</i>	13
2.1.5 <i>Challenges of epoxy resin</i>	13
2.1.5.1 Irreversible degradation of epoxy resin at high temperature.....	13
2.1.5.2 Repairing of damaged epoxy resin	14
2.1.5.3 Recycling of wasted epoxy resin.....	14
2.2 INTRODUCTION OF DYNAMIC COVALENT CHEMISTRY	17
2.2.1 <i>Dynamic covalent reactions</i>	19
2.2.2 <i>Classification of dynamic covalent chemistry</i>	23
2.2.2.1 Associative dynamic covalent chemistry.....	24
2.2.2.2 Dissociative dynamic covalent chemistry	25
2.2.2.3 Mixed-type dynamic covalent chemistry.....	25
2.2.3 <i>Characteristics of dynamic covalent chemistry</i>	26
2.2.3.1 Glass transition temperature (T_g).....	26
2.2.3.2 Topology freezing transition temperature (T_v).....	27
2.2.3.3 Activation energy (E_a) for exchange reaction	29

2.2.3.4 Stress relaxation.....	29
2.2.3.5 Creep.....	29
2.3 EXCHANGEABLE DISULFIDE SYSTEM.....	30
2.3.1 <i>Reaction mechanism of disulfide bonding</i>	30
2.3.1.1 Disulfide-disulfide exchange mechanism.....	31
2.3.1.2 Thiol-disulfide exchange mechanism.....	31
2.3.2 <i>Properties and characteristics of exchangeable disulfide system</i>	32
2.3.2.1 Thermal properties.....	32
2.3.2.2 Mechanical properties.....	32
2.3.2.3 Degradation properties.....	33
2.3.2.4 Mechanochromic effect.....	33
CHAPTER III STRENGTHENING ADHESION EFFECT AT HIGH TEMPERATURE AND REPARABILITY	34
.....	
3.1 EXPERIMENTAL.....	35
3.1.1 <i>Materials</i>	35
3.1.2 <i>Synthesis and preparation of samples</i>	35
3.1.2.1 Synthesis of disulfide-contained epoxy monomer.....	35
3.1.2.2 Synthesis of bulk epoxy resin networks.....	36
3.1.2.3 Preparation of adhesive joints.....	37
3.1.2.4 Rebonding and repairing of adhesive joints.....	38
3.1.2.5 Small molecular model reaction.....	39
3.2 CHARACTERIZATION.....	39
3.3 RESULTS AND DISCUSSION.....	40
3.3.1 <i>Degree of curing</i>	40
3.3.2 <i>Disulfide-bonding determination</i>	40
3.3.3 <i>Thermal analysis</i>	42
3.3.4 <i>Mechanical properties</i>	46
3.3.5 <i>Heat-induced stress relaxation</i>	46
3.3.6 <i>Adhesion performance</i>	49
3.3.6.1 Adhesion strength at ambient temperature.....	49
3.3.6.2 Adhesion ability at the temperature between T_g and T_v	50
3.3.6.3 Reparability at the temperature above T_g and T_v	51
3.3.6.4 Strengthening adhesion effect at high temperature.....	52
3.4 CONCLUSIONS.....	58
CHAPTER IV CHROMOPHORIC INDICATOR OF ADHESION STRENGTH.....	60
4.1 EXPERIMENTAL.....	61
4.1.1 <i>Materials</i>	61
4.1.2 <i>Synthesis and preparation of samples</i>	61

4.1.2.1 Synthesis of disulfide-contained epoxy resin networks (ERD).....	61
4.1.2.2 Preparation of adhesive joints.....	62
4.2 CHARACTERIZATION.....	62
4.3 RESULTS AND DISCUSSION.....	63
4.3.1 <i>Mechanochromic effect</i>	63
4.3.2 <i>Crosslinking density</i>	65
4.3.3 <i>Chain mobility</i>	67
4.3.4 <i>Adhesion strength</i>	68
4.3.5 <i>Correlation among each parameter</i>	68
4.4 CONCLUSIONS.....	70
CHAPTER V DECOMPOSITION AND RECYCLING.....	72
5.1 EXPERIMENTAL.....	73
5.1.1 <i>Materials</i>	73
5.1.2 <i>Synthesis and preparation of samples</i>	73
5.1.2.1 Small molecular model reaction.....	73
5.1.2.2 Synthesis of disulfide-contained epoxy monomer.....	73
5.1.2.3 Synthesis of disulfide-contained epoxy resin networks (ERD).....	74
5.1.2.4 Synthesis of carbon fiber reinforced structure (CFRP).....	77
5.1.2.5 Preparation of peptide-assisted decomposition and recycling system.....	77
5.2 CHARACTERIZATION.....	77
5.3 RESULTS AND DISCUSSION.....	78
5.3.1 <i>Reaction mechanism determination</i>	78
5.3.1.1 Curing.....	78
5.3.1.2 Degradation/decomposition.....	79
5.3.1.3 Recycling.....	86
5.3.2 <i>Thermal and mechanical properties</i>	87
5.3.3 <i>Application for carbon fiber reinforced structure (CFRP)</i>	90
5.4 CONCLUSION.....	91
CHAPTER VI SUMMARY AND PROSPECT.....	92
REFERENCES.....	94
AKNOWLEDGEMENTS.....	107

LIST OF TABLES

Table 2.1 Comparison of chain-growth polymerization and step-growth polymerization	5
Table 2.2 Summary for different types of common dynamic covalent systems	18
Table 2.3 Summary for different types of dynamic covalent reactions	21
Table 3.1 Formulation of all epoxy networks.....	37
Table 3.2 Summarized thermal properties for all epoxy networks in this work	42
Table 3.3 Summarized mechanical properties for all epoxy networks in this work	46
Table 3.4 Summarized T_v and E_a from stress relaxation for all epoxy networks in this work	49
Table 3.5 Summary of T_g , T_v , and activation energy for known dynamic covalent systems.....	58
Table 4.1 Formulation of all epoxy networks.....	62
Table 5.1 All epoxy resin with disulfide bonding (ERD) used in this study.....	75
Table 5.2 Detail formulation of all epoxy networks (ERD) in this work	76
Table 5.3 Photograph of the resultant of decomposed ERD in CHCl_3 / water binary system with GSH. Compositions in which ERD was completely dissolved were marked in pink.	83
Table 5.4 Thermal and mechanical properties for ERD and reworked ERD characterized by dynamic mechanical analysis (DMA).....	88

LIST OF FIGURES

Figure 1.1 Schematic representation of this doctoral thesis.....	2
Figure 2.1 Typical classification of polymeric material and examples of thermoplastics and thermosets.....	4
Figure 2.2 Flow chart of processing the traditional thermoset resins.....	7
Figure 2.3 Typical thermal characterizations of glass transition temperature for epoxy resin: (a) differential scanning calorimetry (DSC) (b) dynamic mechanical analysis (DMA) (c) thermomechanical analysis (TMA) .	8
Figure 2.4 Typical mechanical characterizations for epoxy resin: (a) dynamic mechanical analysis (DMA) (b) tensile test	10
Figure 2.5 Typical adhesion characterizations for epoxy resin: (a) single lap shear test (b) T-peel test (c) wedge test (d) DCB test	11
Figure 2.6 Thee typical adhesive failure modes: (a) adhesion failure (b) cohesion failure (c) substrate failure	12
Figure 2.7 Typical fracture surface determination: (a) ductile fracture (b) brittle fracture	12
Figure 2.8 Summary for current recycling strategies of epoxy resin.....	15
Figure 2.9 Schematic representation of (a) associative and (b) dissociative bond exchange pathways for covalent adaptable networks (CANs).....	24
Figure 2.10 Typical examples of mixed covalent adaptable networks with associative and dissociative pathways (a) urethane exchange (b) disulfide exchange.....	26
Figure 2.11 Schematic representation for calculation of topology freezing transition temperature	28
Figure 2.12 Comparison for the effect of glass transition temperature (T_g) and topology freezing transition temperature (T_v) on viscosity and viscoelastic behavior of dynamic systems with (a) $T_v > T_g$ (b) $T_g > T_v$	28
Figure 2.13 Schematic representation for samples and experimental curve (time-dependent stress or strain curve) at specific temperature on (a) stress relaxation (b) creep	30
Figure 2.14 Disulfide-disulfide exchange mechanism based on [2+1] radical-mediated reaction.....	31
Figure 2.15 Thiol-disulfide exchange mechanism.....	32
Figure 3.1 $^1\text{H-NMR}$ spectrum for bis(4-glycidyoxyphenyl) disulfide	36
Figure 3.2 Synthesis and chemical structure for all epoxy-based network in this study.....	37
Figure 3.3 Schematic representation for (a) samples in lap shear test (b) samples in rebonding procedure	38
Figure 3.4 FTIR-nIR spectra of SS, SC, CS, and CC networks at 4000 to 7000 cm^{-1}	41
Figure 3.5 Raman spectra of SS, SC, CS, and CC networks at 400 to 600 cm^{-1}	41
Figure 3.6 DSC profiles for formula SS, SC, CS and CC synthesized in stoichiometry ratio ($M_{\text{epoxy}} : M_{\text{diamine}} = 2:1$).....	43
Figure 3.7 DSC profiles for formula SS and CS and CC synthesized in stoichiometry ratio ($M_{\text{epoxy}} : M_{\text{diamine}} = 2:1.1$ (dot line)).....	43
Figure 3.8 DMA curve for (a) dynamic epoxy networks SS (b) dynamic epoxy networks SC (c) dynamic	

epoxy networks CS (d) dynamic epoxy networks CC.....	44
Figure 3.9 TGA profiles for formula SS, SC, CS, and CS synthesized in stoichiometry ratio ($M_{\text{epoxy}} : M_{\text{diamine}} = 2:1$).....	45
Figure 3.10 TMA profiles for formula SS, SC, CS, and CS synthesized in stoichiometry ratio ($M_{\text{epoxy}} : M_{\text{diamine}} = 2:1$).....	45
Figure 3.11 Normalized stress relaxation curves of dynamic epoxy networks (a) SS (b) SC (c) CS at different temperatures.....	47
Figure 3.12 Normalized stress relaxation curves of all epoxy networks at 200 °C.....	48
Figure 3.13 Fitting line of the relaxation time to Arrhenius equation for dynamic epoxy networks SS, SC, and CS (R-square = 0.9579, 0.9877, 0.9637).....	49
Figure 3.14 Single lap shear strength for initial and rebonded dynamic epoxy adhesive networks at room temperature	50
Figure 3.15 Demonstration of exchange and healing behavior at 80 °C for formula (a) SS and (b) CA	51
Figure 3.16 Single lap shear strength for initial and rebonded dynamic epoxy adhesive networks at room temperature	52
Figure 3.17 Temperature-dependent Young's modulus for all adhesive epoxy networks	54
Figure 3.18 Temperature-dependent single lap shear strength for all adhesive epoxy networks.....	54
Figure 3.19 Schematic illustration for adhesion strengthening effect for dynamic disulfide bonds at elevated temperature	55
Figure 3.20 NMR spectra for disulfide-exchange model compounds at different temperatures located at the range of 7-7.6 ppm. After the treatment of the mixture at each temperature, all the samples showed the identical spectra which exhibit the composition of the mixture is AA : BB : AB = 1:1:2.....	55
Figure 3.21 Schematic representation of comparison for the effect of glass transition temperature (T_g) and topology freezing transition temperature (T_v) on viscosity, viscoelastic behavior, and network mobility of dynamic systems (a) $T_v > T_g$ (b) $T_g > T_v$	57
Figure 4.1 Synthesis and chemical structure of all epoxy networks in this work.....	61
Figure 4.2 Time-dependent photographic sequence showing the mechanochromic performance for all epoxy networks in this work.....	64
Figure 4.3 Electron spin resonance (ESR) spectrum for ERD-2. The sample was examined immediately after ball-milling into powder. The g-value of thiyl radical ($-S\cdot$) is 2.04.....	64
Figure 4.4 FT-nIR spectra for all epoxy networks at the wavelength from 4000 to 7500 cm^{-1}	65
Figure 4.5 Swelling ratio (Q) for all epoxy networks in toluene at room temperature for 72 hours in swelling test	66
Figure 4.6 Differential scanning calorimetry (DSC) profiles and glass transition temperature (T_g) for all epoxy networks	67
Figure 4.7 Adhesion strength based on single lap shear test for all epoxy networks	68
Figure 4.8 Correlation diagrams between (a) duration time of mechanochromic effect and crosslinking density (R-square=0.9626) (b) crosslinking density and glass transition temperature (T_g) (R-square=0.9293)	

(c) crosslinking density and shear strength of adhesive joint (R-square=0.9259) (d) duration time of mechanochromic effect and shear strength of adhesive joint (R-square=0.9592) 70

Figure 5.1 (a) Chemical structure of compounds used in this study, and (b) schematic representation of GSH mediated recycling system of ERD. 75

Figure 5.2 FT-nIR spectra of (a) uncured (red) and (b) cured (blue) EDR 79

Figure 5.3 NMR spectra of (a) solvent phase and (b) water phase for GSH-assisted thiol-disulfide exchange reaction of model compounds at different reaction time. Time evolution of product by reaction of DTDA with GSH in (c) CDCl₃ and (d) D₂O. Amount of the product was monitored by ¹H-NMR at 7.22, 7.12, 2.8, and 3.12 ppm DTDA, 4-ABT, GSH, and GSH-ABT, respectively. 81

Figure 5.4 Chemical reaction balance for CDCl₃ (CHCl₃) and D₂O (H₂O) phases 81

Figure 5.5 Relation between concentration of glutathione aqueous solution and decomposition time 82

Figure 5.6 Schematic illustration of repeating unit of ERD with (a) cross-link point of amine bonding and (b) degradable disulfide bonding 84

Figure 5.7 (a) FT-nIR and (b) FT-mIR spectra of ERD, decomposed ERD, and reworked ERD after curing. 85

Figure 5.8 (a) Time-dependent UV-vis spectra for decomposed ERD in CHCl₃ phase, and (b) time course of UV spectra of decomposed ERD monitored at 254 nm. 86

Figure 5.9 DSC curve for EDR, 1st-time reworked ERD, and 2nd-time reworked ERD 88

Figure 5.10 Swelling ratio (Q) for ERD, 1st-time reworked ERD, and 2nd-time reworked ERD in toluene at room temperature for 72 hours 89

Figure 5.11 Stress relaxation for ERD and reworked ERD at 130 °C 89

Figure 5.12 Demonstration of recycling procedure for carbon fiber reinforced composite (CFRP) (a) CFRP with ERD, (b) Decomposition test of CFRP-ERD with GSH, (c) after 24 hours, (d) recovered carbon fiber, (e) ERD residue recovered from CHCl₃ phase, and (f) reworked ERD cured at 180 °C for 6 hours. 90

LIST OF ABBREVAITIONS AND SYMBOLS

BGPDS	bis(4-glycidyoxyphenyl) disulfide
CAN	Covalent adaptable networks
CDCl_3	Deuterated chloroform
CHCl_3	Chloroform
CTE	Coefficient of thermal expansion
DCC	Dynamic covalent chemistry
DDM	4,4'-diaminodiphenylmethane
DGEBA	Diglycidyl ether of bisphenol A
DMA	Dynamic mechanical analysis
DMF	Dimethylformamide
DMSO	Dimethyl sulfoxide
DSC	Differential scanning calorimetry
DTDA	4,4'-dithiodianiline
D_2O	Deuterium oxide
EDR	Disulfide-contained epoxy resin
FTIR	Fourier-transform infrared spectroscopy
GSH	glutathione (reduced form)
H_2O	Water
NMR	Nuclear magnetic resonance
TBP	tributylphosphine
TGA	Thermogravimetric analysis
TMA	Thermal mechanical analysis
2-ME	2-mercaptoethanol
E'	Storage modulus
E''	Loss modulus
E_a	Activation energy
R^2	Coefficient of determination
$\tan \delta$	Loss tangent
T_d	Degradation/decomposition temperature
T_g	Glass transition temperature
T_m	Melting temperature
T_v	Topology freezing transition temperature

LIST OF PUBLICATIONS PRESENTED

The following is a list of publications containing the research described in this thesis as well as some additional experiments and results.

1. Hsing-Ying Tsai, Yasuyuki Nakamura, Takehiro Fujita, and Masanobu Naito. Strengthening epoxy adhesives at elevated temperatures based on dynamic disulfide bonds. *Mater. Adv.*, 2020, **1**, 3182-3188
DOI: 10.1039/D0MA00714E
2. Hsing-Ying Tsai, Takehiro Fujita and Masanobu Naito. Environmentally friendly recycling system for epoxy resin with dynamic covalent bonding. *Sci. Technol. Adv. Mater.* (submitted on Jan. 01, 2021)
3. Hsing-Ying Tsai, Takehiro Fujita, Yasuyuki Nakamura, and Masanobu Naito. Mechanochromism of Dynamic Disulfide Bond for Chromophoric Indicator of Adhesion Strength for Epoxy Adhesive. *Chem. Lett.* (submitted on Jan. 04, 2021)

CHAPTER I GENERAL INTRODUCTION

Nowadays, plastics have been widely used in our daily life, such as packaging, construction, automobile, electronic, medical, and so on. According to the statistic announced by EPRO (European Association of Plastics Recycling and Recovery Organizations) plastics material production almost reached 360 million tons due to rapid economic and urbanized development.¹ It is generally accepted that plastics could be categorized into two types, which are thermoplastics and thermosets based on polymeric structure. Thermoplastics material is considered that could be easily reheated, reshaped, and reused by melting and re-hardening. Polyethylene, polypropylene, and polyvinylchloride are typical examples of thermoplastics. On the other hand, thermosetting resin with exceptional thermal, mechanical, and chemical properties due to static covalent crosslinking was more suitable to be extensively applied; polyurethane, unsaturated polyesters, phenolic resins, acrylic resins and epoxy resins are classified into this category.²⁻⁶ Among them, epoxy resin is one of the most common networks that used in adhesive and composite structure for structural application due to excellent mechanical strength, high chemical resistance, and good bonding-compatibility with multiple substrates, such as metals, ceramics, glass, plastics, wood, fibers, and so on.^{7,8} However, there are some critical disadvantages that may limit the operation of epoxy resin: (1) irreversible damage and degradation under heat and/or mechanical stress, which will shorten the service life of epoxy resin (2) absence of simple evaluation method for the crosslinking density and adhesion strength of epoxy resin network in industrial application, so that the rapid pre-screening could not be performed to prevent the failure of epoxy-based adhesive joint (3) lack of decomposability and recyclability due to highly crosslinked structure, which will cause contamination of whole ecosystems.^{7,9} Considering these issues, we tried to develop the advanced epoxy resin that could overcome current challenges.

In the past two decades, the potential system, dynamic covalent chemistry (DCC), also called covalent adaptable networks (CANs), was introduced to bridge the gap between classical thermoplastics and thermosets. The crosslinked networks with dynamic bonds retained the beneficial properties of thermosets resin in normal condition, but behaved as thermoplastic under external stimuli, such as heat, UV-irradiation, ultrasonic, and so on. By cleavage and rearrangement of dynamic bonds, the polymeric networks could be reset, repaired, decomposed, and reused.¹⁰⁻¹⁹ To date, the well-known reactions, Diels-Alder reaction,²⁰⁻²² olefin metathesis,^{23,24} imine/amine exchange,²⁵ siloxane/silanol exchange,²⁶ disulfide metathesis,^{27,28} transamination,^{29,30} and transesterification³¹ have all been utilized to devise exchangeable bond systems. The combination of adaptable bonds and thermosetting networks provides a variety of innovative properties that is hardly observed in traditional thermoset resin, like self-healing, reprocessability, degradability. Among all possible candidates, aromatic disulfide bonding was well-known to be a prospective choice for following reasons. First, reversible disulfide exchange reaction is a catalyst-free mechanism. It can avoid the negative impact that may cause on substrate matrix and/or implanted objects due to insolubility of catalyst such as base, acid, or enzyme, which was usually used in some dynamic systems to activate the reaction. Second, the activation energy (E_a) of exchange reaction for aromatic disulfide bonding (~ 40 kJ/mol) was lower than most dynamic systems, resulting in more rapid cleavage, rearrangement, and recovery efficiency that can reduce the risk of aging. Third, aromatic disulfide bonding possessed relatively high thermal and mechanical

properties; therefore, it provided comparable stability and strength as conventional thermosetting resin.^{28,32-45} Consequently, the phenyl S-S bonds was a proper solution to integrating with epoxy network system, worthy further discussion to produce the reparable, recyclable, and reusable thermosetting material.

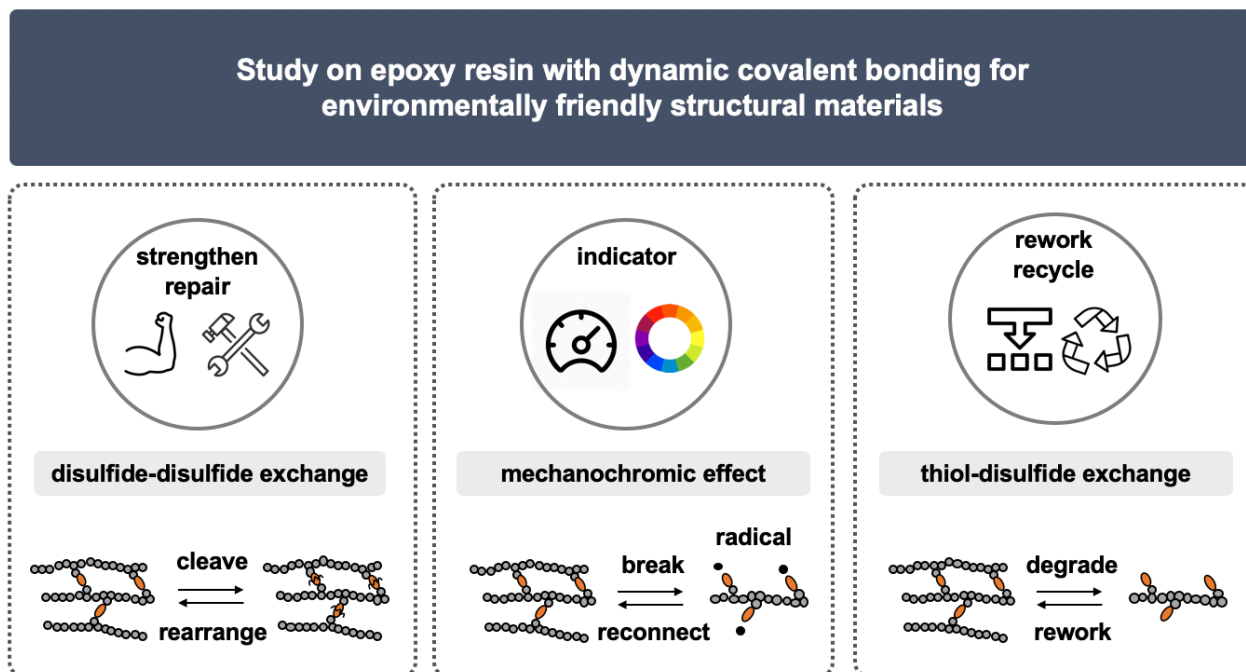


Figure 1.1 Schematic representation of this doctoral thesis

In this doctoral thesis, a novel disulfide-contained epoxy resin was proposed and discussed in three approaches based on different reaction mechanisms. First, reparability and strengthening effect at elevated temperature of epoxy resin used in adhesive were investigated based on disulfide-disulfide exchange reaction. Previously, disulfide-disulfide exchange reaction has been reported that played an important role on reshaping and reprocessing in the form of bulk epoxy resin. In the viewpoint of broadening its practical application in structural adhesive, we fully evaluated the thermal, mechanical, adhesion and reparability performance with different contents of aromatic disulfide bonding for this advanced dynamic epoxy resin. Besides, in order to compare the effectiveness of disulfide bonding system with other covalent adaptable networks, the samples with dynamic ester bonds was also prepared. Moreover, we paid attention on temperature-dependent disulfide exchange reaction and corresponding behavior to solve the problem of declined adhesion strength at elevated temperature and expand the service temperature of epoxy-based adhesive. The mechanism of adhesion strengthening effect under high-temperature environment via dynamic aromatic disulfide bonding was suggested, especially regarding to two thermal indicators in covalent adaptable system, glass transition temperature (T_g) and topology freezing transition temperature (T_v).^{13,46} Second, we applied the mechanochromism of disulfide bonding in evaluation for crosslinking density, chain mobility, and adhesion strength of epoxy network. When the external mechanical stress was applied on the disulfide-contained epoxy resin, the cleavage of disulfide bonding, followed by the generation of thiyl radicals, would cause the color of epoxy resin changing from brown to green. After certain duration time, the color would be returned back to

yellow due to the reconnection of radicals to new disulfide bonding. As a result, we expected that the crosslinking density and chain mobility would have an impact on the lasting time of mechanochromic effect, so that we could further determine the adhesion strength through observing the duration of color change.^{47,48} Finally, the new decomposition and recycling strategy of epoxy resin networks with phenyl S-S bonds would be carried out based on thiol-disulfide exchange reaction. Previously, some researches presented the chemical decomposition method for disulfide-contained epoxy networks by immersing the epoxy resin into thiol-contained compounds such as 2-mercaptoethanol with dimethylformamide.^{39,41,44} Unfortunately, the reworking and recycling of decomposed epoxy residue have never been demonstrated. Besides, 2-mercaptoethanol is toxic chemical, which would not be suitable in practical application. In order to solve this problem, we replaced 2-mercaptoethanol with eco-friendly alternative, the cysteine-contained tri-peptide structure, so called glutathione. Glutathione is well-known as a natural antioxidant by reducing reactive oxygen species using the thiol bond. Therefore, we expected that the thiol-bonding in glutathione enable the cleavage of disulfide bonding in epoxy network by thiol-disulfide exchange reaction, so that the decomposition of disulfide-contained epoxy network could be reached. The degraded liquid epoxy residue was curable back to epoxy network through oxidizing thiol bond back to disulfide bond. Through this water/solvent binary system, the epoxy resin and its composite structure could be degraded and recycled. Overall, the main target of this thesis was to develop the high-performance epoxy resin system with sufficient reparability and recyclability based on dynamic S-S bonds. We hope that the knowledge gained from this thesis for the eco-friendly alternative would contribute towards the understanding of advanced epoxy network and widen the potential range of material design.

This doctoral thesis is composed of six chapters. The first chapter introduces the overall picture of the research, including the purpose, aim and significance of this study. The second chapter presents the background knowledge of thermoset resin, classification, thermal and mechanical properties, and challenge we faced currently. Also, the previous studies about dynamic covalent chemistry, especially aromatic disulfide bonding was reviewed in this chapter to solve the economic and environmental problem of resin accumulation. The study on reparability and strengthening adhesion effect at high temperature of epoxy resin through disulfide-disulfide exchange reaction is disclosed in the third chapter. The fourth chapter demonstrates the application of mechanochromic performance on crosslinking density determination and adhesion strength evaluation. The fifth chapter reveals the advanced degradation and recycling system for thermosetting epoxy-based networks through thiol-disulfide exchange mechanism. Finally, in the sixth chapter, major findings are concluded and possible developments in the future are proposed.

CHAPTER II BACKGROUND AND LITERATURE REVIEW

2.1 Introduction to thermosetting resin science

The conventional polymeric material can be classified into two categories as shown in figure 2.1, thermoplastics and thermosets, based on covalent network structure and their behavior in response to heat. Generally, thermoplastics with high mobility at high temperature provides the pathway to be melted, deformed, and reprocessed when heating above melting point (T_m), which is easy to reshape or reuse; however, this flexibility is not suitable for applications requiring dimensional stability, strong mechanical strength, or resistant ability under harsh environment. To satisfy the requirements, the thermosetting network will be an appropriate alternative. Thermosetting network are three-dimensional crosslinked structure, which are barely decomposed as long as the covalent chemical bonds are not broken or damaged. This characteristic provides excellent thermal stability, mechanical strength, and chemical-resistance, causing wide structural application in aerospace, automobile, construction, and electronics. At the same time, this stability once thermosetting got cured prevents them from being remolded and processed for several times. Typical examples of thermosets are polyurethane, unsaturated polyesters, phenolic resins, acrylic resins, and epoxy resins. This following section provides the knowledge of structure formation and manufacturing process of thermosetting resin. Furthermore, the discussion about fundamental properties, applications, and challenges to be overcome will also be briefly reviewed. ^{7,49,50}

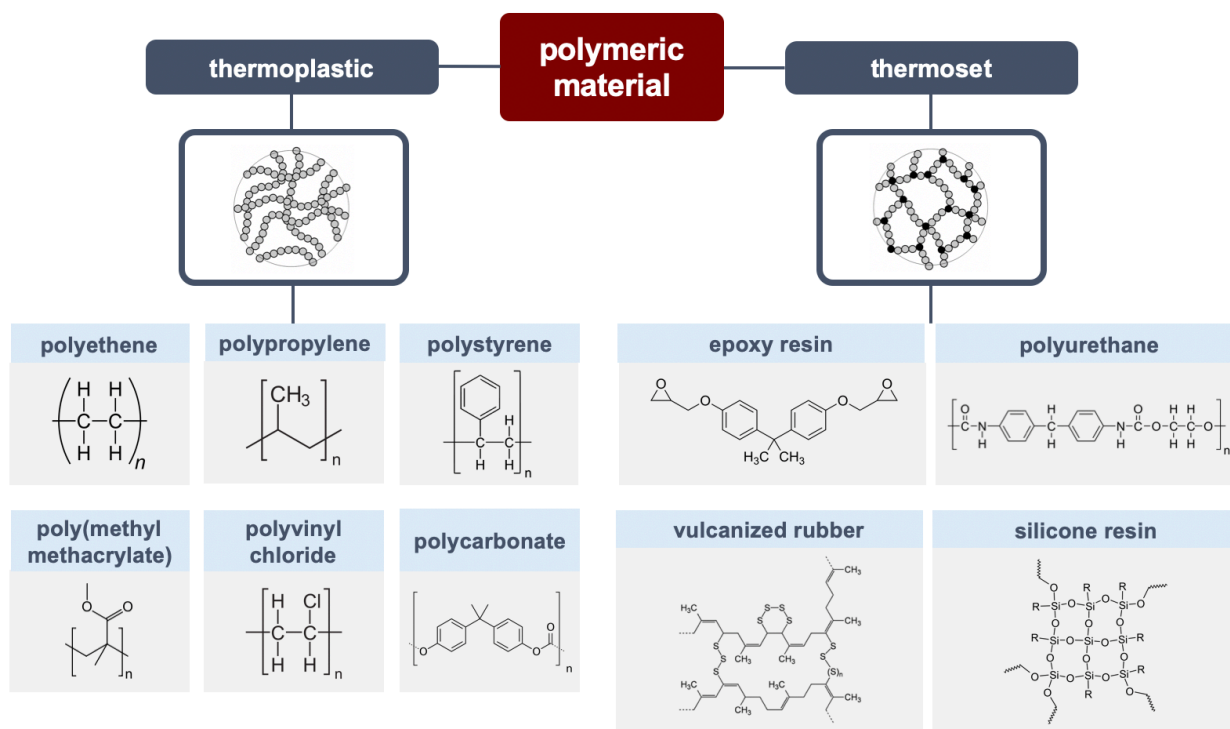


Table 2.1 Comparison of chain-growth polymerization and step-growth polymerization

Chain-growth polymerization	Step-growth polymerization
initiation, propagation, and termination are separated and distinguished	no termination stage during polymerization
monomer consumes slowly, but the degree of polymerization increases rapidly after initiation	monomer consumes rapidly, but the degree of polymerization increases steadily
only monomers react to active position of growing chain	all molecule, including monomer, dimer, trimer, oligomer, and polymer chain can be reacted with each other
primarily composition during polymerization are monomers and polymer chains	primarily composition during polymerization are oligomers with any length
longer reaction time is not directly related to enhancement of molecular weight once it reaches termination	longer reaction time leads to longer polymer chain and larger molecular weight

2.1.1 Structure formation of thermosets

Chain-growth polymerization, step-growth polymerization, combination of chain-growth and step-growth polymerization, and controlled polymerization are most common polymerization techniques to produce thermosetting networks, which will be discussed separately as follows. The differences between two main types, chain-growth polymerization and step-growth polymerization are summarized in table 2.1.

2.1.1.1 Chain-growth polymerization

Chain-growth polymerization is a three-stage procedure to synthesize the polymeric material, which are initiation, propagation, and termination. First, the unsaturated units, such as radical, cation, and/or anion, are critical. This active species acts as chain carriers, that can be initiated by heat, radiation or chemical. Second, one monomer adds onto the active site of polymer chain for growing, leading to formation of new active positions for next attachment. Finally, the reaction is terminated until all active initiation molecule disappears so that the polymer chain becomes deactivated. As a result, the reaction rate is highly depending on the concentration of initiator. Tetrafunctional epoxy monomer with anhydride, methacrylate with dimethacrylate, anion and cation polymerization of diepoxies, and radical polymerization of vinyl esters are classic representatives for chain-growth polymerization.^{51,52}

2.1.1.2 Step-growth polymerization

Step-growth polymerization, also called polyaddition or polycondensation, is a polymerizing technique via continuous step-by-step formation of fundamental reactions. The functional groups A located on main monomer will react with the other functional group B in a comonomer or crosslinker, leading to the formation of polymeric networks. Unlike chain-growth polymerization, there is no obvious initiation or termination of reaction. Also, although polymerization reaction may proceed fast, the molecular weight of polymer could

increase slowly until all long oligomers are reacted with each other. Typical examples of step-growth polymerization are phenolics formed by phenol and formaldehyde, epoxy networks produced by diglycidyl ether of bisphenol A (DGEBA) and diamine, and polyurethanes generated by polyisocyanate and diol. ^{52,53}

2.1.1.3 Mixed polymerization

The combination polymerization contains usually the formation of linear polymer by chain-growth polymerization, followed by crosslinking reaction via step-growth polymerization. This mixed system may be powerful synthesis strategy in commercial and industrial usage. For example, in the system of epoxy-amine with the catalyst such as Lewis acid or Lewis base. The acidic or basic accelerator initiates the chain-growth polymerization reaction of epoxide groups themselves; at the same time, the epoxy-amine crosslinking reaction can occur by step-growth polymerization to form the networks.

2.1.1.4 Controlled polymerization

Controlled polymerization, also called living polymerization, has been developed recently, which is a similar concept with traditional chain-growth polymerization; however, the chain termination is absent in controlled polymerization and the rate of chain initiation is obviously faster than rate of chain propagation, which results in constant growing speed of polymeric chain. Atom transfer radical polymerization (ATRP), nitroxide-mediated free radical polymerization (NMRP), and reversible addition fragmentation chain transfer polymerization (RAFT) are considered as this type. ^{52,53}

2.1.2 Processing of thermosets

Generally, the procedure to manufacturing thermosetting products can be identified into four continuous stages as shown in figure 2.2: (1) mixing and storage of the reactive monomers at specific temperature (2) configuration of shape in the mold or application on the surface of substrates (3) curing for polymerization reaction (4) demolding and post-curing if necessary. The first step is critical to determine ratio of monomers and hardeners and prepare the homogeneous agent in liquid state. It is noticed that the temperature in this stage should be selected carefully to avoid rapid polymerization. The flowing uncured polymer should be poured into mold or paste on the matrix in second stage to set up the configuration. This period can also be defined as the operation windows ranged from minutes to days, since the conventional thermosetting networks could not be reshaped or reprocessed once it cures. In the step of curing, heat or radiation may be applied. For thermal curing, the temperature, duration time, and heating/cooling rate are important parameters that may cause different effect on the final property of thermosetting resin, which must be well-designed. On the other hand, radiation polymerization is curing conversion by ultraviolet or electron beam, that penetrates into the networks accompanied with increase of temperature. In some cases, post-curing considered as a part of curing cycle is required to improve the thermal and mechanical performance of thermosetting polymers by aligning the molecules. The temperature of post-curing is mainly assigned at the temperature near the glass transition temperature of final product. Eventually, the product is obtained after curing and removing from the mold. ⁷

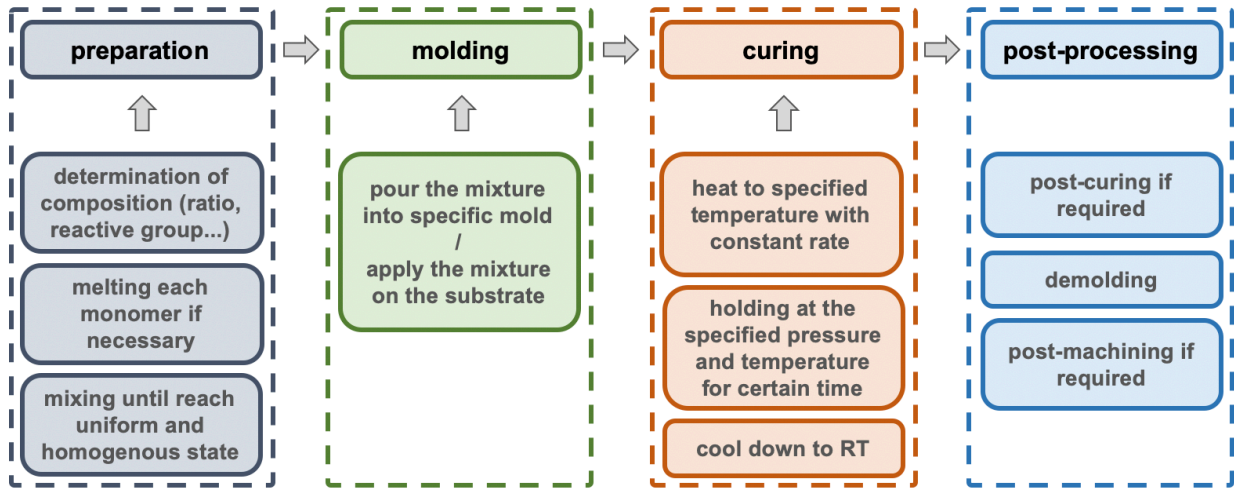


Figure 2.2 Flow chart of processing the traditional thermoset resins

2.1.3 Properties and characteristics of epoxy resin

Among all choices of thermoset resins, epoxy resin is one of the most irreplaceable thermosetting polymers in the fields of adhesive, coating, painting, primer, composites and so on owing to outstanding thermal, mechanical, and chemical resistant properties. Also, it can be bonded with several materials, such as metals, ceramics, glasses, polymers, and woods, which demonstrated extensively potential usage. In following section, the basic background on the behaviors of epoxy resin would be presented, which may promote the development of material design in repairable and recyclable epoxy networks.

2.1.3.1 Thermal properties

The glass transition temperature (T_g), degradation temperature (T_d), and coefficient of thermal expansion (CTE) are most fundamental thermal properties for epoxy-based networks, which will have an impact on the performance in response to temperature. There are several reasons that will change these three indexes, such as chemical nature of bonding, the crosslinking density, molecular weight of whole structure, and uniformity of networks. By realizing the thermal properties, the wider scope of applications would be offered.

Glass transition temperature (T_g) is defined as the temperature where the segmental motion of polymer chain starts, so that the condition changes from rigid glass-like state to flexible rubber-like state. Generally, T_g is examined by differential scanning calorimetry (DSC), dynamic mechanical analysis (DMA), and thermomechanical analysis (TMA). In DSC measurement as given in figure 2.3.(a), an evident change of heat capacity would be appeared, which is represented as a step of baseline, where its mid-point is deemed as T_g . DMA is the other useful instrument for analyzing the thermal transition and viscoelastic property. Storage modulus (E'), loss modulus (E'') and tangent of delta ($\tan \delta$) are three values that can be acquired from DMA measurement. Storage modulus (E') is related to stiffness of material and capacity to store energy elastically. In the other word, E' will decrease sharply when heating above T_g as described in figure 2.3.(b). Loss modulus (E'') is an indicator for viscous behavior, which represents the energy dissipated to heat. E'' will reach maximum value during glass transition, and decrease again in rubbery region. Tangent of delta ($\tan \delta$) is actually the ratio

between loss and storage modulus, which indicates the absorption and dispersion of energy in material. When $\tan \delta$ -value is greater than 1, the material presents more viscous since more energy dissipation; on the other hand, when the value is lower than 1, resin networks acts more elastic. The peak of tangent delta reveals most numbers of segmental motion, which is assumed as T_g . The final method to observe T_g is through the slope in temperature-dependent coefficient of thermal expansion (CTE) tested by TMA as shown in figure 2.3.(c). CTE is the coefficient to describe the tendency of dimensional change in material in response to variations of temperature. The magnitude of CTE usually increases with escalating temperature. Also, the fixed structure in glassy-state is not dimensionally sensitive to temperature change, while malleable networks in rubbery region shows totally opposite trend. Therefore, the turning point of slope in TMA measurement is viewed as T_g . Principally, there are multiple factors that influent T_g -value of epoxy resin, such as molecular weight of polymeric networks, the chemical property of curing agent, and the curing condition applied. Larger molecular weight, more elevated curing temperature, and longer curing time generally lead to higher T_g . Besides, epoxy resin cured by the crosslinker with aromatic ring possesses higher T_g than the one with aliphatic chain. Consequently, the T_g -value of epoxy networks can range from $-30\text{ }^\circ\text{C}$ to $200\text{ }^\circ\text{C}$. Degradation temperature (T_d), also called decomposition temperature, is the other key characteristic to evaluate the thermal stability, which is usually measured by thermogravimetric analysis (TGA). In TGA analysis, the mass of samples is detected as heating, cooling, or holding at fixed temperature under certain atmosphere. T_d -value is the temperature where the 5% loss of initial weight, that implies the limitation of service temperature owing to cleavage of chemical bonds and overheated molecular decay. Coefficient of thermal expansion (CTE) is the other indicator to assess the dimensional and volumetric deformation in response to temperature change. Some factors, such as property of bonding itself, absorption of water, melting point and glass transition temperature have an impact on the value of CTE.

Considering to possible applications of epoxy resin such as aerospace, automobile, electronics industry, remaining good performance at increased temperature may be highly required. Therefore, by assessing T_g and T_d -value of epoxy resin, the service temperature range can be established.^{54–58}

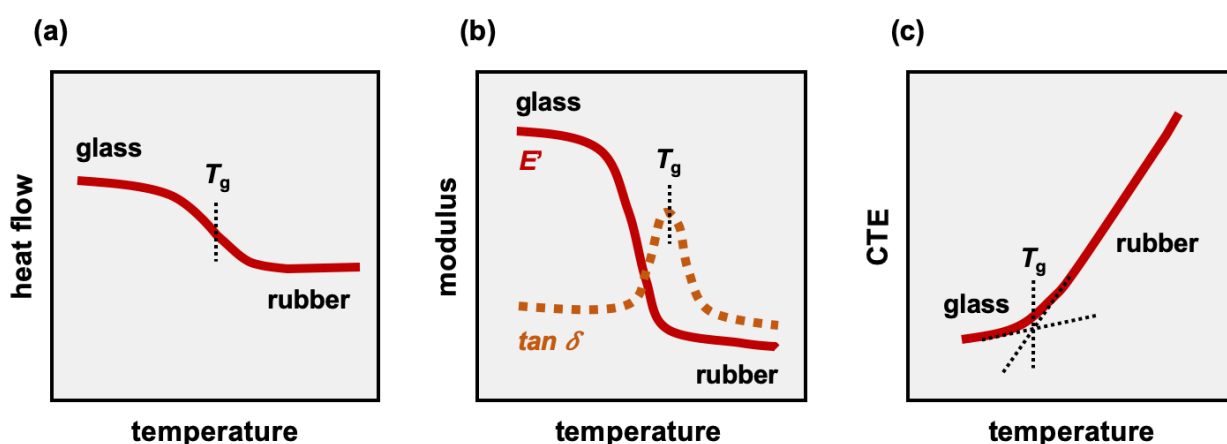


Figure 2.3 Typical thermal characterizations of glass transition temperature for epoxy resin: (a) differential scanning calorimetry (DSC) (b) dynamic mechanical analysis (DMA) (c) thermomechanical analysis (TMA)

2.1.3.2 Mechanical properties

There are lots of common mechanical properties, including stress, strain, modulus, toughness, and fracture mode, used in evaluating the performance of epoxy resin, often identified by dynamic mechanical analysis (DMA) and tensile test.

First, as mentioned previously, DMA provides the knowledge of correlation between modulus and temperature, that help us not only to determine T_g , but also to measure the ability to resist deformation at different temperature under standard testing mode as given in figure 2.4.(a). Also, heat-induced stress relaxation and creep behavior can be observed through DMA. Stress relaxation is defined as the decrease in stress under fixed strain; while creep is increase in strain under constant stress. These two techniques propose the method to estimate the elastic deformation under particular temperature. Tensile test is the other experiment for fundamental mechanical estimation, which performed by samples of dog-bone (dumbbell) shape under uniaxial tensile (pulling) force until fracture occurs. Based on the stress-strain curve as illustrated in figure 2.4.(b), tensile strength and tensile strain can be easily judged; besides, tensile modulus, toughness, and fracture energy can be calculated. Tensile modulus is defined as the slope of curve in specific region, while toughness and fracture energy are elucidated by the area under stress-strain curve. It is worthy to recognize that the mechanical property is for epoxy resin itself; however, by cooperating with adherends or reinforcements, the strength can be additionally improved. For example, the modulus of bulk epoxy resin at room temperature is approximately 1-3 GPa, but is enhanced to near 100 GPa when combining with fibers and fillers to construct reinforced composites structure.

By this overview, the strategy of assessing mechanical performance for epoxy resin is summarized. These approaches are inevitable when an efficient selection of epoxy is decided to utilize in academic and practical industrial application. ^{57,59-63}

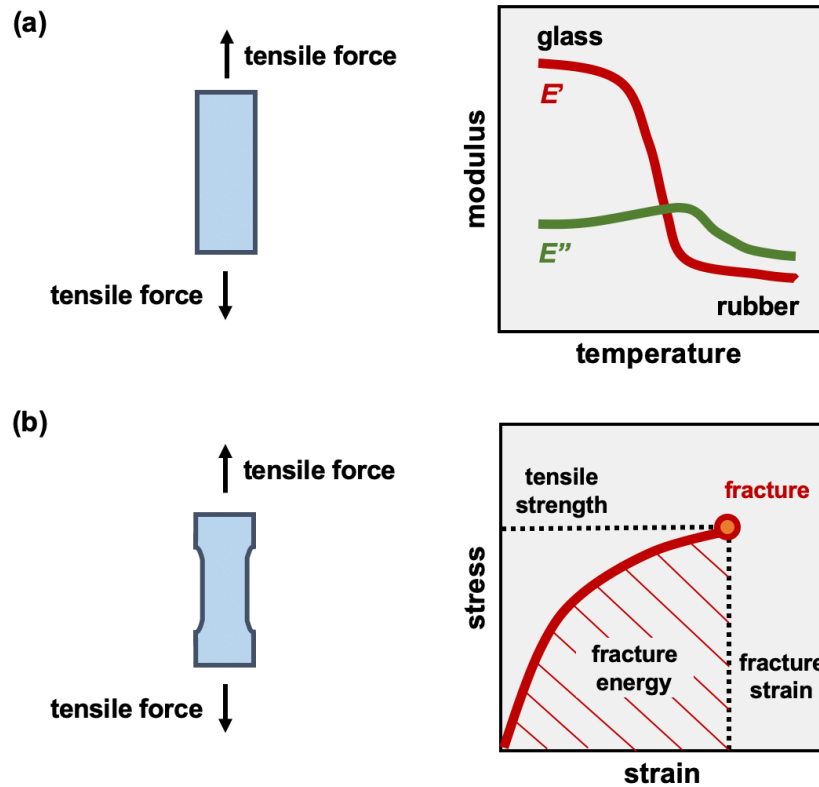


Figure 2.4 Typical mechanical characterizations for epoxy resin: (a) dynamic mechanical analysis (DMA) (b) tensile test

2.1.3.3 Adhesion properties

Unlike basic thermal and mechanical properties, adhesion property is a standard to evaluate the performance of whole adhesive joint system, so that all factors, such as adhesive, adherend, and interface should be scrutinized. Lap shear test, pull-off test, peel test, wedge test, and double cantilever beam (DCB) test are common in adhesive studies. American Society for Testing and Materials (ASTM) is an international organization, that provides the authoritative and technical standards for each testing system. Single lap shear test, double lap shear test, and pull-off test are performed according to ASTM D1002, ASTM D3528, and ASTM D4541. Among these three techniques, single lap shear test is the most typical and simple method that is usually reported in adhesive study as presented in figure 2.5.(a). Two substrates would be bonded together by adhesive under uniaxial shear loading. A shear stress-displacement diagram is obtained, and then the shear strength (σ_{ad}) is calculated as the maximum stress at failure divided by the overlapped area in adhesive joint. Peel test is another important experiment used in prediction of adhesion strength, that can be tested in forms of 90-degree, 180-degree, and T-shape according to ASTM D6862, ASTM D903, and ASTM D1876, separately. T-peel, also called fixed arm peel, is used in determination of peel strength. The specimen is composed of two bonded flexible adherends as given in figure 2.5.(b). The bent and unbonded areas of adherends are fixed by grips of tensile machine, and then the loading at fixed moving rate of machine head is applied. The peeling load is increased sharply at first and then reach the steady state finally. Peeling strength is described as the average load per width/length of bondline. Otherwise, wedge test based on ASTM D3762

is used to characterize the durability of adhesive in specified conditions. In this test, a special wedge is forced to insert into the adhesive and cause initial cracking, as shown in Figure 2.5(c). The propagation of cleavage is recorded periodically so that the environmental bonding lifetime can be speculated. Last but not least, the fracture energy is determined by DCB test according to ASTM D3433. The geometry of the sample is constructed as described in Figure 2.5(d). The force applied on the samples during the test is similar to the T-peel test. After the specimen is first loaded, a linear stress-displacement curve can be observed since the cracking is not yet grown in this stage. The cracking starts propagating when inelastic behavior is found and eventually reaches maximum loading. Then, the load reduces slightly even though the propagation continues. The measurement will be stopped until the cracking grows to a specific length and the specimen is unloaded and pending for the next round. Above cycle is replicated again and again until failure of the adhesive joint. Moreover, the failure mode is also essential for troubleshooting of bonding fracture. Adhesion failure, cohesion failure, and substrate failure, as illustrated in Figure 2.6, are the most notable failure types, which are caused by weak mechanical bonding strength in the interface, the adhesive, and the adherends, individually. Besides, the condition of the fracture surface can be distinguished as ductile fracture or brittle fracture as stated in Figure 2.7 by judging the morphology.

The adhesion property is connected with lots of elements like the adhesive itself, the adherends, and the configuration of joints. Consequently, this information is a critical indicator to evaluate the practical application, which is often proposed in the datasheet of commercial adhesive. Since adhesive is one of the common utilizations for epoxy resin, the high adhesion strength is preferred when considering the structural usage. ⁶⁴⁻⁷³

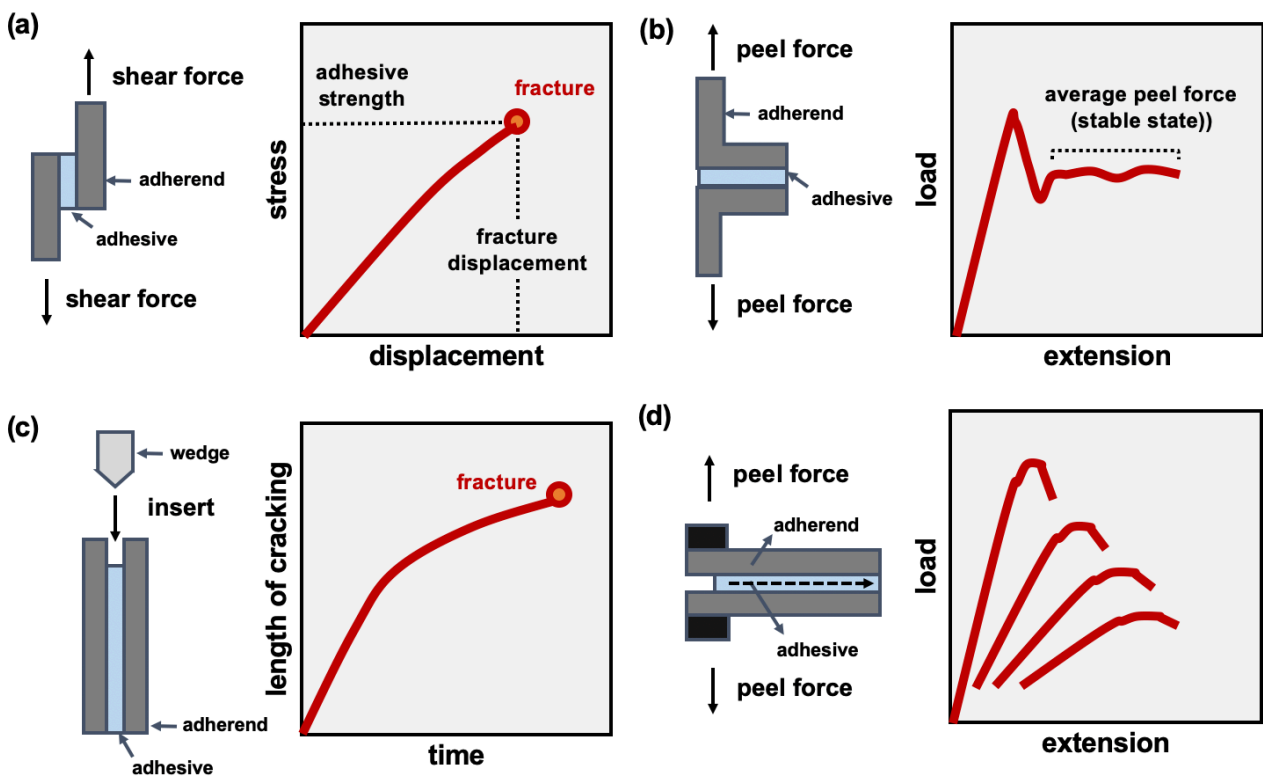


Figure 2.5 Typical adhesion characterizations for epoxy resin: (a) single lap shear test (b) T-peel test (c) wedge test (d) DCB test

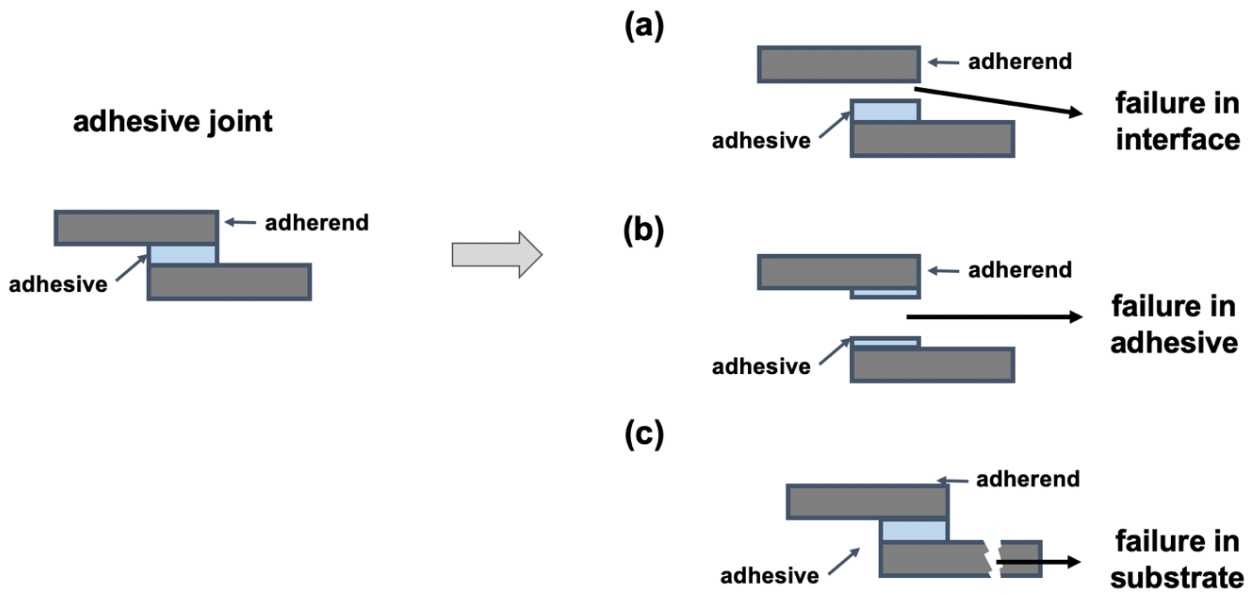


Figure 2.6 Three typical adhesive failure modes: (a) adhesion failure (b) cohesion failure (c) substrate failure

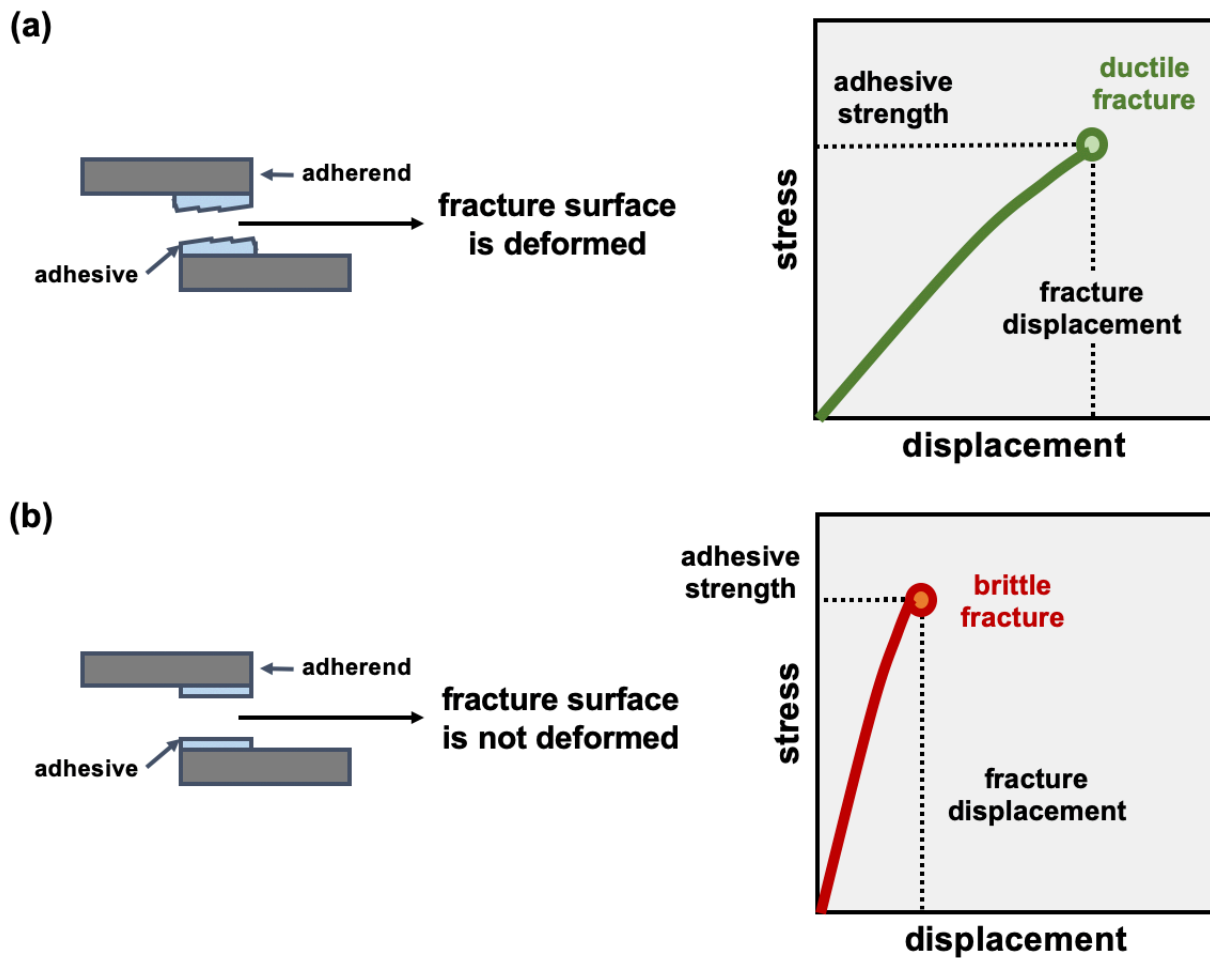


Figure 2.7 Typical fracture surface determination: (a) ductile fracture (b) brittle fracture

2.1.4 Application of epoxy resin

Epoxy resin is generally manipulated in multiple fields, such as aerospace, automobile, and building due to the trend of light-weight design. In general, epoxy resin owns high strength-to-weight ratio, leading to widely replacement of the rivet and fastening. In manufacturing industry, epoxy resin is used in primer, painting, adhesive, and rein matrix of composites. Among these applications, adhesive joint and composites structure are two most common structural applications for epoxy resin.

In the field of adhesive joint, the epoxy resin as adhesive usually bonds with the substrates, such as metal, glass, plastic, wood, and so on. It is well accepted that the adhesion strength of structural adhesive is required at least 10 MPa. The epoxy adhesive resin is generally composed of two parts, epoxy resin monomer and hardener (crosslinker), which would be pre-mixed in specific ratio and temperature. After that, the homogeneous mixture would be applied on the treated substrates. Then, the curing of whole adhesive joint is performed, leading to the manufacturing of adhesive joint. Besides, composite is the other alternative of traditional metal product in past years. Actually, composites structure in the body of advanced Boeing B787 reaches 50%, which is more than aluminum (20%). The composites structure in industry is usually prepared by prepreg, which is made from fibers and partially cured resin matrix. The pre-impregnated fibers in prepreg usually weaves and pre-bonds together by incompletely-cured resin; therefore, prepreg with limited shelf-life needs to store at low temperature to prevent the fully cure. By laminating the prepregs in certain direction and layers, the configuration of structure is established. After that, vacuuming bag is applied to remove the void, and then autoclave is most common equipment for curing. Curing condition is assigned with determination of curing temperature, duration time, vacuum pressure, heating and cooling rate. Finally, the product can be obtained after demolding.

As be known to all, the requirements of materials in these industries is particularly high, demanding dimensional stability, thermal, chemical and fatigue resistance, mechanical strength, and so on, which can be provided by epoxy resin. ^{5,49,74,75}

2.1.5 Challenges of epoxy resin

Although the advantages of epoxy resin are pronounced, there are some drawbacks remained. First, it is common for polymeric material that the mechanical strength at room temperature will be higher than at elevated temperature. Second, due to stable covalent bonding in crosslinking position, the repairing of cracking or cleavage on epoxy resin is not workable once it is cured. At last, traditional thermosetting networks is not decomposable and recyclable, so that the plastic debris, so-called microplastic, defined as the pieces with < 5mm in size not only pollute the atmosphere, habitat, soil, river, and ocean, but also are toxicant for human tissues. Mentioned challenges limited the usage of epoxy resin and resulted in economic misspending and environmental contamination, which become the serious issue needed to be overcome.

2.1.5.1 Irreversible degradation of epoxy resin at high temperature

It is substantially agreed that the mechanical strength will be declined gradually with increasing temperature and sharply decreased above glass transition temperature for all thermosetting resins; hence, this is the reason why the design of epoxy resin structure to enhance both glass transition temperature and

mechanical strength is critical. This decreasing trend is also shown when applying in adhesive joint. Previously, several reports issued the negative effect of high temperature on the adhesion strength, considering the mismatch of adherends and shrinkage of adhesive due to the dissimilar coefficient of thermal expansion. Therefore, if the adhesion strength can be maintained or improved at elevated temperature, the service temperature range can be broadened. ⁷⁶⁻⁷⁸

2.1.5.2 Repairing of damaged epoxy resin

The lifetime of epoxy resin will be shortened by the formation of (micro)cracks caused by internal and external stress. If the cracking is not well-prevented, detected, and repaired immediately, the propagation of cleavage occurs and finally cause the failure of material; therefore, the technique for repairing the epoxy resin has been studied with the concept of self-healing thermosetting polymers. In the past, the approach in this direction is to introduce different types of microsphere contained reactive groups into networks. The recovery agent is released and reacted when the cracking is generated, which leads to the breaking of microspheres. However, this method is only feasible within limited time. Once the microspheres are consumed, the healing reaction will not happen. ^{15,31,47,79}

2.1.5.3 Recycling of wasted epoxy resin

There has been a general awareness about environmental protection recently. Lots of regulations, such as Restriction of certain Hazardous Substances (RoHS) and Registration, Evaluation and Authorization of Chemicals (REACH) are contributed to reducing the toxic material in our daily life. Also, European Union (EU) paid more attention and pressure on the problem of waste management issue. Because conventional thermoset resin cannot be decomposed or dissolved, the recycling is not effective. The usual methods as described in figure 2.8 include thermal degradation to break specific bonding, mechanical proposal to grind bulk resin into powder as fillers, and chemical modification by integration epoxy networks with bio-degradable or renewable precursors that can be decomposed by solvent or other reaction agents as stated in following sections for more details. Nevertheless, existed recycling method not only consumes energy and time, but also limits in implanted objects embedded into the resin matrix or substrates. That means the recycling efficiency is not sufficient enough. Still, recycling of epoxy resin is a huge challenge owing to lack of efficient and mild degradation and recycling strategy. ⁸⁰⁻⁸⁸

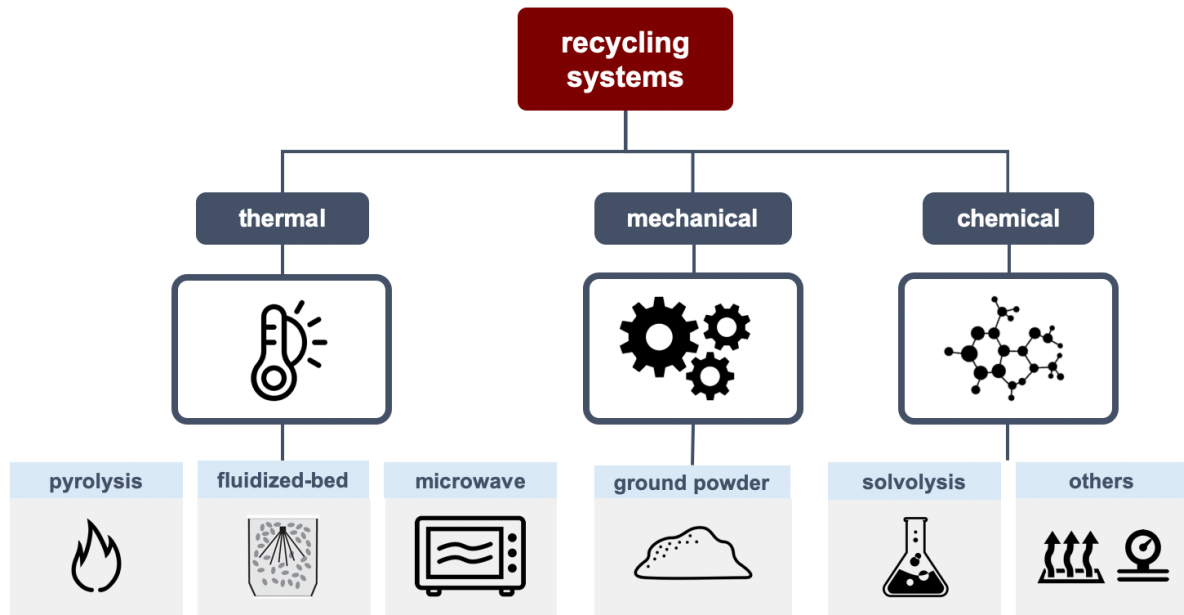


Figure 2.8 Summary for current recycling strategies of epoxy resin

2.1.5.3.1 Thermal recycling techniques

Common thermal recycling techniques include pyrolysis, fluidized bed pyrolysis, and microwave assisted pyrolysis. These methods promote the recovery of fibers, fillers, and inserts, but resin itself is hardly reused because it is usually volatilized to small molecular monomers. Otherwise, the gas like carbon dioxide, hydrogen, and methane and char of embedded substances are generated because it is generally processed at the temperature range from 400 °C to 700 °C. Fundamentally, the thermal recycling techniques causes the higher expense of energy, time, and, cost than other recycling systems.

Pyrolysis is most well-known thermal process. Because of high processing temperature, the decomposition of resin matrix is accompanied with formation of oils, gases, and solid char. Therefore, the implanted objects are often contaminated so that the post-treatment to remove the contaminations is required in this system. This procedure results in the degradation of fibers, fillers, and reinforcements sometimes; therefore, the determination of mechanical property for these materials is critical when practical application. For instance, mechanical strength of glass fibers after high-temperature procedure would be decreased 50 % minimum, while carbon fibers are more resistant with heat but produce more char during high temperature, which will remain on the surface of fibers that limited the bonding when re-using. Besides the heating temperature, the atmosphere during degradation is another key characteristic. Some previous indicated that epoxy resin is easily decomposed under oxygen than inert condition, which present better performance in removing the attached resin; hence, the air control is helpful to establish the pyrolysis procedure. In practical applications, ELG Carbon Fiber in United Kingdom and Hadeq Recycling Ltd. are companies who provided the service using pyrolysis as recycling method for carbon fibers. Fluidized-bed process is another type of thermal recycling process by applying the bed of silica sand. This technique proposes faster heating and separation of fibers from resin matrix. Also, the content of oxygen shall be precisely monitored to avoid the formation of char. Foregoing research carefully evaluated the surface of recycled fibers, finding out that little

reduction of surface can provide better bonding with new matrix. The uniqueness of this procedure is that it can be processed with mixed materials like sandwich-structure, so that it is appropriate recycling system for end-of-life products. On the other hand, the weakness of this procedure is that the fluidized sand used may damage the structure of fibers. Microwave-assisted pyrolysis is deemed as potential technique since the heat is directly to the core of composites, resulting in faster heat transfer and less energy consumption. However, the problem of char residue on the surface of recycled fibers is remained. In summary, there are still several challenges needed to be overcome in thermal recycling method. ⁸⁹⁻⁹¹

2.1.5.3.2 Mechanical recycling techniques

This technique is consisted of two steps, that are first shredding and crushing stage and second grinding stage. The first part is common for every recycling strategies in order to reduce the volume of whole waste accumulation. After that, the broken epoxy resin fragments would be roughly separated by sieving into resin-rich pieces and fibers with different lengths that implanted inside the resin. The ground epoxy-based composite is usually used in two applications, that are fillers or reinforcements. The utilization as fillers is not commercially available since the price of virgin fillers such as silica is not expensive. In comparison, processing and sorting are needed for the ground epoxy resin, which increases the cost actually. Besides, this type of recycled material as fillers could only be incorporated less than 10 wt.% because the mechanical property is degraded and the processing problems occur owing to higher viscosity with increasing the contents of fillers. On the other hand, the reinforcement would be more suitable for ground powder, which has been proven that can be successfully integrated with original polyether-ether-ketone (PEEK) resin; yet, the epoxy resin with much more complexed structure is still difficult to decompose. Industrial application of this technique is basically in glass fiber reinforced composites manufacturers. For example, Filon Products Ltd. and Hableside Danelow in United Kingdom, Fiberline-Zajons-Holcim AG/Geocycle in Germany, Eco-Wolf Inc. in United States focus on reincorporating with other products or energy recovery in cement kiln. However, the problem of this recycling method is that the bonding strength between these ground powders possess low bonding strength with new resin and implanted objects, causing declined mechanical property of produced composites, that will limit the usage of this recycling technique. ^{25,88,89}

2.1.5.3.3 Chemical recycling techniques

In general, chemical recycling, also defined as solvolysis, is attained with assistance of solvent, acid, or base reagent and/or catalyst under specific temperature and pressure. In comparison with thermal techniques, solvolysis to degrade the epoxy resin can be triggered in lower temperature. Through this decomposition system, the reagent can diffuse into the thermosetting networks and then break certain chemical bonds. Therefore, the damage of fibers and fillers may be minimized. Depending on the temperature and pressure applied in the reaction, the solvolysis discussed in following sections will be separated into high temperature and pressure (HTP) and low temperature and pressure (LTP). The temperature above 200 °C and higher pressure are indispensable in HTP process. Supercritical water with temperature higher than 374 °C and the pressure larger than 221 bar is main reagent for HTP process in recycling the carbon fibers inside the resin matrix. In order to lower the temperature and pressure, some solvent like alcohol, methanol and acetone have

been reported to add into water. The drawback of this method is that the organic solvent remained on the surface of fibers. In fact, based on the analysis for recycled fibers in previous study, the oxygen content of recycled fibers is lower than original state, resulting in lower interfacial shear strength; whereas, this problem can be solved by reaction in oxidant condition, but causing the significant decay of tensile strength. On the other hand, the LTP process is defined as the reaction occurs below 200 °C and at atmosphere pressure. Due to low reaction temperature, the addition of catalysts and mechanical stirring force are usually required. In this case, strong reagent, such as nitric, sulfuric, and acetic acid is the common reaction medium, which may cause safety and disposition problem. The advantage of this method is that it is almost impossible to observe the side reaction because of low temperature, enabling the higher recyclability.^{79,92-97}

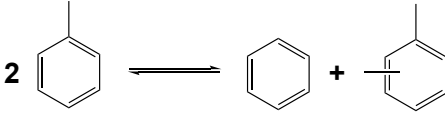
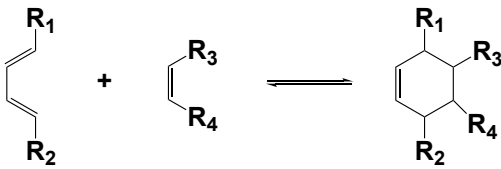
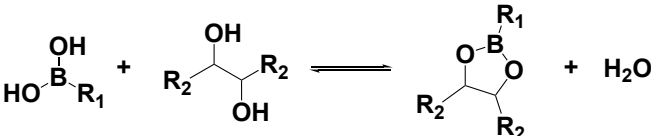
2.1.5.3.4 Conclusion of current recycling techniques

Pyrolysis and solvolysis are the most common strategies for recycling epoxy resin, particularly in the form of carbon fiber reinforced composites structure. The initial cracking and/or shredding epoxy resin into smaller fragments is needed in both techniques because the size of products is usually large in industrial application. These two recycling systems have been proven that fibers embedded in resin matrix can be reused through suitable processing condition. Compared with pyrolysis, the recycled fibers through solvolysis is generally cleaner due to lack of char attached on the surface. However, there may be some residual solvent, acid, or base. In conclusion, the recycling method operated with maximized recycling efficiency under mild condition, which means low reaction temperature, pressure, and gentle chemical, is highly necessary. Also, it had better to develop the advanced decomposition strategy that can not only reclaim embedded fibers and fillers, but also reuse degraded resin monomer as reactive agent to form new thermosetting networks.

2.2 Introduction of dynamic covalent chemistry

To address the demand of repairable and recyclable epoxy resin, in the past decades, the potential polymeric system, dynamic chemistry, become the powerful tool to change the traditional understanding of thermoplastics and thermosets. In general, the dynamic crosslinks could be classified into two categories, covalent exchange and non-covalent interaction, based on types of chemical bond undergone reversible reaction. It is generally accepted that dynamic covalent chemistry (DCC), also known as covalent adaptable networks (CANs) is considered as a more beneficial system owing to higher mechanical strength, better chemical stability, and stimuli-responsive property. In dynamic covalent chemistry, the reversible bond would be broken, rearranged, and recombined under specific stimuli, such as heat, UV-irradiation, pH, or mechanical force, enabling recovery, reprocessability, and recyclability as thermoplastics but also retains thermal and mechanical stability of thermosetting, which provides the possibility to create the repairable, reprocessable, and recyclable epoxy resin. The prototypical reactions and corresponding exchange conditions that possess dynamic nature are summarized in table 2.3. Therefore, following sections will focus on reviewing the principles, classifications, and characteristics of dynamic covalent networks.^{12-19,98,99}

Table 2.2 Summary for different types of common dynamic covalent systems

reaction types	conditions	chemical equation	ref.
transesterification	basic or acidic catalyst	$R_1-C(=O)-OR_2 + R_3-OH \rightleftharpoons R_1-C(=O)-OR_3 + R_2-OH$	100
transalkylation	zeolite catalysts		101,102
thiol-thioester exchange	neutral medium	$R_1-C(=O)-S-CH_2-OOH + R_2-SH \rightleftharpoons R_1-C(=O)-S-R_2 + HS-CH_2-OOH$	103–105
disulfide exchange	room temperature or mild temperature	$R_1-S-S-R_1 + R_2-S-S-R_2 \rightleftharpoons 2 R_1-S-S-R_2$	27,32,34,45, 106,107
diselenide exchange	visible light	$R_1-Se-Se-R_1 + R_2-Se-Se-R_2 \rightleftharpoons 2 R_1-Se-Se-R_2$	108,109
Diels-Alder reaction	low temperature for forward reaction; high temperature for reverse reaction		21,22,110,111
olefin metathesis	metal catalyst	$R_1-C(R_2)=C(R_1)-R_2 + R_3-C(R_4)=C(R_3)-R_4 \rightleftharpoons R_1-C(R_2)=C(R_3)-R_4 + R_3-C(R_4)=C(R_1)-R_2$	23,24
imine exchange	room temperature or mild temperature	$R_1-NH_2 + R_2-C(=O)-H \rightleftharpoons R_1-N=C(R_2)-H + H_2O$	112–114
siloxane/silanol exchange	basic or acidic catalyst	$R_1O-Si(OR_1)_2 + R_3O-Si(OR_3)_2 \rightleftharpoons R_1OSi(OR_1)-Si(OR_3)_2 + R_2-OH$	26
boronic ester exchange	room temperature or mild temperature		115–117

2.2.1 Dynamic covalent reactions

Dynamic covalent bonds with certain examples will be described in following sections as summarized in table 2.4. First, most of reversible covalent bonds can be categorized into dynamic polar reactions, which interprets that there is charged active intermediates existed during the reversible exchange reaction. The general examples of this types that bonds are generated and/or broken are C-N (C=N) bonds, C-C bonds, C-O bonds, C-S bonds, S-S bonds, Se-Se bonds and B-O bonds. Besides, dynamic covalent pericyclic reactions and dynamic covalent radical reactions are other two classifications.

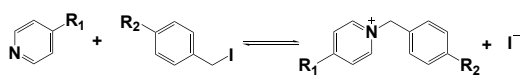
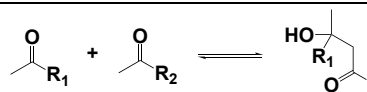
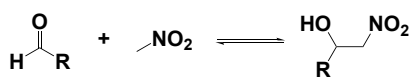
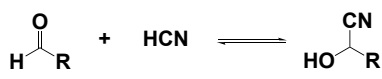
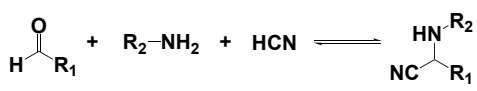
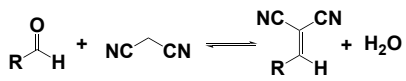
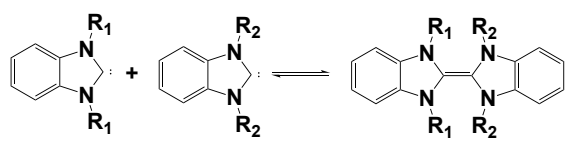
In dynamic polar reactions, C-N bonds are the most common dynamic covalent bonds. Exchange with imine and exchange with imine intermediates are significantly used. Imines formed via condensation of amine and aldehyde/ketone can be exchanged through hydrolysis/re-condensation or imine metathesis mechanism without catalyst or with acid accelerator. Except for this imine, there are some examples that imine intermediates participated in exchange reaction, such as aminal formation and imine rearrangement. The intermediates with lower stability in this type of exchange is regarded as virtual and temporary compositions of whole reaction systems. Moreover, C=N bonds is also extensively used, which applying N- or O- substituted amines as nucleophiles. These substituted amines usually possess higher nucleophilic characteristic because of free electron pairs on reactive nitrogen, which also promotes the stability of generated imine owing to reduction of electrophilicity. The oxime ligation, uncharged hydrazone, and acylhydrazone are belonged to this C=N reaction, that catalyst is needed due to the relatively steady state, leading to slower exchange rate. C-C bond plays an important role in organic chemistry, but its utilization is limited because of the difficulty in side reactions and property catalyst. Classic C-C group formations include formation by nucleophilic addition of carbon nucleophiles, carbene building blocks, electrophilic aromatic substitution, and organometallic intermediates with transition-metal catalyst. Related studies for these mechanisms are contributed to seeking the improvement of stability problem and faster reversibility with suitable catalyst. The dynamic exchange of C-O bonds can be classified into two categories, that are formation of C-O bonds from nucleophilic additions for C=O bonds and C-O bonds exchange via transition-metal catalyst. The well-known transesterification is considered as this type, which generally exchange with the assistance of basic or acidic catalyst to increase the equilibrium rate. Besides, transallylesterification with palladium catalyst and Nicholas ether exchange with strong acid have been reported. Reversible reaction with C-S bonds is another powerful exchange strategy. Since the related positions of sulfur and oxygen atom in periodic table, the reaction mechanism of C-S bonds and C-O bonds is similar, but with more nucleophilic property, causing different reaction rate and catalyst. For example, compared thioester exchange with ester exchange, thioester exchange occurs without catalyst under mild reaction condition. S-S bonds and Se-Se bonds are also utilized dynamic covalent reactions. The exchange is activated by nucleophilic attack of thiolate anion to disulfide bond, which cause the generation of new disulfide and thiolate anion. The reversible disulfide reaction can be triggered without catalyst and accelerated in basic condition or addition of phosphines. On the other hand, diselenide exchange presents sufficient equilibrium rate in general condition with the assistance of visible light. The last dynamic polar bonds are B-O bonds. The main exchange reactions including B-O bonds generally react with diols because of its stability. Boronic ester formation and boronate ester formation are two instances for reversible B-O bonds, which usually happen in the presence of nucleophile, such as alcohol, water, nitrogen-contained aromatic

heterocycles, and phosphonic acids at room temperature.

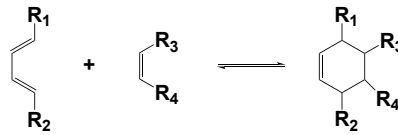
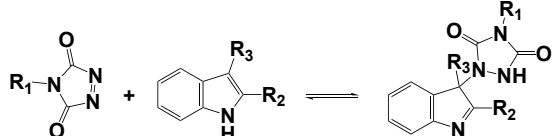
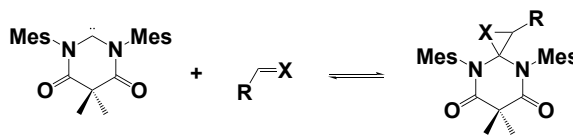
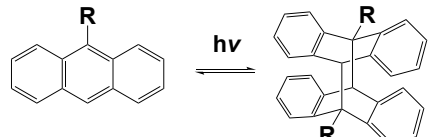
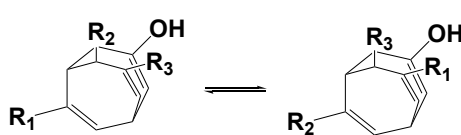
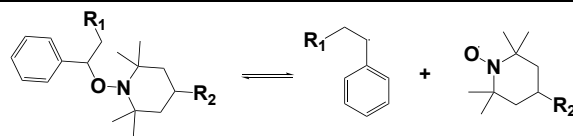
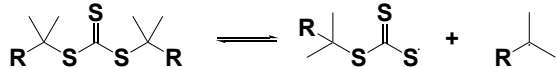
Dynamic covalent pericyclic reaction includes Diels-Alder reaction, [2+1] cycloadditions, [4+4] cycloadditions, ene reaction, and cope rearrangement. The benefit of this exchange system is its self-contained nature of reaction, which interprets that all atoms in reagents are incorporated into the resulting product without the additives. Diel-Alder reaction is the most typical pericyclic reaction, which can be defined as the generation of two C-C σ bonds with the consuming of two weaker C-C π bonds. Also, dynamic [2+1] cycloadditions between diamidocarbenes and olefins or aldehydes to establish reversible three-membered ring, and [4+4] cycloadditions of anthracenes to form dimers, have been developed. Besides the cycloaddition subtype, dynamic sigmatropic rearrangements via bullvalone derivatives is also reported. Mostly, the growing numbers of discussions about pericyclic reactions have been proposed recently to explore more steady exchange pathways and wider variety of functional groups. The last one of covalent bonds is dynamic radical reactions. Alkoxyamine exchange, diarylbibenzofuranone exchange, and trithiocarbonate exchange are belonged to this category. Among them, alkoxyamine exchange is best-explored of this type, which is used in producing self-healing and reprocessable crosslinking networks for multiple materials unlike its application in radical polymerization.

In conclusion, dynamic covalent bonds with side applicability in several fields in modern chemistry. Different types of reversible covalent bonds possess unique properties, which is worthy discussing the various areas, such as material design, catalyst discovery, advanced molecular structure establishment, nanotechnology and so on.¹⁸

Table 2.3 Summary for different types of dynamic covalent reactions

classification	type of bonds	examples	reaction equation
dynamic polar reactions	C-N bonds	imine exchange	$R_1-NH_2 + R_2-C(=O)H \rightleftharpoons R_1-N=CH-R_2 + H_2O$
		transimination	$R_1-NH_2 + R_1-N=CH-R_2 \rightleftharpoons R_1-N=CH-R_1 + R_2-NH_2$
		imine metathesis	$R_2-N=CH-R_1 + R_1-N=CH-R_2 \rightleftharpoons R_1-N=CH-R_1 + R_2-N=CH-R_2$
		aminal formation	$2 R_1-NH_2 + R_2-C(=O)H \rightleftharpoons R_2-C(H)(R_1)_2 + H_2O$
		imine rearrangement	$R_1-N=CH-R_2 \rightleftharpoons R_2-N=CH-R_1$
	C=N bonds	oxime ligation	$R_1-O-NH_2 + R_2-C(=O)H \rightleftharpoons R_1-O-N=CH-R_2 + H_2O$
		hydrazone formation	$H_2N-NH-R_1 + R_2-C(=O)H \rightleftharpoons R_1-NH-N=CH-R_2 + H_2O$
		acylhydrazone formation	$H_2N-NH-C(=O)R_1 + R_2-C(=O)H \rightleftharpoons R_1-C(=O)-NH-N=CH-R_2 + H_2O$
		nitron exchange	$R_2-N^+=CH-R_1 + R_1-NHOH \rightleftharpoons R_1-N^+=CH-R_1 + R_2-NHOH$
		transamidation	$R_2-NH-C(=O)R_1 + R_1-NH_2 \rightleftharpoons R_1-NH-C(=O)R_1 + R_2-NH_2$
		urea formation	$R_1-N=C=O + R_2-NH-R_2 \rightleftharpoons R_1-NH-C(=O)-NR_2$
		nucleophilic substitution	
	C-C bonds	Aldol reaction	
		nitroaldol reaction	
		cyanohydrin formation	
		Strecker reaction	
		Knoevenagel reaction	
		carbene dimerization	

	electrophilic aromatic substitution	
	alkene metathesis	
	alkyne metathesis	
C-O bonds	hemiacetal exchange	
	acetal exchange	
	orthoester exchange	
	ester exchange	
	transallylesterification	
	Nicholas ether exchange	
C-S bonds	hemithioacetal exchange	
	thioacetal exchange	
	thioester exchange	
	thiol-nitrone addition	
	Thia-Michael addition	
S-S / Se- Se bonds	disulfide exchange	
	selenylsulfide exchange	
	diselenide exchange	
B-O bonds	boronic ester formation	
	boronate ester formation	

dynamic pericyclic reactions	-	Diels-Alder reaction	
		ene reaction	
		[2+1] cycloadditions	
		[4+4] cycloadditions	
		cope rearrangement	
dynamic radical reactions	-	alkoxyamine exchange	
		trithiocarbonate exchange	

2.2.2 Classification of dynamic covalent chemistry

Depending on the exchange mechanism, dynamic covalent chemistry can be further classified into two sorts. The first group is associative exchange mechanism as described in figure 2.9. In this reaction, the breaking and reformation of bonding are occurred concurrently, resulting in the minimal change in crosslinking density and maintaining more stable viscosity during the exchange. The other group is dissociative exchange pathway, the new linkages only forms after some linkage dissociates; therefore, the dramatic decrease of network connectivity can be observed, causing obvious difference in macromolecular structure while exchanging. This section will further introduce associative CANs, dissociative CANs, and CANs with mixed exchange mechanisms. ^{12,16–19,98,118}

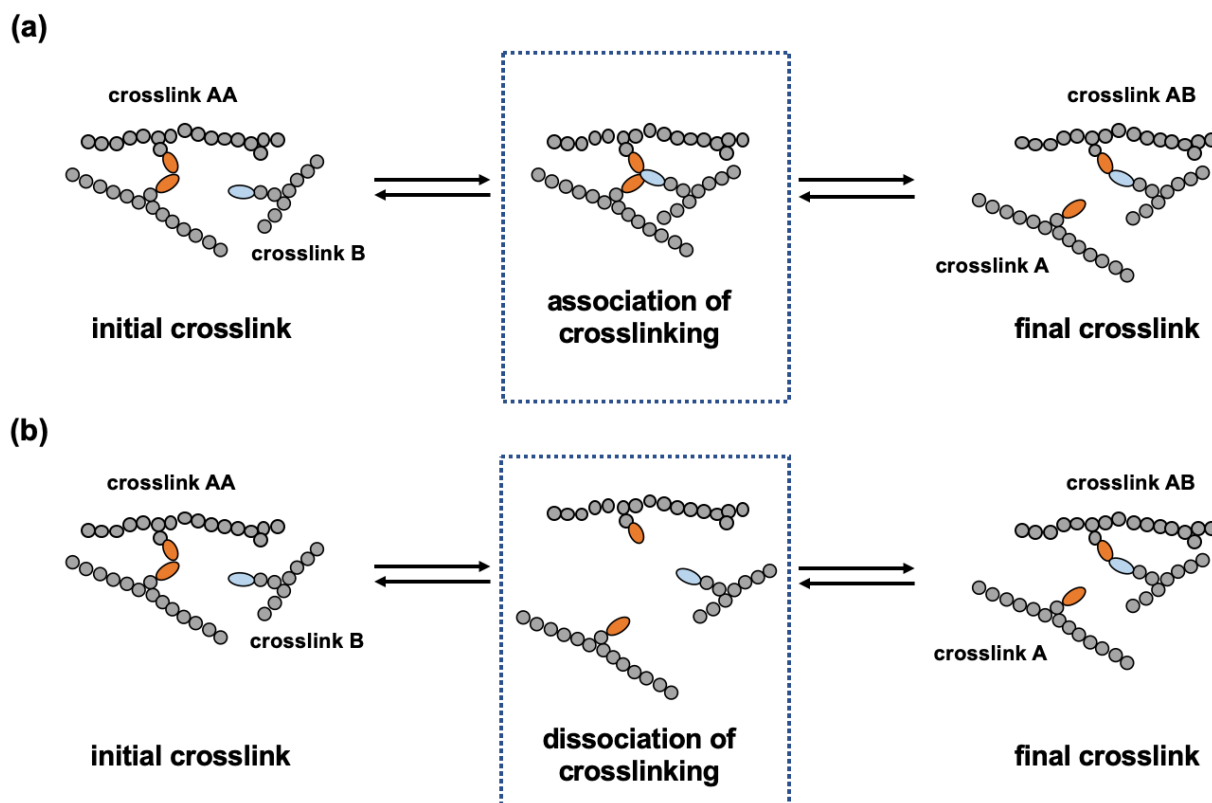


Figure 2.9 Schematic representation of (a) associative and (b) dissociative bond exchange pathways for covalent adaptable networks (CANs)

2.2.2.1 Associative dynamic covalent chemistry

In associative covalent adaptable networks, the cleavage and re-connection of dynamic bonding happens in one single step during interchange reaction. This characteristic provides the constant crosslinking density, showing stable viscosity-temperature relationship. In 2011, Leibler and his research team firstly designed the associative dynamic covalent networks with thermosetting structure based on transesterification. The resulting malleable materials presented viscosity variation like inorganic silica as calculated by Arrhenius Equation. Inspired by this work, this new concept, also called “vitriimer”, is defined as the networks with covalent adaptable bonds that change its topology but remaining the fixed number of chemical linkages regardless of temperature change. Therefore, the steady crosslinking structure limits the diffusion and motion of whole networks, so that the vitriimer system presents gradual decrease in viscous flow with increasing temperature.

Transesterification is the most common associative dynamic reaction in academic and industrial application. This reaction is established on the exchange between ester bond and hydroxyl group activated by enough heat and/or catalyst. The carbonyl carbon located in starting ester bond is attacked by alkoxide ion or nucleophilic attack depending on the type of catalyst, bringing out the intermediate tetrahedral structure, and then the transesterified products is obtained finally. By adjusting the molecular percentage and changing the type of catalyst, the activation energy of exchange reaction will be different. Transamination of vinylogous urethanes is another alternative in vitriimer systems. The associative exchange of vinylogous urethane is

similar to transesterification, which is based on the concept of addition-elimination reaction. Vinylogous urethane β -carbon is attacked by free amine, and then released the new amine moiety. The advantage of this system is that it exhibits stress relaxation within short time in absence of catalyst due to comparably low activation energy (~ 60 kJ/mol). Olefin metathesis is another example for associative dynamic covalent chemistry, which has been widely used in ring opening metathesis polymerization. Also, it is reported that shows excellent stability and functional compatibility in the presence of catalyst. Besides, there are some previous studies reported the mechanism, properties, and applications of other associative pathway, such as transamination of diketoenamine, transalkoxylation of triazolium salts, and dioxaborolane metathesis.^{14,17-19,99,119}

2.2.2.2 Dissociative dynamic covalent chemistry

In dissociative covalent adaptable networks, the bond-breaking and bond-reconnecting of dynamic bonds are two separated steps. The crosslinking structure is cleaved after dissociation of dynamic bonds. The broken segments may diffuse and then re-form to another bonds, resulting in sharply decrease of viscosity during exchanging and sensitive flowing change in response to external stimuli. As a result, the equilibrium between opening and connecting of crosslinks and the crosslinking density can be actually expressed as a function of temperature. Also, it seems that such exchange mechanism possesses fast network rearrangement, leading to rapid reversibility efficiency and stress relaxation because of temporary loss in network integrity and increase in flowing of whole structure.

Reversible Diels-Alder reaction, also considered as a [4+2] cycloaddition, is the typical dissociative covalent adaptable systems. The high reaction temperature or highly tailored electron-rich dienes and electron-deficient dienophiles are usually needed for reversible reaction. One of the most common utilization of Diels-Alder reaction is mechanism between maleimides and furans, which required high temperature to overcome the kinetic barrier of reversible reaction. Another reaction of dissociative covalent adaptable network is ring-opening/closing metathesis polymerization, which requested the usage of transition-metal catalyst like ruthenium. Otherwise, nucleophilic transalkylation, urethane/urea exchange and Michael adduct exchange are also deemed as the dissociative covalent adaptable networks.^{13,18}

2.2.2.3 Mixed-type dynamic covalent chemistry

This type of dynamic covalent chemistry is also called vitrimer-like networks because it possesses partial property of associative covalent adaptable networks (vitrimer material) with multiple bond exchange mechanisms as described in figure 2.10. The most utilized networks of this type are disulfide exchange reaction, and urethane exchange.

In this type, there are two pathways, dissociative or associative one, depending on the reaction condition and catalyst. For example, urethane exchange can be triggered in associative way when reacting with free hydroxyl groups, but in dissociative way via acid catalyst. Similarly, different exchange mechanisms for vinylogous urethane reversible reaction are detected in low or high reaction temperature. Also, disulfide exchange can be separated into two classifications, that are radical-mediated exchange reaction through radical addition in associative method, or radical reconnection in dissociative strategy. Generally, the reactions

with associative or dissociative pathways are demonstrated obvious change in activation energy (E_a), which have been confirmed in several previous researches.⁹⁹

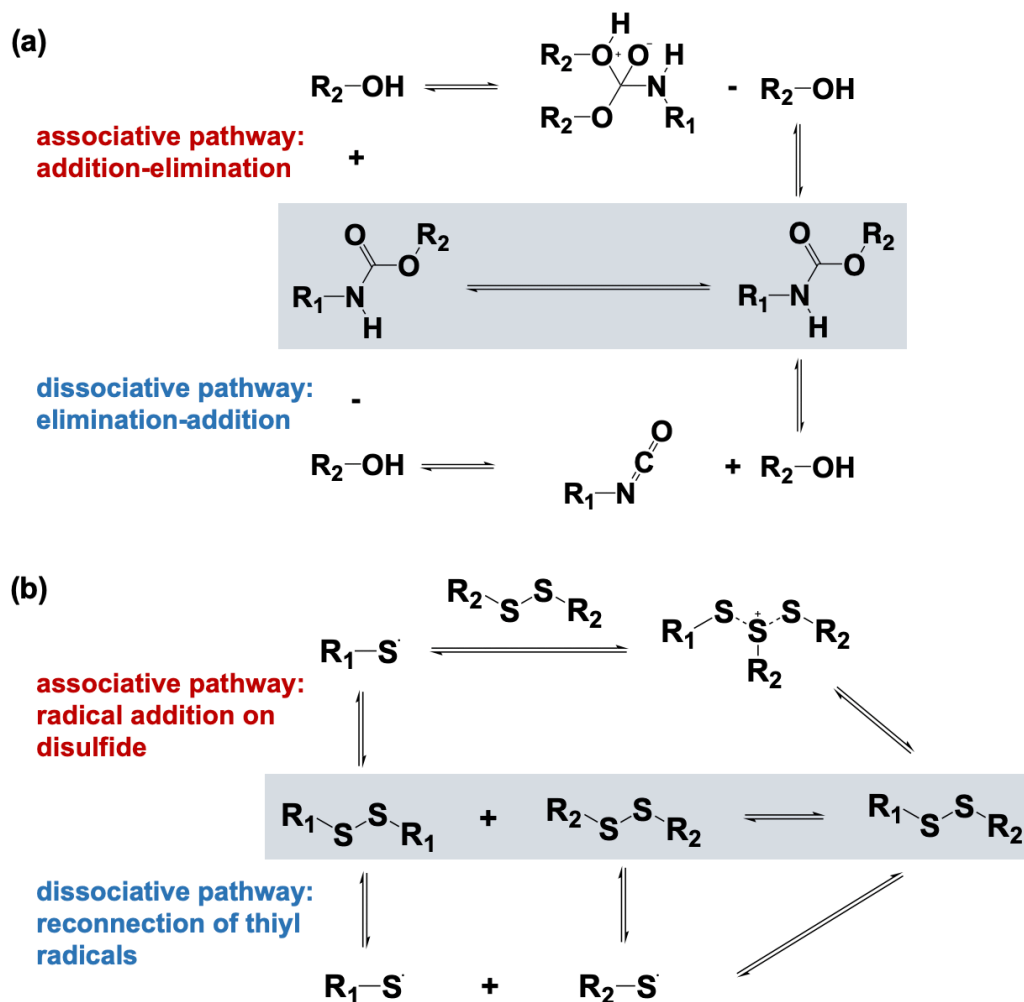


Figure 2.10 Typical examples of mixed covalent adaptable networks with associative and dissociative pathways (a) urethane exchange (b) disulfide exchange

2.2.3 Characteristics of dynamic covalent chemistry

There are some classic indicators and unique property from traditional thermosetting resin in dynamic system, including glass transition temperature (T_g), topology freezing transition temperature (T_v), stress relaxation, and creep behavior. The following sections will review the definition, measurement, calculation, and interpretation of these performances.

2.2.3.1 Glass transition temperature (T_g)

In dynamic covalent system, the exchange reaction and viscoelastic behavior are generally described according to two transition temperatures. The first transition temperature is glass transition temperature (T_g),

which indicates the transition of polymeric material from rigid and fixed polymer chain in glass state to flexible and movable segmental motion in rubbery situation. The common methods to identify T_g of dynamic networks structure is basically same as traditional epoxy resin as stated in paragraph 2.1.3.1, which are differential scanning calorimetry, dynamic mechanical analysis and thermomechanical analysis.

2.2.3.2 Topology freezing transition temperature (T_v)

The other critical transition temperature to evaluate the exchange reaction and viscoelastic behavior in dynamic covalent system is topology freezing transition temperature (T_v). T_v is defined as the point at which the material exhibits a viscosity of 10^{12} Pa·s. T_v is generally considered as the critical point at which the exchange rate becomes sufficiently rapid such that cleavage and rearrangement of dynamic bonds can occur dynamically. Therefore, at the temperature above T_v , exchange reaction occurs in rapid rate, so that the reprocessing, reshaping, and reusing of dynamic covalent networks can be obtained. On the other hand, at the temperature below T_v , the reversible reaction happens slowly, resulting in similar property as traditional thermosetting structure. As a result, T_v is an important indicator to establish the remolding and recycling procedure.

However, the determination of intrinsic T_v is not as direct as T_g because totally different reaction rate below and above T_v . When the exchange reaction occurs in the network structure, it is extremely difficult to monitor the kinetics of reversible reaction. Currently, stress relaxation test examined by rheometer or dynamic mechanical analysis is the most common strategy. Through the data of stress relaxation, the relaxation time at each testing temperature can be evaluated as a function of the temperature followed Arrhenius Equation as shown in Equation 2.1.

$$\tau(T) = \tau_0 \exp\left(\frac{E_a}{RT}\right) \quad (\text{Equation 2.1})$$

where $\tau(T)$ and τ_0 are the relaxation time at specific temperature and initial state, respectively. E_a is activation energy. R is the gas constant and T is the absolute temperature in kelvins. Based on this calculation as presented in figure 2.11, the Arrhenius fitting line to a certain relaxation time (depending on the modulus in rubbery state and Poisson ratio of material) was extrapolated so that the exact T_v -value can be obtained. However, the T_v -value measured by this method may be affected under external force since the additional tensile force is often applied on the sample in rheometer or DMA test, which has a slight influence on the breaking rate of dynamic bonds. Therefore, by introducing the aggregation-induced-emission luminogens, the T_v can be determined more accurately by fluorescence change.

The relationship between T_g and T_v is critical for viscosity change and viscoelastic behavior at different stage of temperature. Therefore, the dynamic networks can be categorized into two cases (a) $T_v > T_g$ (b) $T_g > T_v$ as described in figure 2.12. In case (a) and case (b), the viscoelastic behavior in region I is same, which shows the stable network structure as traditional thermosetting resin. However, the state of materials presents totally opposite at the temperature in region II. For case (a), in the region II above T_g but below T_v , it is expected to undergo the transition from glassy to rubbery state with high mobility, and then transfer to elastomer without exchange reaction due to lack of sufficient exchange reaction kinetics. In the contrary, the case (b) with greater

T_g than T_v , the intrinsically fast exchange reaction of disulfide bonding is embedded in the epoxy network even at the intermediate temperature region II above T_v and below T_g . In such the situation, the dynamic motion of the epoxy networks seems to be limited due to lack of chain mobility, but the exchange reaction of disulfide may sufficiently occur because of enough high temperature than the T_v values. When the temperature is further increased to the region III, where the temperature above both T_v and T_g , the viscoelastic state is reached because both segmental movement and exchange reaction of dynamic bonds are fast enough; therefore, the reprocessing and recycling can be performed in this stage. In case (a), the viscosity in region III follows the typical Arrhenius fitting because the exchange reaction of crosslinking is dominated in rearrangement of networks. On the other hand, the case (b) in region III is firstly diffusion-controlled in WLF model then changed to exchange-controlled mechanism based on Arrhenius law because the cleavage and recombination of network topology is controlled by segmental motions in initial situation. In the viewpoint of these two different relationships between T_v and T_g , the starting flow of viscoelastic state is determined by the higher transition temperature. ^{13,17,120,121}

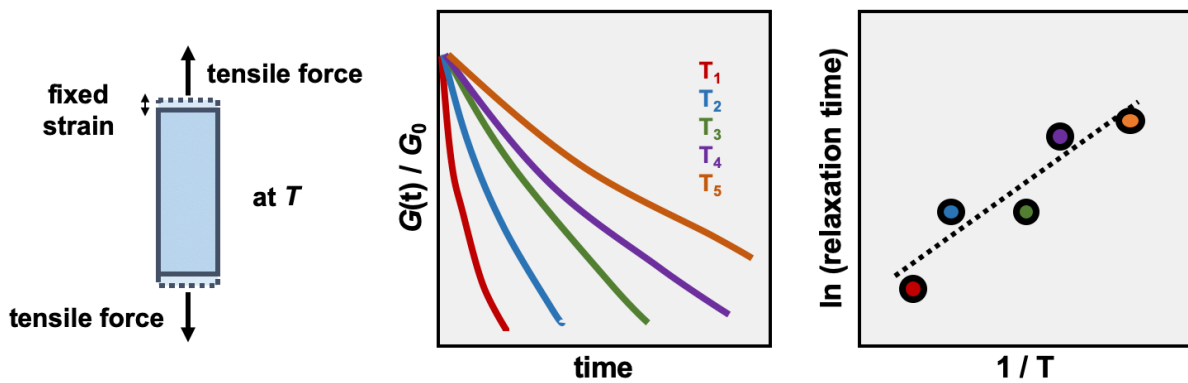


Figure 2.11 Schematic representation for calculation of topology freezing transition temperature

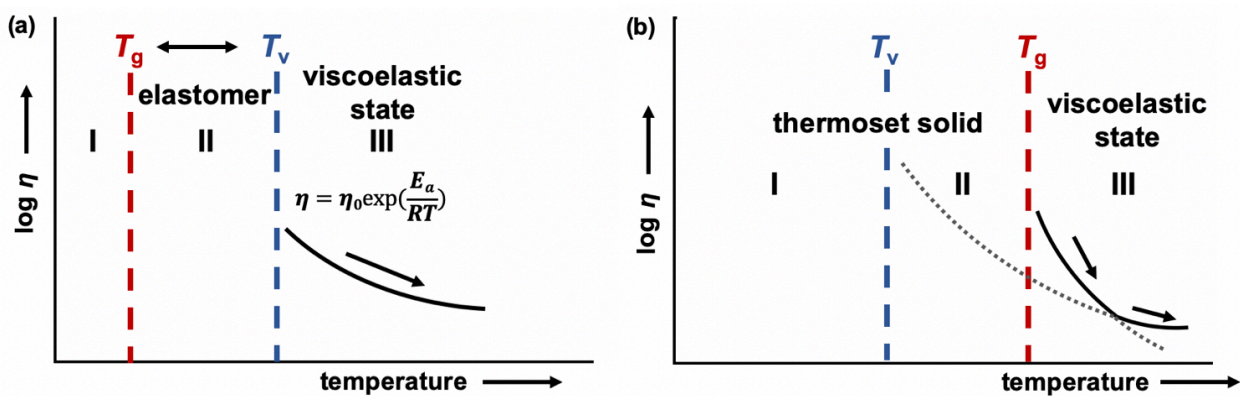


Figure 2.12 Comparison for the effect of glass transition temperature (T_g) and topology freezing transition temperature (T_v) on viscosity and viscoelastic behavior of dynamic systems with (a) $T_v > T_g$ (b) $T_g > T_v$

2.2.3.3 Activation energy (E_a) for exchange reaction

Activation energy is defined as the energy provided to trigger the chemical reaction or the potential barrier needed to be overcome. In covalent adaptable networks, the activation energy can be acquired with the calculation of topology freezing transition temperature (T_v) in the experiment of stress relaxation as presented in figure 2.11, which meant that the activation energy is actually about the viscous flowing detected via stress relaxation behavior instead of exchange reaction itself. Besides, this value may be reduced with the assistance of catalyst. ^{25,34,37,96,107,119,122,123}

2.2.3.4 Stress relaxation

Stress relaxation is the experiment that observe the decrease of stress in response of persistent strain applied on the structure under specific temperature as stated in figure 2.13.(a). This effect mainly results from remaining the configuration of network under fixed deformation, that is the unique heat-induced ductility property for dynamic covalent chemistry. Unlike dynamic networks, the traditional thermosetting network usually presented no stress relaxation in most conditions.

Based on the Maxwell model for viscoelastic material, the stress relaxation time is defined as the time required to release 63% of initial stress, which is highly correlated to the kind of dynamic bond, the amounts of dynamic bonds in the whole network, the testing temperature, and additives modified with functional groups. Generally, more elevated temperature (but should be lower than decomposition temperature) and higher density of dynamic bonds lead to more speedy relaxation. ^{124–127}

2.2.3.5 Creep

Creep is the other indicator that is easily confused with stress relaxation. In polymer science, creep is the tendency of deformation by loading the constant stress in certain temperature as illustrated in figure 2.13.(b). Similarly, the creep is also attributed to viscoelasticity that static stress results in localized molecular rearrangement of polymer chains. Therefore, the conventional thermoset resin demonstrates more excellent creep resistance at elevated temperature due to its thermal stability and less flexibility of covalent crosslinked network structure.

In practical application, creep resistance is an important consideration. The extent of creep is associated with same factors as stress relaxation, mainly determined by environmental temperature and concentration of dynamic bonds. Therefore, several previous researches have paid attention on exploring the balance between creep resistant ability and acceptable vitrimer performance by adjusting the optimized content of dynamic bonds in the networks. ^{128,129}

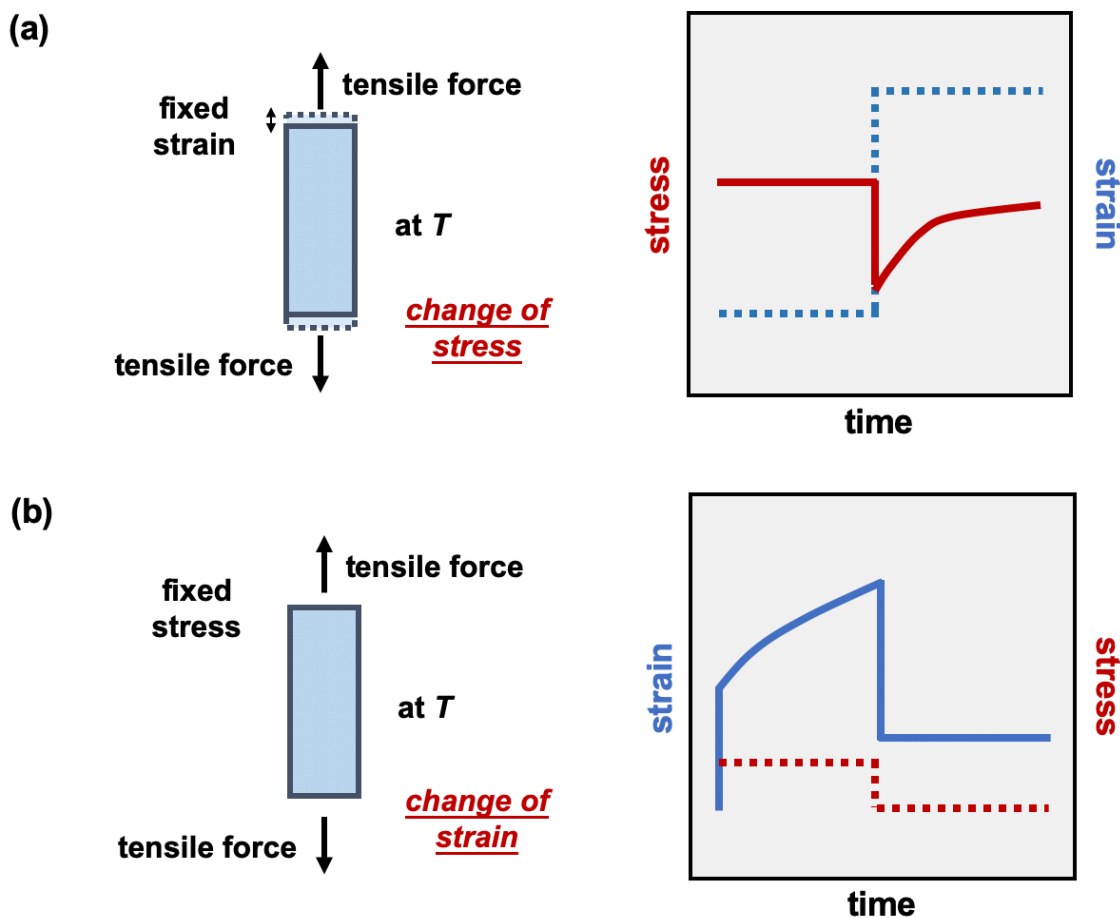
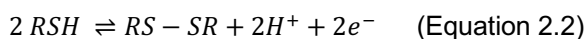


Figure 2.13 Schematic representation for samples and experimental curve (time-dependent stress or strain curve) at specific temperature on (a) stress relaxation (b) creep

2.3 Exchangeable disulfide system

Reversible disulfide system is one of the most common covalent adaptable networks because sulfur-sulfur bond is often incorporated with vulcanized rubber in chemistry industry. This reaction provides rapid exchange rate via the dynamic characteristic of S-S linkages. In recent years, several studies have been explored the exchange reaction mechanism, which can be associative or dissociative types depending on the reaction conditions and catalyst, that will be further discussed in following sections. Generally, disulfide bonding is formed from the oxidation of thiol (-SH) groups as shown in Equation 2.2.



2.3.1 Reaction mechanism of disulfide bonding

The most vital aspect of disulfide bonds is the disulfide-disulfide exchange reaction through cleavage and rearrangement, and thiol-disulfide exchange reaction via reduction-oxidation reaction. Both of two reactions will be reviewed in following sections for their mechanisms, properties, benefits, and possible applications.

2.3.1.1 Disulfide-disulfide exchange mechanism

In general condition, the reversible disulfide mechanism is actually a [2+1] radical-mediated reaction under the condition without catalyst, including three stages as shown in figure 2.14. First, the cleavage of one S-S bond leads to the formation of sulfur-centered radicals. Second, the other disulfide bonding is attacked by thiyl radical, causing the generation of three-membered transition state and then production of new sulfur radical. Finally, the other free sulfur radical is recombined with new thiyl radical to create another disulfide compound. With the assistance of catalyst such as triethylamine and tri-*n*-butylphosphine, radical-mediated and thiol-mediated exchanges can be triggered simultaneously; therefore, the sulfur-based anion is formed instead of sulfur radical in this situation and the amount of anion can be increased by more nucleophilic catalyst. Besides, this reaction is pH-sensitive, so that the pH-value shall be controlled in the range of from 7 to 9 in most cases to promote the formation of thiolate for exchange reaction.

Chemical structure of disulfide bonding provides different performance in reversibility rate, since the reaction is started by the cleavage of S-S bonds; hence, the effect of functional group on dissociation energy has been studied in molecular level previously. Based on the results, the aromatic disulfide bonding is considered as the more efficient reversible reaction than aliphatic one due to chemical modification of phenyl rings, especially in *para* positions. The dissociation energy would be reduced resulting from two factors: (1) the decrease of spin density on sulfur atom of the new-generated thiyl radical leads to delocalization and stabilization. (2) the number of antibonding orbitals is increased that will promote the cleavage of bond.

27,36,42,43,106,107,130

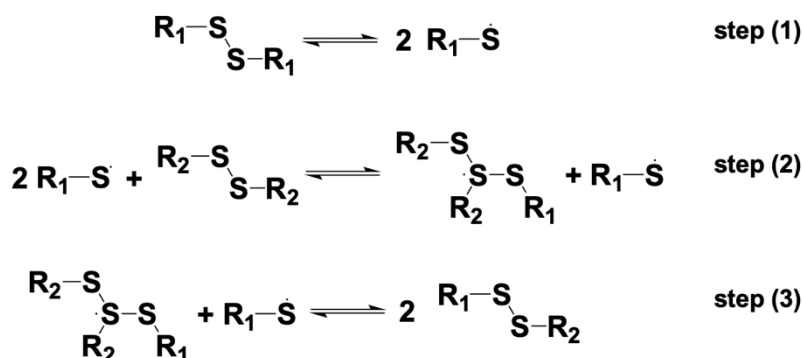


Figure 2.14 Disulfide-disulfide exchange mechanism based on [2+1] radical-mediated reaction

2.3.1.2 Thiol-disulfide exchange mechanism

The reaction of thiol-disulfide exchange is an anion-mediated reaction. Unlike thiyl radical initiated in disulfide-disulfide exchange, the thiol-disulfide exchange reaction is triggered from initial ionization from thiol group to thiolate anion group. Then, the sulfur atom of disulfide bonding nucleophilic is attacked by anion to cleave and generate new S-S bonds, and finally lead to protonation of the formed thiolate anion. Besides, the thiol-disulfide reaction can also be deemed as reduction-oxidation reaction. In this case, the thiyl group is applied as reducing agent, while disulfide is acted as oxidizing agent. After redox reaction, the SH bond is

oxidized into new disulfide bonding and S-S bond is reduced to thiolate group. Thiol-disulfide exchange reaction is commonly used in biochemistry, especially in folding and stabilizing of proteins. Also, some previous researches provided the decomposition strategy of disulfide-contained epoxy network via thiol-disulfide exchange by using the 2-mercaptoethanol and dithiothreitol, which will be further reviewed in section 2.3.2.3.

39,44,122,131–136

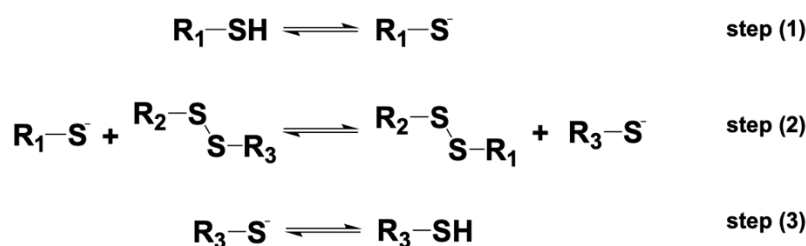


Figure 2.15 Thiol-disulfide exchange mechanism

2.3.2 Properties and characteristics of exchangeable disulfide system

Previously, many researches discussed the thermal, mechanical, degradation, and other properties of reversible disulfide bonding incorporated with epoxy networks structure, which will be briefly reviewed in following sections.

2.3.2.1 Thermal properties

Typical thermal performance reported in previous studies for disulfide-contained networks includes glass transition temperature (T_g) and topology freezing transition temperature (T_v). In most of cases, disulfide-contained networks exhibit the higher T_g than T_v . For example, the structure synthesized by diglycidyl ether of bisphenol A (DGEBA) and 4-aminophenyl disulfide (AFD) has been explored that possess T_g in 130 °C and T_v in -13 °C. Another epoxy material prepared by isosorbide-derived epoxy and aromatic disulfide diamine hardener also presents same trend, which shows T_g in 41 °C and T_v in 31 °C. To summarize, the networks consisted of S-S bond displayed lower T_g than conventional C-C bonds due to less thermal stability; however, the T_v -value is much lower because of high-speed reversibility rate. This thermal property can offer the comparable service temperature of epoxy resin as traditional epoxy resin; besides, reprocessing and remending can be reached through exchangeable bonds. ^{37,39,44}

2.3.2.2 Mechanical properties

The bulk epoxy-disulfide combination system demonstrates the commensurate mechanical property with traditional thermosetting resin for modulus in dynamic mechanical analysis (DMA) and tensile test. The storage modulus at room temperature examined by DMA for dynamic networks with disulfide bonding is approximately 2.2-2.6 GPa, while the value of reference samples is 2.5 GPa. When this material is used in composite structure, the related strength test, such as compression strength, interlaminar shear strength, flexural strength,

and impact strength is also performed and reported with comparable values. Therefore, the incorporation of S-S bond with epoxy networks has no negative influence on mechanical property compared to regular epoxy resin structure. ^{39,41}

2.3.2.3 Degradation properties

The degradation for disulfide -contained epoxy resin is generally occurred in the presence of thiol group via thiol-disulfide exchange reaction. Similar to conventional epoxy resin, the dynamic networks with disulfide bonding presents excellent chemical resistant ability, so that common chemical media like ethanol, acetone, toluene, dimethylformamide (DMF), dimethyl sulfoxide (DMSO), tetrahydrofuran (THF), NaOH, and HCl cannot cause decomposition. Nevertheless, the depolymerization can be easily obtained by 2-mercaptoethanol and dithiothreitol in DMF solution due to the existence of SH bond. DMF solvent is usually chosen to assist the swelling of epoxy structure. Depending on the amount of disulfide bonding inside the polymeric network, the reaction temperature, the type of thiol group, and the concentration of reagent, the degradation of epoxy-disulfide networks can be finished within 1 to 24 hours. This technique can also be applied in composite structure to recycle the fibers without damage. ^{39,41,44,45}

2.3.2.4 Mechanochromic effect

Mechanochromic effect is known as the obvious color change of material that induced by mechanical force like crushing, pressing, shearing, or scratching, which is very critical in monitoring the fracture of material. In dynamic disulfide bonding, the reversible mechanochromic effect can be detected when it integrated with epoxy resin since there is no mechanochromic effect observed in pure aromatic disulfide diamine. This phenomenon results from the formation of phenyl thiyl radicals, leading to the color change from yellow to green. After placing for 24 hours at room temperature or heating above T_g in few seconds, the sulfur-centered radicals will be recombined with each other, causing the disappearance of mechanochromic effect. Interestingly, this behavior is controlled change in dipole moment when nitrogen and sulfur atoms in *para* position. It is accepted that the duration of mechanochromic effect lasting is related to the crosslinking density and chain mobility of polymer network. The higher crosslinking density results in less segmental movement, leading to longer time of reconnection of free radicals. Therefore, the disulfide-contained epoxy network with higher crosslinking density exhibited longer lasting time of mechanochromism. ^{47,48,137-140}

CHAPTER III STRENGTHENING ADHESION EFFECT AT HIGH TEMPERATURE AND REPARABILITY

Thermosetting structural adhesive is one of the most common utilizations for epoxy resin, which has been widely applied in aerospace, automobile, and infrastructure because of light-weight design to replace conventional fastening, rivet, and insert. Epoxy-based adhesive composed of highly-crosslinked network structure, providing the excellent thermal stability, strong mechanical strength, superior chemical resistant ability, and applicability with multiple kinds of substrates. However, there are two disadvantages that restricts the performance of epoxy-based adhesive. First, although this material is required to be steady in harsh elevated-temperature environment, the adhesive strength of conventional epoxy-based adhesive usually reduces with increasing temperature. Second, because of low toughness property for epoxy-based adhesive, the poor ability to absorb the mechanical energy and avoid fracture may cause some micro-cracking on the adhesive itself. There are several techniques used in enhance the toughness previously, but few reports discussed the repairing of epoxy resin since it is difficult to recover the broken covalent crosslinking structure once it is cured. Therefore, we tried to develop the new-generation epoxy resin as adhesive that can solve above two issues.^{49,64,65,67,73,76,141-144}

To address this demand, our research has focused on the use of dynamic covalent bonds. Polymeric networks with dynamic bonds behave as traditional thermosetting structure, but exhibit thermoplastic property due to reversible exchange reactions under external stimuli. By introducing the dynamic bonding into thermosetting epoxy-based adhesive, the network presents the unique properties, such as healing, reprocessability, degradability, and recyclability. Among all choices, aromatic disulfide bonding is really suitable to integrate with epoxy networks because of catalyst-free reactivity, relatively stable thermal and mechanical performance, and rapid reversibility efficiency. These dominances can avoid the damage on substrate caused by insoluble catalyst, offer steady performance in structural utilization, and decrease the reaction time at high temperature during repairing, which may cause aging and oxidation of epoxy resin.^{27,28,32,34,35,43,107,130}

In this study, we carefully assessed the chemical composition, thermal stabilities, and mechanical strength for epoxy resin with different amounts of aromatic disulfide bonding, leading to the thorough understanding of the relationship between content of S-S bonds and each property. In order to emphasize on the unique performance of disulfide exchange reaction compared with other dynamic bonds, the sample with ester bonds was prepared. Moreover, although previous researches have reported the degradation, self-healing and electrical resistance properties for epoxy-disulfide combination system, the adhesive characteristics of these substances, especially the effects of temperature change on adhesion strength, have not been fully evaluated; therefore, the detail temperature-dependent behavior in both bulk sample and adhesive joint was also elucidated.^{39,41,44}

The results revealed that the reparability of broken epoxy resin could be obtained by simple hot-pressing procedure and recovered adhesive joint maintained approximately 90% of initial adhesion strength. The epoxy resin with most content of S-S bonds exhibited best reparability within shorter reaction time than the one reprocessed via transesterification. On the other hand, the unusual adhesion strengthening effect at high temperature was observed in the case of disulfide-contained networks. This improvement was discussed in the concept of the relationship between glass transition temperature (T_g) and topology freezing transition

temperature (T_v) and the special speculated strengthening mechanism via disulfide-disulfide exchange reaction was proposed.

3.1 Experimental

In this section, the material used in this project, synthesizing procedure of epoxy monomer, polymerization of epoxy resin network, preparation of adhesive joint, establishment of small model, and characterization techniques are described.

3.1.1 Materials

Diglycidyl ether of bisphenol A (DGEBA) (JER 825) with the epoxide equivalent weight of 170-180 g/mol was purchased from the Mitsubishi Chemical Corporation. As a diamine hardener, 4,4'-diaminodiphenylmethane (DDM) with an amine hydrogen equivalent weight of 49.6 g/mol and dithiodianiline (DTDA) with an amine hydrogen equivalent weight of 62.1 g/mol were purchased from the Tokyo Chemical Industry Co., Ltd. Citric acid monohydrate, sebacic acid and 1-methylimidazole used in reference samples with ester bonds were purchased from the Tokyo Chemical Industry Co., Ltd. Also, in order to synthesize the epoxy monomer with aromatic disulfide bonding ((in this case, bis(4-glycidylphenoxyphenyl) disulfide (BGPDS)), bis(4-hydroxyphenyl) disulfide, epibromohydrin were purchased from the Tokyo Chemical Industry Co., Ltd. and anhydrous dimethylformamide (dehydrated DMF), hexane, chloroform, methanol, anhydrous potassium carbonate, anhydrous magnesium sulfate, and sodium chloride were purchased from Wako. Chemicals. All chemicals were used as purchased without any purifying and post-treating.

On the other hand, aluminum alloy (6061-T6) used as substrates in adhesive joint was purchased from Standard-Testpiece Company. Ethanol, hexane, acetone, ethanol, sodium hydroxide, sodium carbonate and sodium dodecylbenzene sulfonate used in the cleaning of the aluminum substrates were purchased from Wako. Chemicals.

3.1.2 Synthesis and preparation of samples

This section includes three parts, which are procedures used in synthesizing disulfide-contained epoxy monomers, curing epoxy-based resin, and constructing the adhesive joint in this study.

3.1.2.1 Synthesis of disulfide-contained epoxy monomer

The mixture of bis(4-hydroxyphenyl) disulfide (10 g, 40.0 mmol), anhydrous potassium carbonate (55.28 g, 400 mmol), epibromohydrin (54.79 g, 400 mmol), and dehydrated dimethylformamide (200 mL) was heated at 60 °C and stirred overnight under nitrogen or argon atmosphere. The completion of the reaction was confirmed by thin layer chromatography (TLC), and solid substrates were removed from the reaction mixture by a suction filtration. Then, 250 mL of water was added into the reaction mixture, and the mixture was extracted by chloroform/hexane solution (2/3 v/v) for three times. The combined organic phase was washed by water for three times and brine. The organic phase was dried by anhydrous magnesium sulfate and concentrated by rotary evaporation. The residue was re-crystallized from methanol to afford the product as a white solid (10.8 g, 29.8 mmol, 75 %). $^1\text{H NMR}$ (CDCl_3 , 400 MHz): 7.40-7.36 (d, 4H, Ar-H), 6.87-6.84 (d, 4H,

Ar-H), 4.25-4.20 (dd, 4H, OCH₂CH(O)CH₂), 3.96-3.90 (dd, 4H, OCH₂CH(O)CH₂), 3.37-3.32 (m, 2H, OCH₂CH(O)CH₂), 2.92-2.89 (dd, 4H, OCH₂CH(O)CH₂), 2.76-2.74 (dd, 4H, OCH₂CH(O)CH₂) as presented in figure 3.1. ⁴¹

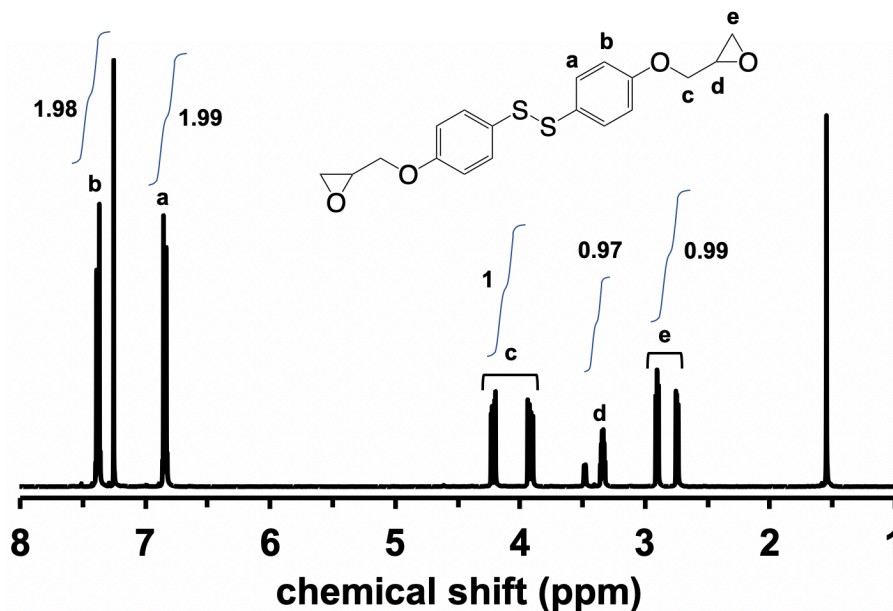


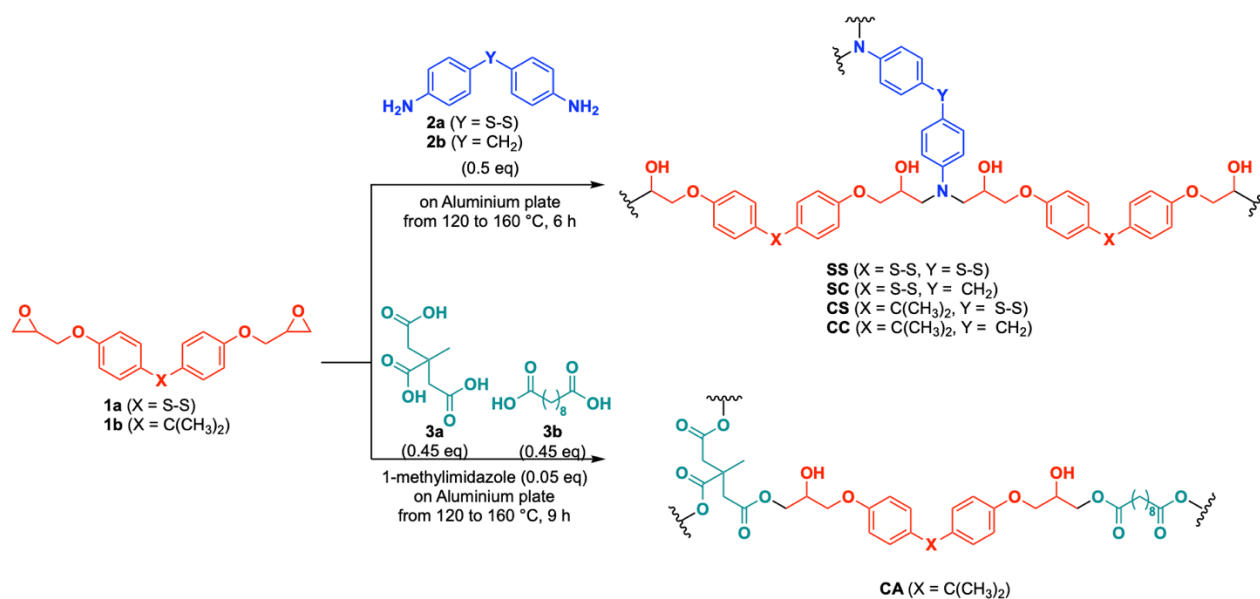
Figure 3.1 ¹H-NMR spectrum for bis(4-glycidyoxyphenyl) disulfide

3.1.2.2 Synthesis of bulk epoxy resin networks

Five types of epoxy resin were prepared according to table 3.1 and figure 3.2. The disulfide system comprised bis(4-glycidyoxyphenyl) disulfide (BGPDS, termed the 1a herein) and dithiodianiline (DTDA, 2a) as the epoxy monomer and diamine crosslinker, respectively. The diglycidyl ether of bisphenol A (DGEBA, 1b) and diaminodiphenyl methane (DDM, 2b) were employed as controlled samples of BGPDS and DTDA, respectively, without phenyl S-S bonds. The chemical reactivities of the aromatic disulfide in the epoxy monomer and diamine hardener were assumed to be almost identical. The epoxy adhesives SS, SC, CS, and CC were synthesized by combining the epoxy monomer (either 1a or 1b) and the diamine hardener (2a or 2b), combining in a 2:1 molar ratio in a glass vial and mixed at 90 °C for 30 min then rapidly poured into a Teflon mold. Each sample was cured in an oven at 120 °C for 2 hours, 140 °C for 2 hours, and 160 °C for 2 hours. Also, to compare between various dynamic reaction mechanisms, formula CA, made from a 1:0.45:0.45 mixture (on a molar basis) of epoxy monomer, citric acid monohydrate and sebacic acid was prepared in a glass vial. Citric acid monohydrate and sebacic acid were preheated for melting and then mixed with DGEBA at 125 °C. The catalyst 1-methylimidazole was added to catalyze the transesterification and epoxy-acid reactions. After obtaining the homogenous yellow mixture, the sample was cured in an oven at 120 °C for 3 hours and 160 °C for 6 hours. ¹²³

Table 3.1 Formulation of all epoxy networks

Network	epoxy monomer		diamine crosslinker		
	S-epoxy BGPDS (mol. ratio (g))	C-epoxy DGEBA (mol. ratio (g))	S-diamine DTDA (mol. ratio (g))	C-diamine DDM (mol. ratio (g))	
SS	2 (1)	-	1 (0.343)	-	
SC	2 (1)	-	-	1 (0.274)	
CS	-	2 (1)	1 (0.365)	-	
CC	-	2 (1)	-	1 (0.291)	
Network	epoxy monomer		acid crosslinker		catalyst
	C-epoxy DGEBA (mol. ratio (g))		citric acid monohydrate (mol. ratio (g))	sebacic acid (mol. ratio (g))	
CA ¹²³	1.1 (1)		0.5 (0.183)	0.5 (0.264)	1-methylimidazole 0.055 (0.024)

**Figure 3.2** Synthesis and chemical structure for all epoxy-based network in this study

3.1.2.3 Preparation of adhesive joints

Aluminum substrates (AA6061-T6) with dimensions of 100 (length) × 25 (width) × 2 (thickness) mm as shown in figure 3.3.(a) were prepared by mechanical surface polishing with 800 grit sandpaper, followed by ultrasonic cleaning in ethanol, hexane and acetone for 15 minutes in each solvent. Each substrate was subsequently immersed in an alkaline degreasing solution at 70 °C for 10 minutes (according to the ASTM D2651 standard procedure). Finally, substrates were rinsed with water at room temperature for 10 minutes and then dried at 70 °C as necessary to remove the residual water. In each trial, an epoxy monomer and amine

hardener were combined in a glass vial and mixed at 90 °C for 30 min, then immediately applied on the overlapped area of treated metal substrates. The adhesive joint was held together using two clips. The overlapped area was fixed at 25 × 12.5 mm and the thickness of the adhesive was controlled within 100-150 micron (µm) by adding 1 wt.% glass beads to the polymer. Finally, the adhesive joints were cured in an oven under the same conditions as applied to the bulk samples. (120 °C for 2 hours, 140 °C for 2 hours, and 160 °C for 2 hours)

3.1.2.4 Rebonding and repairing of adhesive joints

The initial adhesive joints were broken after the first single lap shear test. Following such tests, each detached specimen was hot-pressed at 200 °C under 20 kN of compressive force for 20 minutes (in the case of the SS, SC and CS specimens) or 160 °C under 20 kN of compressive force for 60 minutes (in the case of the CA specimen) to rebond and/or repair the broken adhesive joints as demonstrated in figure 3.3.(b). After cooling to room temperature, these specimens were again subjected to single lap shear tests. The rebonding procedure would be repeated for three times. Please note that specimen CC without any dynamic bonds could not be rebonded through hot-pressing procedure.

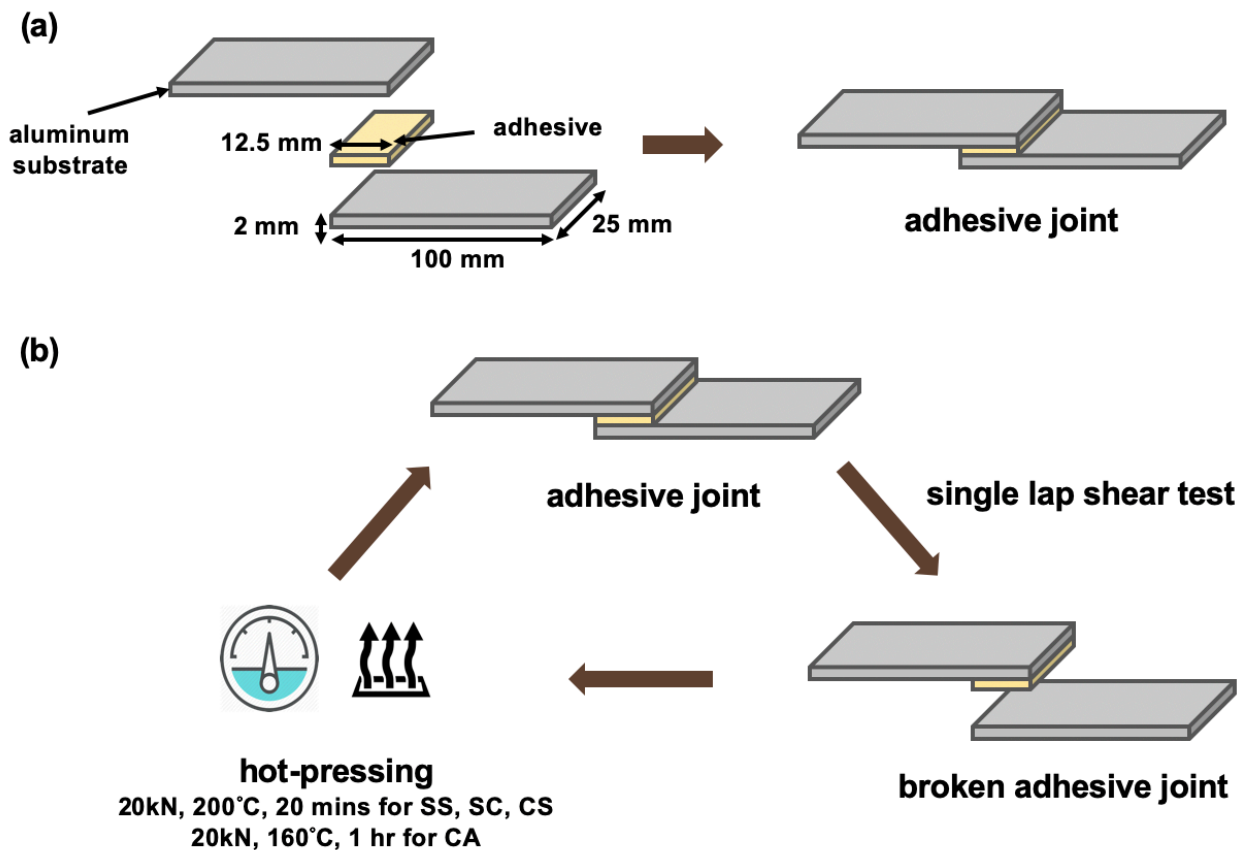


Figure 3.3 Schematic representation for (a) samples in lap shear test (b) samples in rebonding procedure

3.1.2.5 Small molecular model reaction

Solutions of diphenyl disulfide and 4,4'-dithiodianiline in DMSO- d_6 (0.45 M each), prepared separately, were mixed in 1:1 (v/v) ratio in an NMR tube covered with aluminum foil to shed the light. After the treatment of the sample at ambient, 50, 75, 100, and 150 °C. for 2 hours, the composition of the mixture was monitored by ^1H NMR.

3.2 Characterization

^1H nuclear magnetic resonance spectra were collected using a JEOL-ESC 400 instrument at 400 MHz for CDCl_3 solution of sample, and reported in ppm δ (ppm) from internal tetramethyl silane signal.

The existence and intensity of aromatic disulfide bonding was confirmed by in via confocal Raman microscope from Renishaw Qontor at the wavelength settled from 200 to 1800 cm^{-1} . A 532-nm laser was used in this experiment and the power was controlled in 0.1%. Exposure time for each count was 200 seconds and 10 counts were accumulated totally for each composition.

The efficiency of curing was assessed using Fourier transform infrared-near infrared spectroscopy, employing the JASCO 6100 spectrometer over the range of 4000 to 7000 cm^{-1} in transmission mode. A spectrum of the ambient air was used as a background. The samples were prepared in the 1-millimeter thickness. The spectra were recorded at a resolution of 8 cm^{-1} with total 32 scans.

Thermal analysis was performed by differential scanning calorimetry (DSC) by equipment from Shimadzu DSC-60 plus. Approximately 10 milligrams of sample were placed in aluminum cell and aluminum oxide was used as reference with weight of 20 milligrams. Temperature range was from 0°C to 250°C with heating and cooling rate of 10°C/min under nitrogen flow at 50 ml/min. Glass transition temperature was obtained from second heating cycle.

Thermogravimetric analysis (TGA) was obtained by equipment from TA instrument SDT Q600 under argon atmosphere. Approximately 5 milligrams of sample were loaded in aluminum pan. Temperature range was from 25°C to 500°C with heating rate of 10°C/min under argon flow at 100 ml/min. Air was used as reference. Degradation / decomposition temperature was identified by the points of intersection of tangents to the two branches of the curve.

Thermal mechanical analysis (TMA) was used in identifying the coefficient of linear thermal expansion (CTE) by equipment from Netzsch DMA242E on TMA detection in tensile mode. All samples were pre-heated to 120°C for one hour to remove the water on the surface. Then, the temperature was decreased to room temperature for additional one hour to reach thermal equilibrium. After above procedure, characterization started by heating until 200°C at the heating rate of 5°C /min. CTE would be calculated at the range of 70°C to 110°C (below glass transition temperature) for glass state.

Dynamic mechanical analysis was performed using a Netzsch DMA242E instrument in the tensile test mode with sample dimensions of 10 × 5 × 0.2 mm over the temperature range from 25 °C to 200 °C at a heating rate of 3 °C/min. The oscillation frequency was maintained at 1 Hz.

Stress relaxation tests were carried out using the same equipment at different temperatures (at least five different temperature for each dynamic compositions), allowing 30 extra minutes for thermal equilibration. A minimum force of 0.006 N was applied to each sample in order to maintain straightness. A strain of 1% was

applied and this deformation was maintained during the measurement process.

Adhesion test was examined for formula SS and CA only. Each composition represented two types of dynamic systems, which are disulfide exchange owns T_v higher than T_g and transesterification possesses T_g higher than T_v to compare the difference. The temperature used to bond two bulk samples was set up at 80 °C under 10 kN of compressive force for 1 hour, since this temperature located in the region between T_v and T_g for both cases.

Single lap shear tests were carried out by using a Shimadzu autograph AG-X plus instrument with a crosshead speed of 0.1 mm/min. The sample temperature was controlled using an environmental chamber and the test temperatures were ambient, 50, 75, 100, 150 and 200 °C. A thermocouple was used to confirm that the internal chamber temperatures were correct. After attaining the desired temperature, the sample was held at that temperature for 1 hour to allow for equilibration. The reported values represent the averages of three samples along with the standard error.

3.3 Results and discussion

3.3.1 Degree of curing

First, it is important for confirming the curing procedure is complete to prevent the unstable chemical composition. In order to determine the curing condition (120 °C for 2 hours, 140 °C for 2 hours, and 160 °C for 2 hours) we used in this study that could result in fully curing, near-infrared spectroscopy (n-IR) was carried out in evaluation. In n-IR spectra as given in figure 3.4, the peak of aromatic ring at 4680 cm^{-1} is suitable for normalization for comparison since the phenyl group was not participate and involve in the curing reaction, presenting the same transmittance before and after curing. Therefore, the well-defined bands related with the epoxy and primary amine were observable in the combination band of the second overtone of the epoxy ring stretching with the fundamental C-H stretching (ca. 4530 cm^{-1}) and the combination band of NH stretching and bending (ca. 5000-5100 cm^{-1}). Thus, the epoxy monomer decreased upon curing process, resulting in decrease of the band of the fundamental C-H stretching and the weak overtone of terminal CH_2 at ca. 4530 cm^{-1} and ca. 6060 cm^{-1} , respectively. The primary amine combination band at ca. 5000 cm^{-1} also decreased. On the other hand, the band of O-H overtones at ca. 7000 cm^{-1} increased as a consequence of the oxirane ring opening reaction.¹⁴⁵

3.3.2 Disulfide-bonding determination

Since aromatic disulfide bonding was too weak to be detected in FTIR spectra, Raman microscope was applied to confirm the existence of aromatic disulfide bonding. The band at 485-500 cm^{-1} was characterized as phenyl S-S bond as demonstrated in figure 3.5, which revealed that the aromatic disulfide bonding existed in chemical structures SS, SC, and CS as expected except for composition CC. Besides, in order to compare the intensity of aromatic disulfide bonding, the peak of aromatic ring at 1610 cm^{-1} was used in normalization because the content of aromatic ring was not changed with different epoxy networks. Localized spectra at the wavelength of 400 to 600 cm^{-1} were as also revealed as illustrated in figure 3.5. The intensity of peak proved that the composition SS possessed more aromatic disulfide bonding than other compositions (SC and CS) as our assumption. Moreover, there was obviously no peak shown in networks CC.^{146,147}

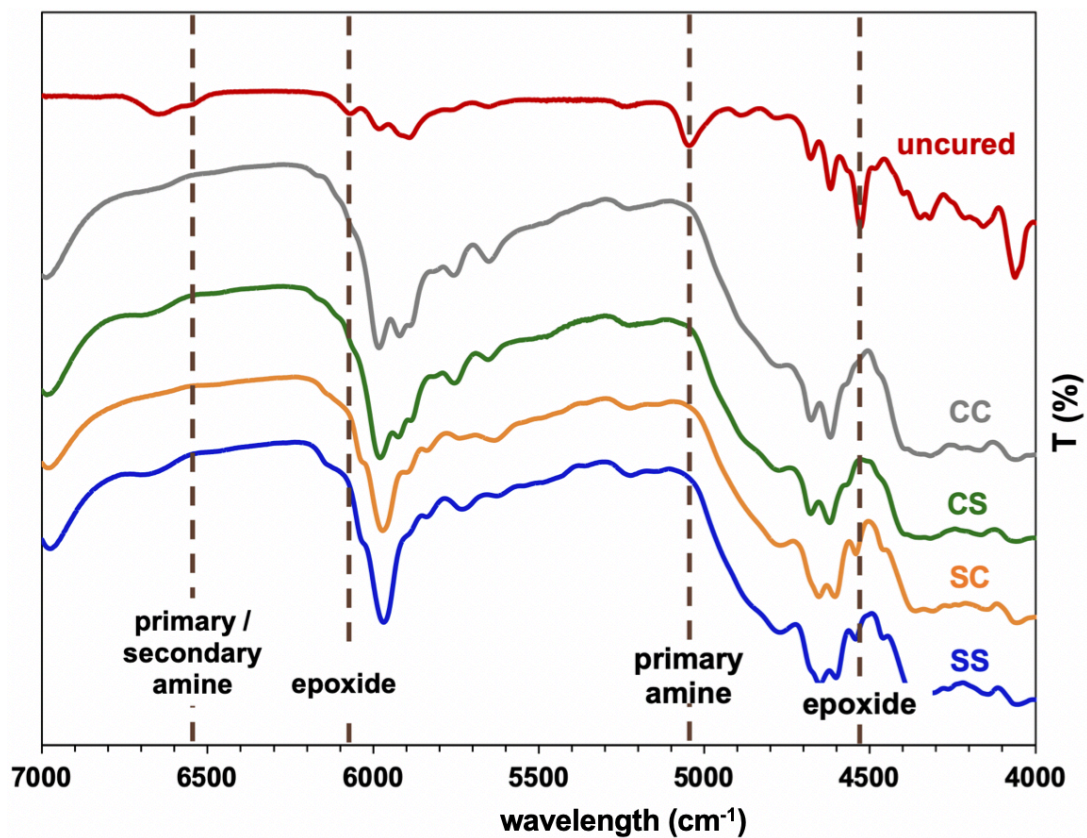


Figure 3.4 FTIR-nIR spectra of SS, SC, CS, and CC networks at 4000 to 7000 cm^{-1}

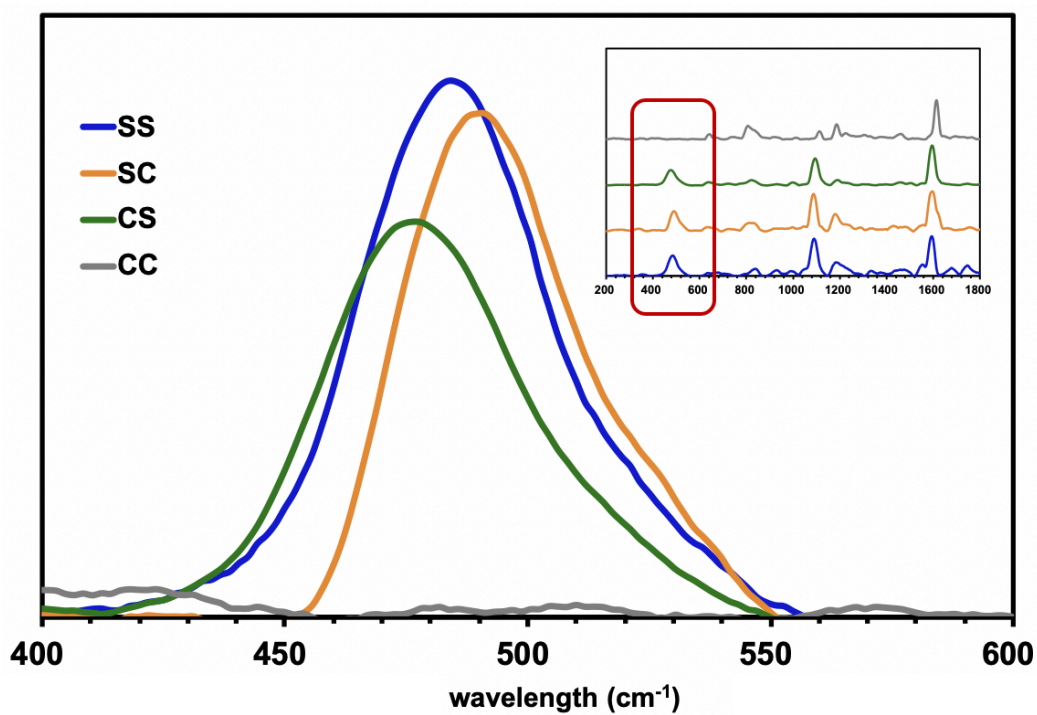


Figure 3.5 Raman spectra of SS, SC, CS, and CC networks at 400 to 600 cm^{-1}

3.3.3 Thermal analysis

The thermal analysis in this study for all epoxy resin networks, including glass transition temperature (T_g) from differential scanning calorimetry (DSC) and dynamic mechanical analysis (DMA), degradation or decomposition temperature (T_d) thermogravimetric analysis (TGA), and coefficient of thermal expansion (CTE) from thermal mechanical analysis (TMA) was discussed as summarized in table 3.2 of this section. Although the topology freezing transition temperature (T_v) is the other essential transition temperature in dynamic system, this hypothetical value was generally discussed and calculated with heat-induced stress relaxation experiment, which would be explored in paragraph 3.3.5.

Table 3.2 Summarized thermal properties for all epoxy networks in this work

Networks	T_g (DSC) ($^{\circ}\text{C}$)	T_g (DMA) ($^{\circ}\text{C}$)	T_d (TGA) ($^{\circ}\text{C}$)	CTE (TMA) ($10^{-5}/^{\circ}\text{K}$)
SS	127.0	133.7	272.3	7.8
SC	138.8	144.0	271.3	7.2
CS	162.6	160.5	296.1	6.5
CC	182.7	177.9	361.2	6.2
CA ¹²³	-	73	-	-

First, the second heating cycle in DSC profile was usually used to define the T_g -value because there was no exothermic or endothermic peak existed. In our case, the DSC profiles of composition SS, SC, CS, and CC prepared in stoichiometry ratio, where $M_{\text{epoxy}} : M_{\text{diamine}}$ was 2:1, were as shown in figure 3.6. The results indicated the shift of baseline in heat flow was located at 127.0 $^{\circ}\text{C}$, 138.8 $^{\circ}\text{C}$, 162.6 $^{\circ}\text{C}$, and 182.7 $^{\circ}\text{C}$ for formula SS, SC, CS, and CC, respectively, corresponding to the glass transition temperature. Besides, if the ratio between epoxy monomer and diamine hardener was changed to 2:1.1, the T_g -value would be approximately 10 $^{\circ}\text{C}$ lower than original composition. Also, the T_g -value could be analyzed by dynamic mechanical analysis as described in figure 3.7. The peaks of tangent delta for composition SS, SC, CS, and CC were at 133.7 $^{\circ}\text{C}$, 144.0 $^{\circ}\text{C}$, 160.5 $^{\circ}\text{C}$, and 177.9 $^{\circ}\text{C}$, separately. In summary, the T_g -value was decreased with increasing the content of aromatic disulfide bonding inside the network structures. Otherwise, the disulfide bonding in epoxy monomer promoted more reduction of T_g -value than the one in diamine crosslinker. This effect may result from two reasons. First, dynamic phenyl S-S bond provided more flexibility than traditional C-C bonds, causing more mobility and lower T_g . Second, there were two more alkyl groups located in diglycidyl ether of bisphenol A (DGEBA), so that it would be more difficult to cause chain motion for the composition synthesized from the DGEBA due to the more branches and side groups. However, even though the glass transition temperature was declined, the T_g -value of this new system was still higher than most known dynamic system, such as similar epoxy networks CA based on transesterification, which was previously reported that possessed the T_g -value of 73 $^{\circ}\text{C}$.

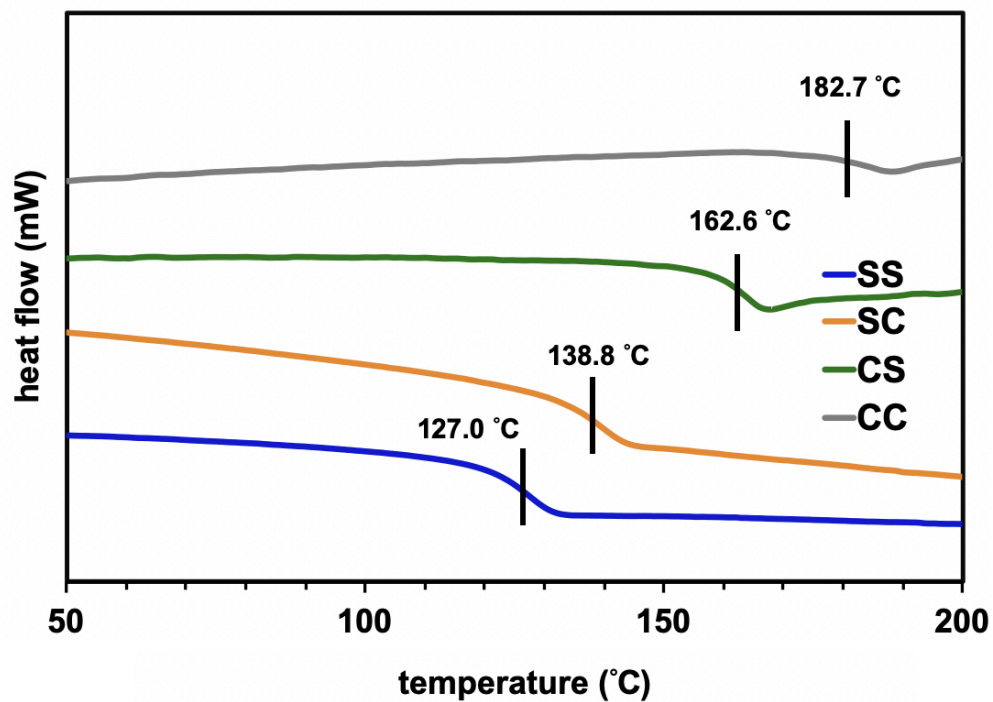


Figure 3.6 DSC profiles for formula SS, SC, CS and CC synthesized in stoichiometry ratio ($M_{\text{epoxy}} : M_{\text{diamine}} = 2:1$)

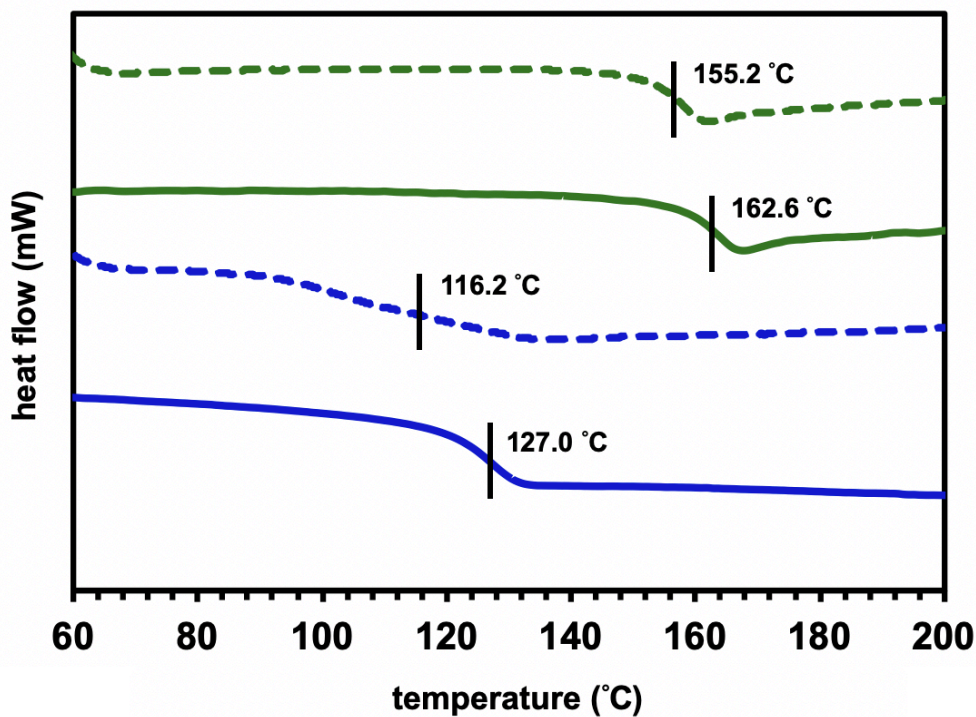


Figure 3.7 DSC profiles for formula SS and CS and CC synthesized in stoichiometry ratio ($M_{\text{epoxy}} : M_{\text{diamine}} = 2:1.1$ (dot line))

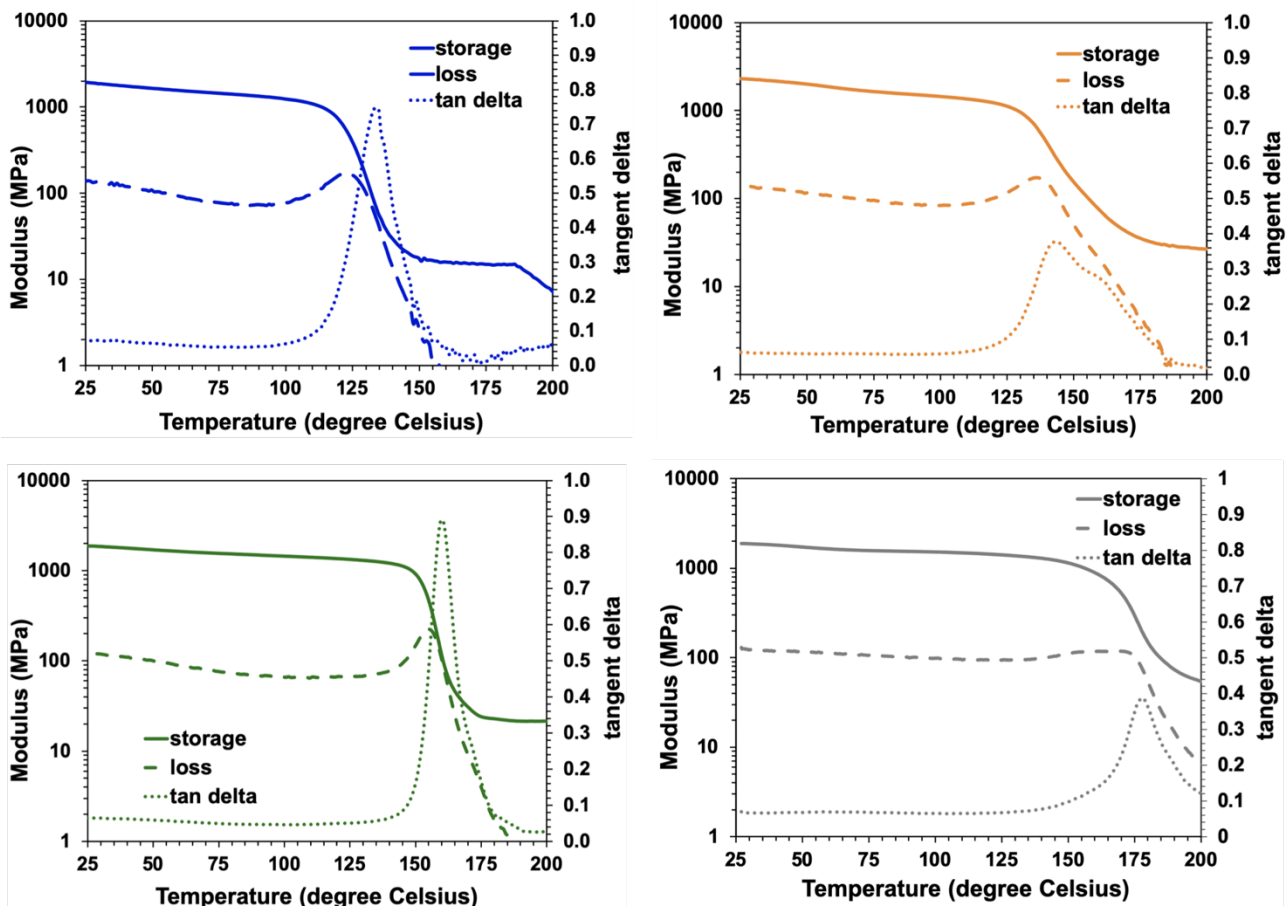


Figure 3.8 DMA curve for (a) dynamic epoxy networks SS (b) dynamic epoxy networks SC (c) dynamic epoxy networks CS (d) dynamic epoxy networks CC

Degradation/decomposition temperature was defined as the temperature chemically decomposed into smaller fragments by heat, also an indicator to evaluate the thermal stability, which usually performed by TGA. Based on the results analyzed from TGA as presented in figure 3.9, the 5% loss of weight started from 272.3 °C, 271.3 °C, 296.1 °C, and 361.2 °C, for formula SS, SC, CS, and CC, respectively, which was interpreted as degradation/decomposition temperature. The profiles of TGA exhibited that more contents of aromatic disulfide bonding resulted in lower degradation/decomposition temperature, attributed to less energetic stability of disulfide bonding. Also, the result was consistent with the relatively good mobility at high temperature for S-S bonds as suggested by the DSC results. Also, coefficient of thermal expansion (CTE) was indicated that the deformation in response to heat, which was generally measured by TMA as stated in figure 3.10. The CTE-value determined in the range from 70 °C to 110 °C, which was corresponding to the glass state of all epoxy resins. The measured CTE-values of formula SS, SC, CS, and CC were 7.8, 7.2, 6.5, and 6.2 ($10^{-5}/^{\circ}\text{K}$), separately. The enhancement of CTE-value with increasing amounts of phenyl S-S bonds might be ascribed to lower bond energy of sulfur-sulfur bonds than carbon-carbon bonds.

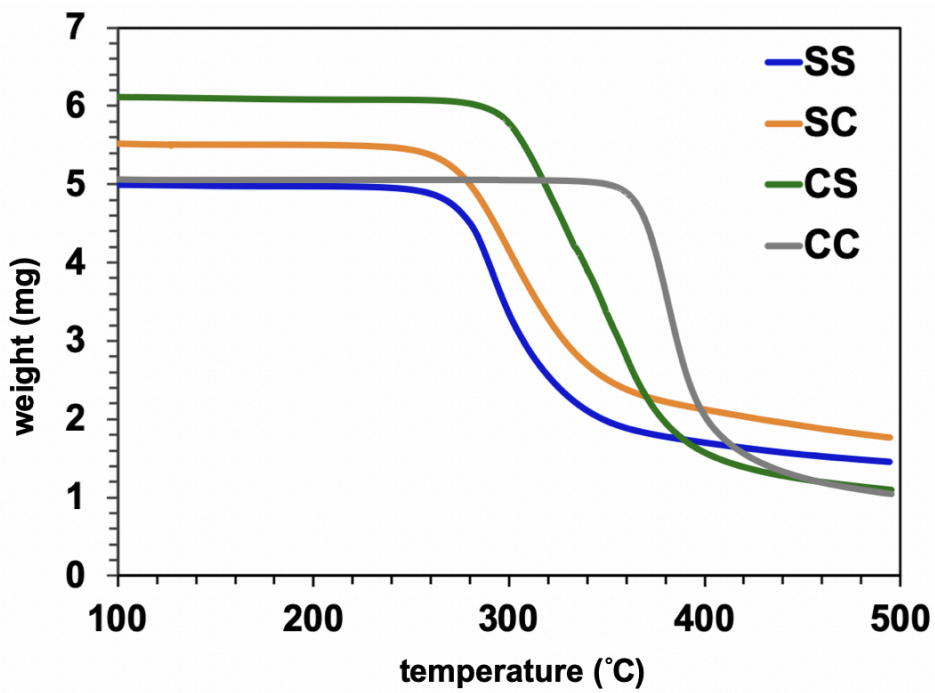


Figure 3.9 TGA profiles for formula SS, SC, CS, and CS synthesized in stoichiometry ratio ($M_{\text{epoxy}} : M_{\text{diamine}} = 2:1$)

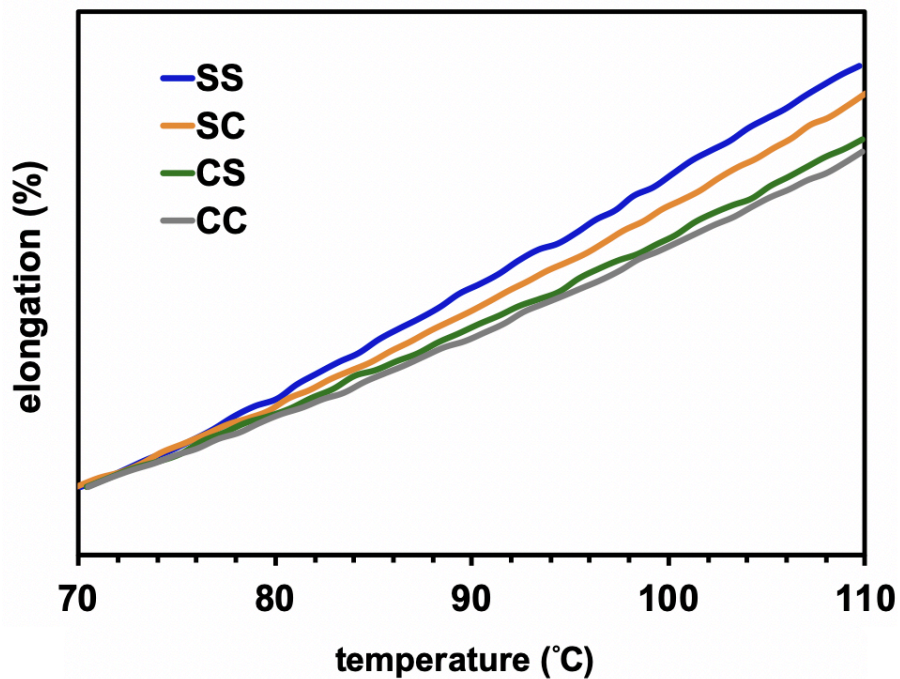


Figure 3.10 TMA profiles for formula SS, SC, CS, and CS synthesized in stoichiometry ratio ($M_{\text{epoxy}} : M_{\text{diamine}} = 2:1$)

3.3.4 Mechanical properties

As the DMA curve shown in figure 3.8, the mechanical strength of all bulk resin used in this work was summarized into table 3.3. The storage modulus assessed by DMA at room temperature (25 °C) were reported in 1.93, 2.02, 1.88, 1.88, and 1.65 GPa for formula SS, SC, CS, CC and CA, respectively. Therefore, incorporation of dynamic disulfide bonds into epoxy networks had no negative impact on mechanical property in glassy state under ambient environment. When the temperature was increased above T_g (the peak of tangent delta), the storage modulus would be reduced significantly by approximately two orders of magnitude because of glass-rubber transition. Also, the storage modulus at rubbery state (defined as the temperature at T_g+30 °C) for each composition was varied from 10-50 MPa due to relatively low thermal stability and flexibility for aromatic disulfide bonding.

Table 3.3 Summarized mechanical properties for all epoxy networks in this work

Networks	storage modulus (E') (at 25 °C) (GPa)	storage modulus (E') (at T_g+30 °C) (MPa)
SS	1.93	15
SC	2.02	30
CS	1.88	20
CC	1.88	50
CA ¹²³	1.5 - 1.8	4 - 5

3.3.5 Heat-induced stress relaxation

Heat-induced ductility was the critical characteristic for dynamic networks; therefore, the time- and temperature-dependent relaxation modulus was evaluated by DMA. The normalized stress relaxation curves testing at different temperatures for composition SS, SC, and CS were as described in figure 3.11. For dynamic networks CA, stress relaxation curve was referred to the reference 123. Based on Maxwell's model for viscoelastic materials, the relaxation time is defined as the time required to release 63% of the initial stress. The acquired relaxation times (τ) was ranged from 10 seconds at 200 °C to 5 minutes at 160 °C for formula SS, 90 seconds at 200 °C to 22 minutes at 160 °C for formula SC, and 3 minutes at 210 °C to 25 minutes at 170 °C for formula CS. Besides, the fully release of stress could be detected in all formula at highest testing temperature. The results indicated the speedy relaxation performance above T_g could be detected in all dynamic networks. Also, the relaxation rate was highly correlated to two factors: the amount of dynamic bonds and the testing temperature. Generally, as given in figure 3.12, when testing temperature was set up at 200 °C for all compositions, the formula SS showed most rapid release rate, while formula CC without any dynamic S-S bond presented no stress relaxation. This trend revealed that the more contents of disulfide bonding led to shorter relaxation time. Otherwise, the higher temperature promoted the speed for cleavage and rearrangement of dynamic bonds, which also contributed to faster release of stress.

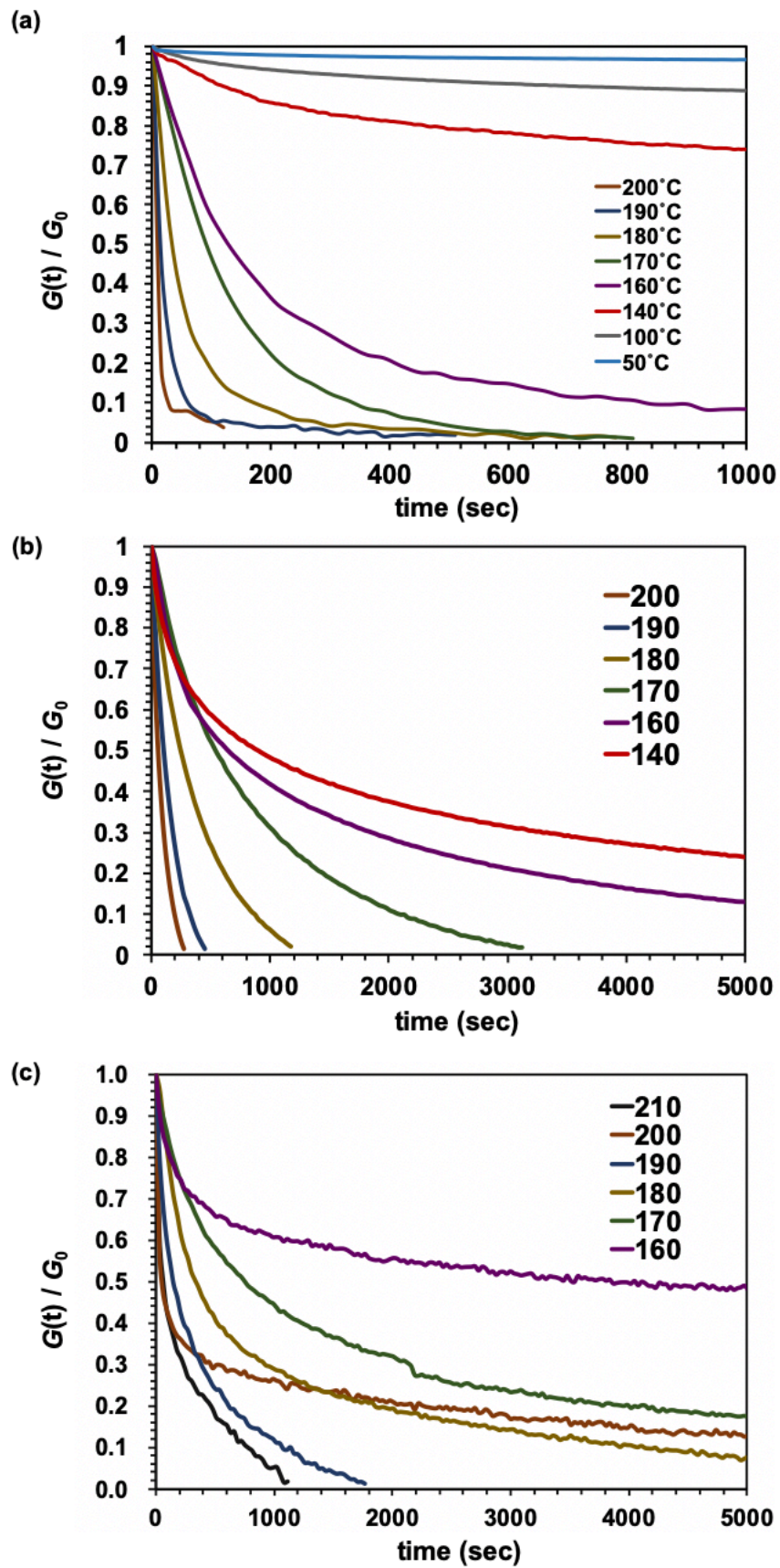


Figure 3.11 Normalized stress relaxation curves of dynamic epoxy networks (a) SS (b) SC (c) CS at different temperatures

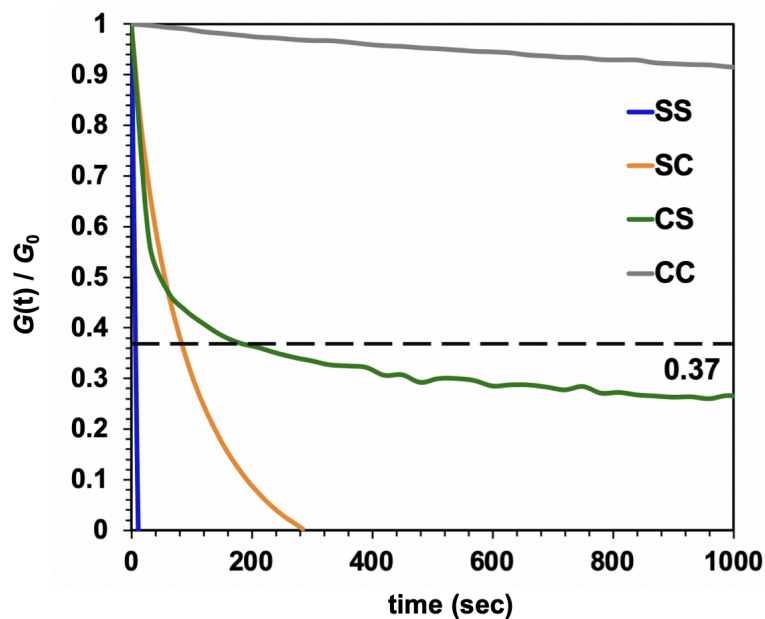


Figure 3.12 Normalized stress relaxation curves of all epoxy networks at 200 °C

The determination of topology freezing transition temperature (T_v) was critical in vitrimer-like system since the T_v -value was considered as the point where the exchange rate was sufficiently fast to bring out the breaking and reorganization of dynamic bonds. Therefore, the assessment of T_v -value can help us to decide the proper service and reprocessing temperature for each dynamic system. This transition temperature was calculated according to the stress relaxation time plotted as a function of temperature in the manner of an Arrhenius plot as revealed in figure 3.13. The T_v -values of formula SS, SC, CS, and CA were -22 °C, 65 °C, 93 °C, and 105 °C, respectively as concluded in table 3.4.* As a result, the data disclosed that more aromatic disulfide bonding caused lower topology freezing transition temperature due to the increased probability of exchange reactions with higher densities of disulfide bonds, which accelerated the bond cleavage and bond recombination. This rapid behavior can also be interpreted by considering activation energy, and the activation energy value for the stress relaxation of each composition could be calculated from the data in figure 3.13 based on the Arrhenius equation. The resulting activation energy values were also summarized in table 3.4, which were 40, 64, 88, 106 kJ/mol, separately. Although the exchange reaction of dynamic bonds would result in relaxation, significant rearrangement of whole polymer network would also be required for stress release; hence, the mobility of polymeric chain was also important for relaxation behavior. The SS specimen was found to have the lowest activation energy among all the compositions. The results for both the T_v -values and activation energies proposed that higher concentrations of aromatic disulfide bonds promoted the release of stress because of the easier reorganization of the polymer network and the increased possibility of exchange occurring.

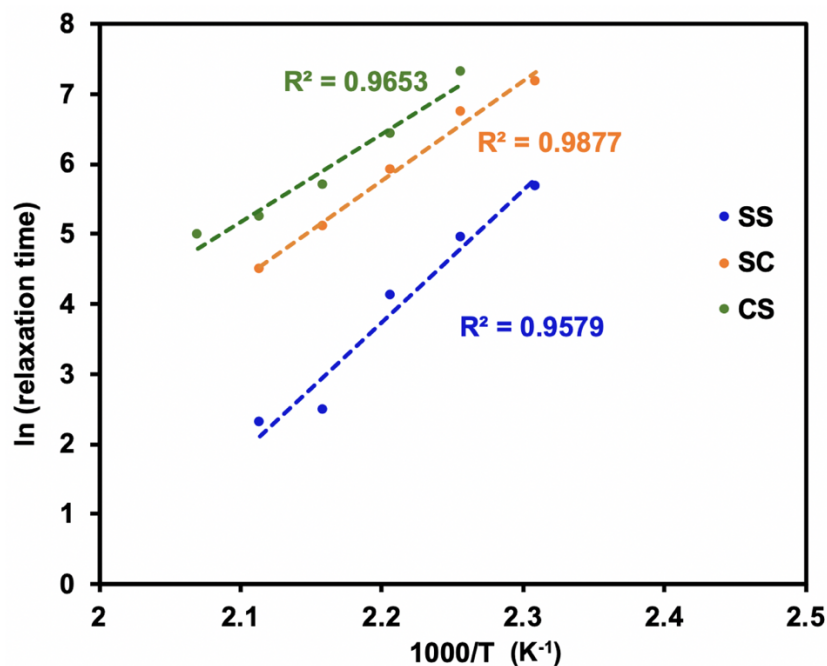


Figure 3.13 Fitting line of the relaxation time to Arrhenius equation for dynamic epoxy networks SS, SC, and CS (R-square = 0.9579, 0.9877, 0.9637)

Table 3.4 Summarized T_v and E_a from stress relaxation for all epoxy networks in this work

Networks	topology freezing transition temperature (stress relaxation) (T_v) (°C)	activation energy (stress relaxation) (E_a) (kJ/mol)
SS	-22	40
SC	65	64
CS	93	88
CC	-	-
CA ¹²³	105	106

3.3.6 Adhesion performance

3.3.6.1 Adhesion strength at ambient temperature

The viscoelastic properties derived from the T_g and T_v of these materials had a significant effect on their performance as adhesives, so that the adhesion property was performed by two sections. First, single lap shear test is the most common characterization to evaluate adhesion ability. In this case, the adhesive joints were prepared by applying thin adhesive resin on the surface of aluminum substrates. The curing condition in the temperature higher than above both T_g and T_v of epoxy resins with dynamic covalent bonds that had already been proven to be almost fully cured. Adhesion strength obtained under this condition was 13.4 ± 1 , 12 ± 0.8 , 18.9 ± 0.8 , 15.7 ± 0.9 , and 9.4 ± 2.4 MPa at room temperature for formula SS, SC, CS, CC and CA, respectively as stated in figure 3.14. Thus, introducing dynamic disulfide bonding into the epoxy-based

adhesive would not significantly affect the adhesive strength, regardless of whether such bonding resulted from the phenolic epoxy or the aromatic diamine hardener. It is worth to note that the failure mode in our case for all epoxy-based adhesives was shown the adhesion failure, which indicated that the mechanical strength of adhesive itself was higher than the bonding strength between metal substrate and polymeric resin. Consequently, the shear strength may be improved if the more suitable surface treatment applied on the aluminum matrixes.

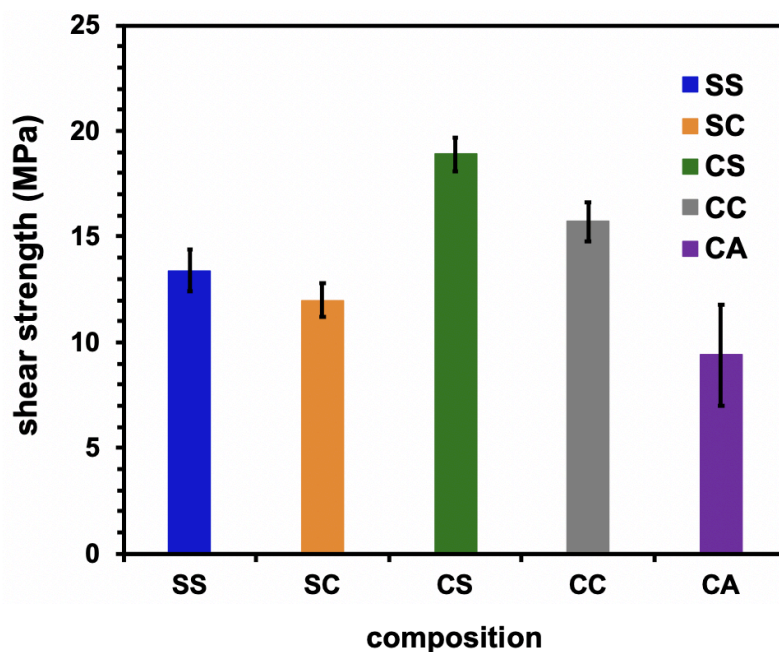


Figure 3.14 Single lap shear strength for initial and rebonded dynamic epoxy adhesive networks at room temperature

3.3.6.2 Adhesion ability at the temperature between T_g and T_v

In order to investigate the adhesion ability for two dynamic covalent systems, aromatic disulfide exchange in formula SS and transesterification in formula CA, at the different temperatures, we separated the testing temperatures into two regions, the temperature between and above T_g and T_v . Through this experiment, we assumed that the relationship between the viscoelastic properties derived from the T_g and T_v of these materials and adhesion performance could be realized.

First, a simple adhesion demonstration at the temperature between T_g and T_v was performed as presented in figure 3.15. Although there were some researches concerning the adhesive characteristics of covalent adaptable networks, the effect of temperature had hardly been discussed, especially in this intermediate region. This temperature range may be important for practical application of adhesive since it was coincided with general service temperate of adhesion joints. In this demonstration, two cured bulk resins of formula SS and CA were hot-pressed at 80 °C to explore the adhesion condition because this temperature

was located at the range between T_g and T_v for these two compositions but in totally opposite way. This bonding temperature was above T_v (-26 °C) and below T_g (134 °C) for formula SS, but above T_g (73 °C) and below T_v (105 °C) for formula CA. There were obvious differences in this intermediate region. The subsequent testing of these specimens indicated that the formula SS showed excellent adhesion property as shown in figure 3.15.(a); whereas, the CA film pieces did not adhere but presented evident deformation from their original shapes during hot-pressing as demonstrated in figure 3.15.(b). When the SS film was heated to 80 °C, the exchange reaction of dynamic bonds was initiated but chain mobility of whole epoxy network could not be triggered efficiently because the material was below its T_g . As a result, the film shape could be maintained so that it exhibited solely good adhesion. In comparison, the transesterification process in this polymer is thought to have been dormant below T_v , while chain motions would have been able to occur at the same temperature. Therefore, only deformation of the film occurred without adhesion between the CA films.

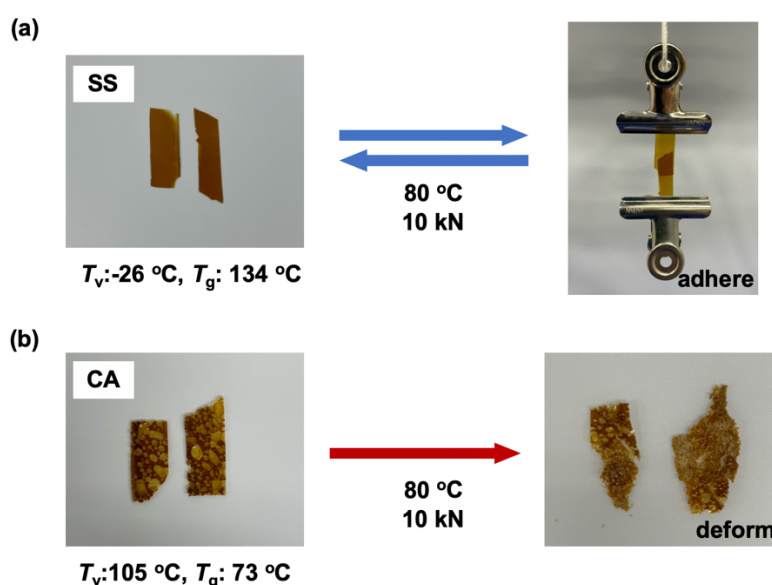


Figure 3.15 Demonstration of exchange and healing behavior at 80 °C for formula (a) SS and (b) CA

3.3.6.3 Reparability at the temperature above T_g and T_v

The other temperature range was the region above T_g and T_v . In this temperature, it was generally accepted that the epoxy resin would exhibit high viscoelastic property, which led to the reparability and reprocessability of networks. The results disclosed that the shear strength with dynamic bonds could be recovered to 83 to 95% of initial adhesion strength, while the specimens without any covalent adaptable bonding (formula CC in this case) did not present any re-adhesion when rebonding was attempted. These results could be explained in terms of both the viscoelastic nature of the dynamic epoxy networks and the exchange reaction associated with the covalent adaptable bonding. In the case that an epoxy adhesive with adaptable bonding was heated above both its T_g and T_v , the state of polymeric material was transferred to viscoelastic liquid. Simultaneously, the bond exchange reaction proceeded among the adaptable bonds at a

fast speed to rearrange the polymer network, resulting in recovery of the shear strength. Evidence for these effects was revealed by the correlation between the rebonding of shear strength and the content of aromatic disulfide bonding, leading to the adhesion strength of the SS sample was 95% of the initial value. This was higher than the recovery percentages exhibited by two other compositions (the formula SC and CS). Moreover, the CC specimen without exchangeable dynamic bonding could not adhere again once it was broken. These results confirmed that high density of dynamic bonds was required for the effective repairing of the polymer network, leading to recovery of the adhesive strength. Same phenomenon could be also observed in formula CA. The CA sample also showed good restoration of shear strength when heated to a viscoelastic state because of the presence of dynamic ester bonds, even so it took a longer time to repair. As a result, there were no significant differences between the rebonding strengths of the epoxies with the aromatic disulfide and ester bonds when the specimens were repaired by heating above both T_g and T_v .

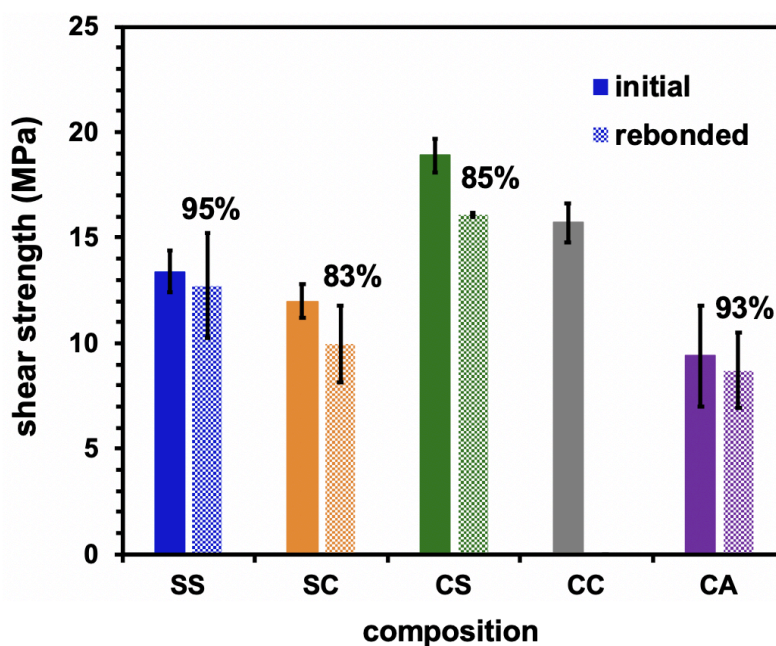


Figure 3.16 Single lap shear strength for initial and rebonded dynamic epoxy adhesive networks at room temperature

3.3.6.4 Strengthening adhesion effect at high temperature

The effect of temperature on the Young's modulus and shear strength values of all epoxy-based adhesive joints in this work was further assessed by performing single lap shear strength tests at temperatures ranging from ambient to 200 °C as described in figure 3.17 and 3.18. As shown in figure 3.17, the Young's modulus values of all compositions were slightly decreased with increasing in temperature below T_g but dramatically declined once it was heating above T_g . This phenomenon was occurred for both the dynamic systems and the conventional thermosetting networks. Consequently, the heat-induced change in the mechanical properties of

the adhesive resins is primarily attributed to the drastic segmental movement in rubbery state and relatively stable chain motion in glassy situation. However, when epoxy resins are applied as adhesives, their adhesive strength in response to temperature change in figure 3.18 showed more complicated behavior that could be classified into two categories. In the case of a standard thermosetting adhesive, the adhesive strength tended to gradually decrease with increase in temperature and then sharply dropped at the T_g of the material, as was also observed for bulk samples as given in figure 3.17. This effect originated from the transition from rigid glassy to flexible rubbery state. Corresponding to these typical thermoset adhesives, the lap shear strength of the CC samples transitioned from moderate value to extremely low bonding strength at the temperature range of 150 to 200 °C, which contained the T_g of the sample CC (178 °C).

Conversely, the epoxy adhesives with aromatic disulfide bonding (that were formula SS, SC and CS) exhibited unusual increases in lap shear strength when heating from room temperature to 100 °C. Particularly, the SS specimen revealed a 30% increase of initial lap shear strength at 100 °C in comparison with testing at room temperature as emphasized in figure 3.18. In general, internal stresses were generated and accumulated in the three-dimensional network structures of adhesive resulting from volume shrinkage during the curing process and the cooling process after curing as shown in figure 3.19. When external shear forces were applied to these polymer networks at room temperature during lap shear test, these materials tended to exhibit brittle fracture because of micro-cracking caused by internal stress and/or decreases in the elongation of the three-dimensional network structure, resulting in the cleavage of chemical bonds and then the fracture of whole adhesive joint system like figure 3.19.(a). Otherwise, since thiol group would barely be reacted with aluminum and/or aluminum oxide surfaces, the exchange reaction of the dynamic disulfide bonds was thought to be the primary approaches of relieving localized internal stress via rearrangement and reorganization of the polymer network as given in figure 3.19.(b).

In order to assess the efficiency of reversible exchange reactions among the aromatic disulfide bonds, diphenyl disulfide and dithiodianiline were dissolved into dimethyl sulfoxide (DMSO) as small molecular-weight model compounds. The temperature-dependent nuclear magnetic resonance (NMR) spectra as displayed in figure 3.20 proved that the exchange reactions of these two compounds occurred even at room temperature.¹⁴⁸ Although it should be noted that the exchange of dynamic disulfide bonds may be more restricted in a fixed polymeric structure at room temperature, we assumed that the dissociation and association of aromatic disulfide bonds could still be proceeded within such rigid networks. Besides, increasing the temperature would be expected to enhance the rate for both the bond breaking and reorganization as well as the probability of exchange and rearrangement. Therefore, epoxy networks containing dynamic sulfur-sulfur bonds would become tougher at higher temperatures because of the rapid exchange and rearrangement above T_v . Simultaneously, if the sample was below its T_g , the mechanical strength of the adhesive resin will be maintained owing to its rigid structure. As a sample was heated to its T_g , the adhesive strength would significantly be reduced and adhesive joints would be tended to break, as was presented in traditional thermosetting polymeric materials. The presented data established that the high concentration of aromatic disulfide bonds demonstrated the adhesion strengthening effect. However, similar trend could not be observed in formula CA. When the CA sample was heated, the bond strength was decreased with elevating the environmental temperature. This effect may be resulted from two reasons: (1) high T_v , the transesterification exchange

reaction could not be easily triggered in the testing temperature, so that the internal stress could not be relieved during testing; (2) relatively low T_g , the high-speed chain motions in the sample was occurred but lack of exchange reaction since the T_v was not reached.

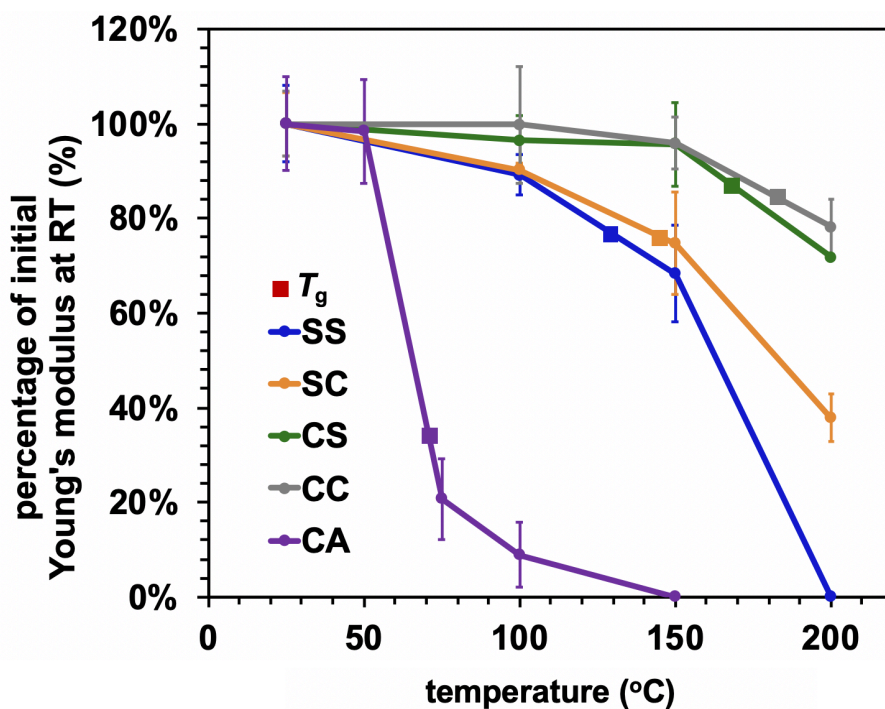


Figure 3.17 Temperature-dependent Young's modulus for all adhesive epoxy networks

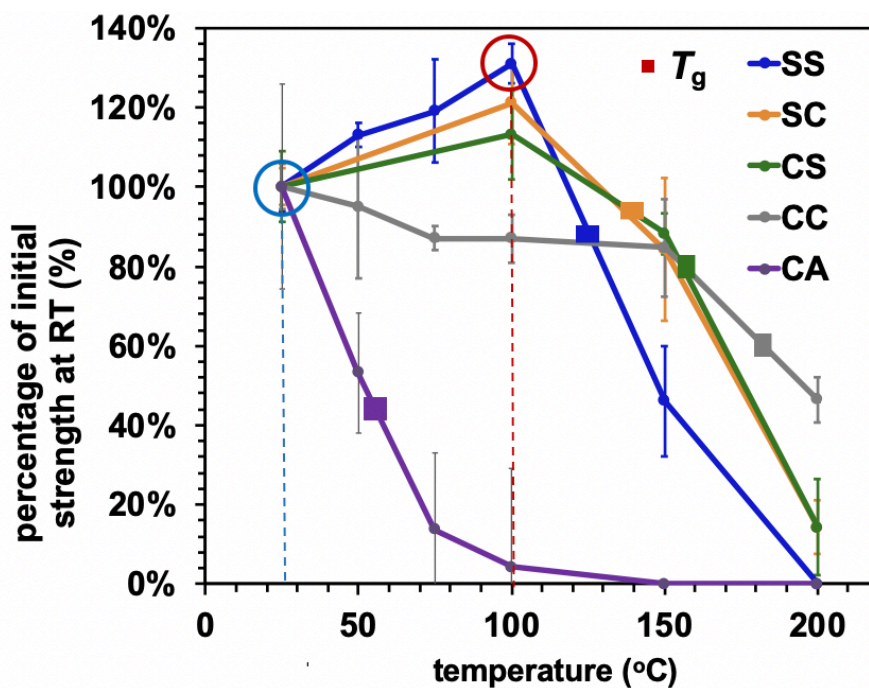


Figure 3.18 Temperature-dependent single lap shear strength for all adhesive epoxy networks

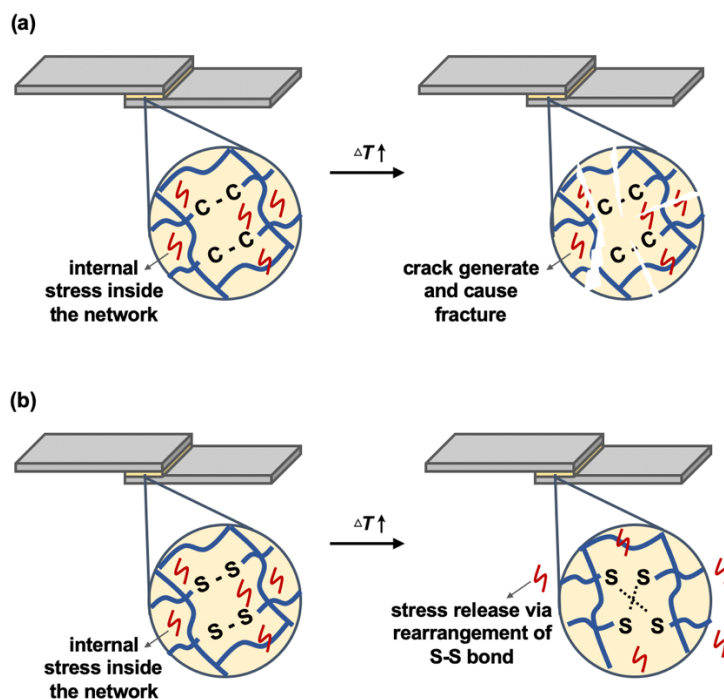


Figure 3.19 Schematic illustration for adhesion strengthening effect for dynamic disulfide bonds at elevated temperature

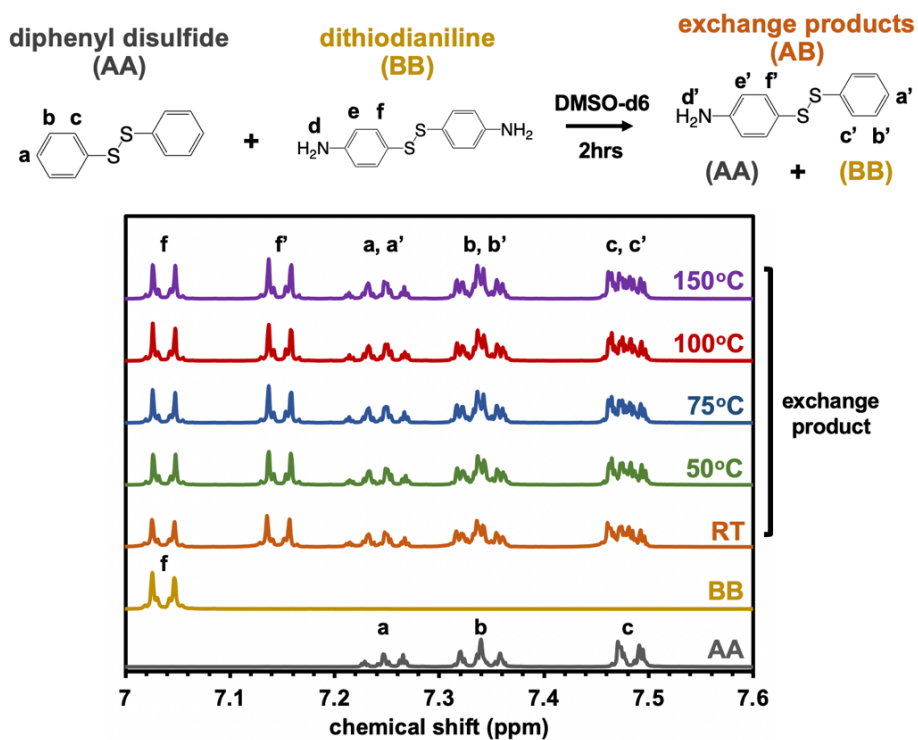


Figure 3.20 NMR spectra for disulfide-exchange model compounds at different temperatures located at the range of 7-7.6 ppm. After the treatment of the mixture at each temperature, all the samples showed the identical spectra which exhibit the composition of the mixture is AA : BB : AB = 1:1:2.

Therefore, we can conclude the T_g and T_v were critical for dynamic covalent systems regarding to mechanical property of bulk samples and adhesion strength of adhesive joints. All covalent adaptable networks could be categorized into two types based on the relationship between T_g and T_v of materials as stated in figure 3.21. Formula CA was classified to first case where the T_v -value was much higher than T_g -value in figure 3.21.(a). The heating of epoxy resin to temperature within the intermediate region II (above T_g but below T_v) was expected that the transition from glassy to rubbery state was occurred so that the chain mobility was highly increased. Therefore, the material transferred from rigid thermoset resin to elastomer, but no exchange reaction could be triggered since the reversibility rate was not sufficient. Once it was further heated to the temperature above T_v (region III), the transesterification reaction started so that the polymeric material changed from elastomer to viscoelastic state, which presented the thermal reprocessing and resetting strategy. In contrast, the SS, SC, CS specimens with aromatic disulfide bonding were specified into second case that possessed T_g -value higher than T_v -value as given in figure 3.21.(b). In this category, the intrinsically fast exchange reaction connected with aromatic disulfide bonding was able to take place in the rigid epoxy network even at the intermediate temperature in region II, where was above T_v but below T_g . Although the disulfide exchange reaction was able to proceed at temperature higher than T_v , a lack of chain mobility below T_g was expected to restrict the segmental motion of whole epoxy network, leading to the rigid and stiff structure. When the temperature was enhanced to T_g (located at region III), these networks also transferred to viscoelastic liquids because both polymeric chain movement and reversible exchange reaction of dynamic aromatic disulfide bonding were occurred.

In fact, both glass transition temperature (T_g) and topology freezing transition temperature (T_v) were associated with changes in viscosity of polymer, but originated from entirely different reasons. The T_g -value reflected the transition from rigid brittle solid to flexible ductile state due to chain movement, which resulted in viscosity change in intramolecular chain motion. In comparison, T_v -value was attributed to the exchange reaction of dynamic bonding, which related to intermolecular bond reaction. This difference led to totally dissimilar behavior in terms of bulk sample and adhesion properties. In bulk sample, the mechanical strength would be decreased with increasing temperature, and significant declined when heating above T_g . However, the adhesion joint was more complicated than bulk samples, considering the factors of volume shrinkage caused from different thermal property among adhesive resin and substrates. In this scenario, bonding strength was greatly decreased above T_g , but adhesion would be strengthened due to the minimized occurrence of fractures as a result of exchange reaction of dynamic bonds above T_v . Among common covalent adaptable networks as given in table 3.5, aromatic disulfide bonding generally exhibited low T_v and activation energy and high T_g ; hence, the rates of dissociation, diffusion, and association of disulfide bonding were increased and the decline of mechanical strength due to glass-rubber transition could be postponed. This characteristic would widen the service temperature range of these materials when it was applied in industry usage. On the other hand, the adhesives with ester bond owned higher T_v -value than T_g -value, so that the glass transition would be triggered before strengthening performance provided by dynamic exchange reaction. ^{13,46,76-78}

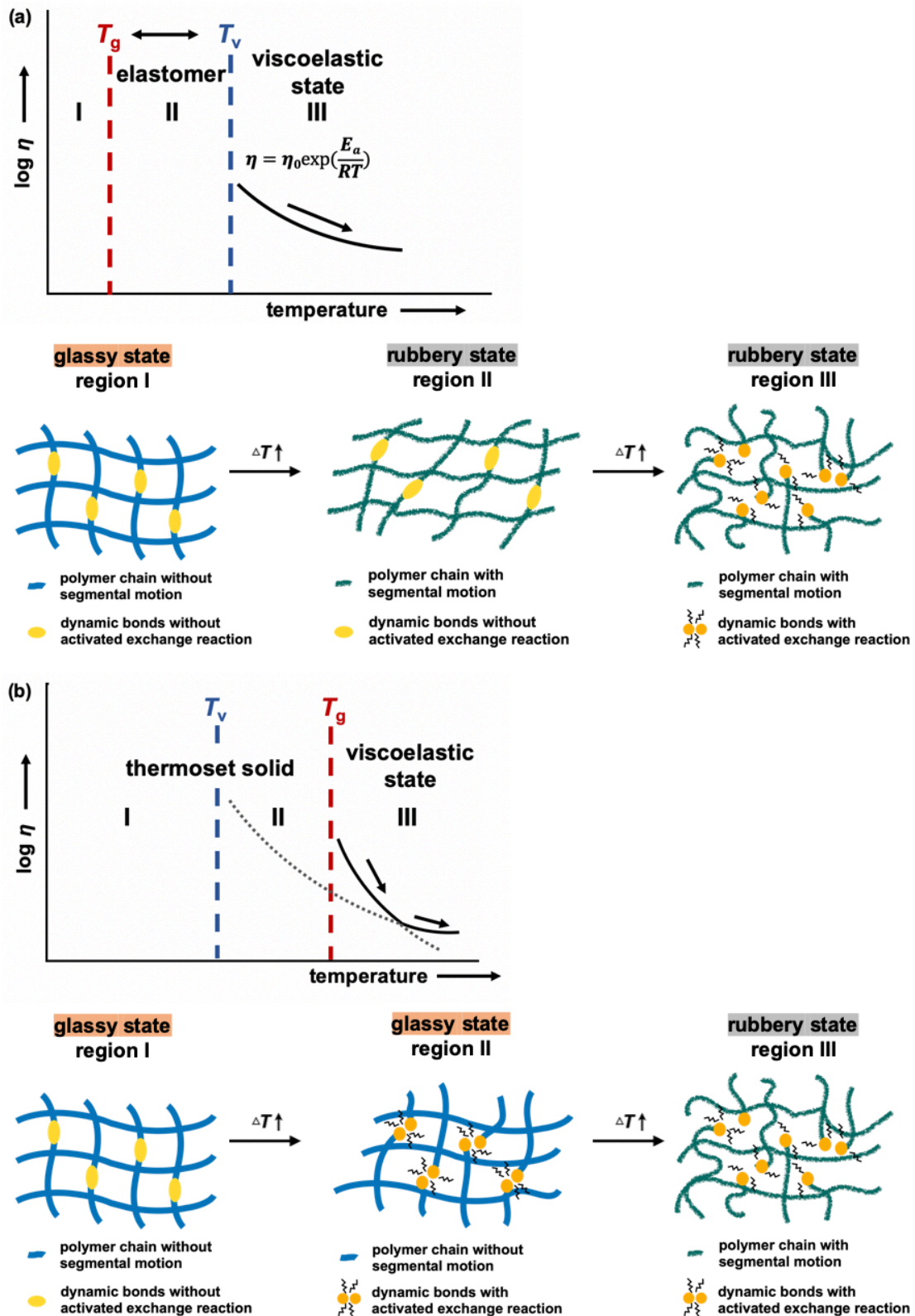


Figure 3.21 Schematic representation of comparison for the effect of glass transition temperature (T_g) and topology freezing transition temperature (T_v) on viscosity, viscoelastic behavior, and network mobility of dynamic systems (a) $T_v > T_g$ (b) $T_g > T_v$

Table 3.5 Summary of T_g , T_v , and activation energy for known dynamic covalent systems

dynamic covalent system	T_g (°C)	T_v (°C)	activation energy (kJ/mol)	ref
aromatic disulfide	127 - 133	-18 - 86	38 - 55	39,44
transesterification	45 - 65	105 - 120	88 - 119	123,149,150
imine exchange	121	36	90	151
siloxane exchange ^a	123 - 125	47-117	81 - 174	152
transamination ^a	-77 - -51	22 - 35	52 - 80	29
transalkylation ^a	-11	98	140	102

^a the system was not incorporated with epoxy network

3.4 Conclusions

This study demonstrated the results for the performance of epoxy polymers incorporating aromatic disulfide bonds and its application as adhesives. In the case of bulk sample, first, due to less thermal stability, more flexibility, and lower bond energy of aromatic disulfide bonding in comparison with carbon-carbon bonds, the thermal properties such as glass transition temperature (T_g), decomposition temperature (T_d), and coefficient of thermal expansion (CTE) were slightly reduced with increasing the amount of S-S bonds. Second, the mechanical strength of bulk samples was not influenced by the content of dynamic bonds at ambient condition. Finally, the results of heat-induced stress relaxation determined that the high density of dynamic bonds presented the more rapid stress release, resulting in lower theoretical topology freezing transition temperature (T_v) and activation energy.

In the adhesion characterization, the introduction of adaptable S-S bonds into epoxy networks still suggested the high shear strength at room temperature, which provided the possibility of practical structural application of dynamic adhesive. Also, the reparability of dynamic thermosetting networks could be obtained by hot-pressing procedure because of the transition to viscoelastic state with sufficiently fast exchange reaction. Most interesting part of this research was that the improved adhesive properties of these materials at elevated temperatures below the glass transition region (compared with other dynamic systems and traditional thermosets) is ascribed to their extremely low T_v and activation energy values contributed by dynamic disulfide bonding. These factors resulted in stronger adhesion because the easier cleavage and rearrangement of aromatic disulfide bonds stimulated the release of internal stress. This study also established that a high concentration of disulfide bonds accelerated the exchange process by increasing the likelihood of bond cleavage and rearrangement, which in turn improved adhesion. It is also worth to notice that this adhesion strengthening effect could be only observed in the dynamic system with low T_v and high T_g because exchange reaction of dynamic bonds could be proceeded under the rigid structure that would not result in decline of adhesion strength.

With regard to industrial applications, epoxy-based adhesive systems with dynamic disulfide bonding represented the more environmentally-friendly and economical option. These resins not only showed good adhesion properties and permit simple rebonding procedures, but also demonstrated the obvious improvement in high-temperature adhesion performance as a result of the incorporation of exchangeable disulfide bonds

that expand their usable temperature range. These factors could permit the development of next-generation adhesives based on dynamic covalent chemistry and broaden the potential range of material design. The knowledge gained from this study should also be applicable to other epoxy adhesive systems, especially because bisphenol A is often used in epoxy adhesives, which should be further investigated in the future.

CHAPTER IV CHROMOPHORIC INDICATOR OF ADHESION STRENGTH

Epoxy-based adhesive has been widely applied in industries because of the trend of light-weight design. In general, it exhibits excellent thermal stability and mechanical strength due to the covalent thermoset network structure, leading to the outstanding adhesion performance. It is well accepted that there are multiple factors that affect adhesion strength; for example, the chemical structure and molecular weight of epoxy resin and hardener, surface morphology of substrate, curing condition, and so on. Particularly, for two-component curing system of epoxy resin, if the ratio of the main agent (in this case, epoxy resin monomer) to the curing agent (in this case, diamine hardener) is not accurate, the adhesive performance could be greatly degraded, resulting in adhesive failure. Therefore, the crosslinking density of adhesive network is considered as a critical factor, which has a significant impact on its adhesion strength. However, it is difficult to evaluate the crosslinking density of epoxy adhesive by its appearance in practical application; otherwise, current evaluation of crosslinking density, such as dynamic mechanical analysis, differential scanning calorimetry (DSC), solid state nuclear magnetic resonance (NMR), and X-ray powder diffraction (XRD) is limited in the laboratory. Consequently, the more efficient indicator in crosslinking density of adhesive network in industrial application is highly desired to rapidly screen the low-crosslinked adhesive network, resulting in decreasing the occurrence of failure of adhesive joint. ^{64,66,71–73,141,153–161}

In order to address this demand, the dynamic disulfide bonding is introduced into epoxy resin network. This combination polymeric material belongs to dynamic covalent networks, also known as vitrimer, which presents the reversible network topology under external stimuli through exchange reaction of dynamic bonds. Dynamic disulfide bond plays an important role not only as dynamic covalent bond to exhibit the vitrimer characteristic, but also in additional mechanochromic functionality for epoxy resin. Previously, the research demonstrated the mechanochromic effect applied in damage detection of disulfide-contained epoxy resin and its composite structure. When the composites with disulfide-contained epoxy resin was crushed by a hammer, the broken area would show green coloration and then returned to yellow after several hours at room temperature or heating to specific temperature. The green coloration was attributed to the generation of sulfur-centered radicals (thiyl radical) by mechanical stress; whereas, the color turned to yellow after certain time due to the reconnection of radicals to bridge the new disulfide bonding. Here, we expected that the highly crosslinked networks with less chain mobility resulted in longer reconnection time of thiyl radicals to reform the disulfide bond. In other words, this time-dependent mechanochromic property offered the approach to evaluate the crosslinking density of epoxy resin, finally leading to the determination of its adhesion strength. ^{47,48}

In this study, we firstly utilized mechanochromism of disulfide bonds to assess both crosslinking density and adhesion strength. We assumed that the duration time of mechanochromic effect would be longer in the disulfide-contained epoxy network with higher crosslinking density and less segmental chain movement (in this case, means higher glass transition temperature (T_g)), finally suggesting the tougher adhesion strength. The disulfide-contained epoxy resin with different ratio of epoxy monomer and diamine hardener was prepared. The duration of mechanochromic behavior, crosslinking density, chain mobility, and adhesion strength of each formula was thoroughly investigated, providing the evidence of correlation among each property; therefore, we could utilize this color change phenomenon as an indicator to assess the crosslinking density and adhesion strength of disulfide-contained epoxy network. Through the results obtained from this work, the

mechanochromic property for dynamic polymer applied in the crosslinking density and adhesion strength evaluation could be further discussed.

4.1 Experimental

4.1.1 Materials

Diglycidyl ether of bisphenol A (DGEBA) (JER 825) with the epoxide equivalent weight of 170-180 g/mol used as epoxy monomer for synthesizing the epoxy resin was purchased from the Mitsubishi Chemical Corporation. As a diamine hardener, 4,4'-dithiodianiline (DTDA) with an amine hydrogen equivalent weight of 62.1 g/mol were purchased from the Tokyo Chemical Industry Co., Ltd.

On the other hand, aluminum alloy (6061-T6) used as substrates in adhesive joint was purchased from Standard-Testpiece Company. Ethanol, hexane, acetone, sodium hydroxide, sodium carbonate and sodium dodecylbenzene sulfonate used in the cleaning of the aluminum substrates were purchased from Wako Chemicals. Glass bead used in controlling the thickness of adhesive was purchased from Monotaro Co., Ltd.

4.1.2 Synthesis and preparation of samples

This section includes two parts, which are procedures used in curing epoxy-based resin and constructing the adhesive joint in this study.

4.1.2.1 Synthesis of disulfide-contained epoxy resin networks (ERD)

Epoxy resin with high content of aromatic disulfide bonding was prepared as shown in figure 4.1. The disulfide system comprised diglycidyl ether of bisphenol A (DGEBA) and 4,4'-dithiodianiline (DTDA) as the epoxy monomer and diamine crosslinker, synthesized by combining the epoxy monomer and the diamine hardener in a 3:1, 2:1, 2:2, and 2:3 molar ratio in a glass vial and mixed at 90 °C for 30 min then rapidly poured into a Teflon mold as figure 4.1 and table 4.1. Sample was cured in an oven at 120 °C for 2 hours, 140 °C for 2 hours, and 160 °C for 2 hours, given the epoxy resins with disulfide bonding referred as ERD-1, ERD-2, ERD-3, and ERD-4.

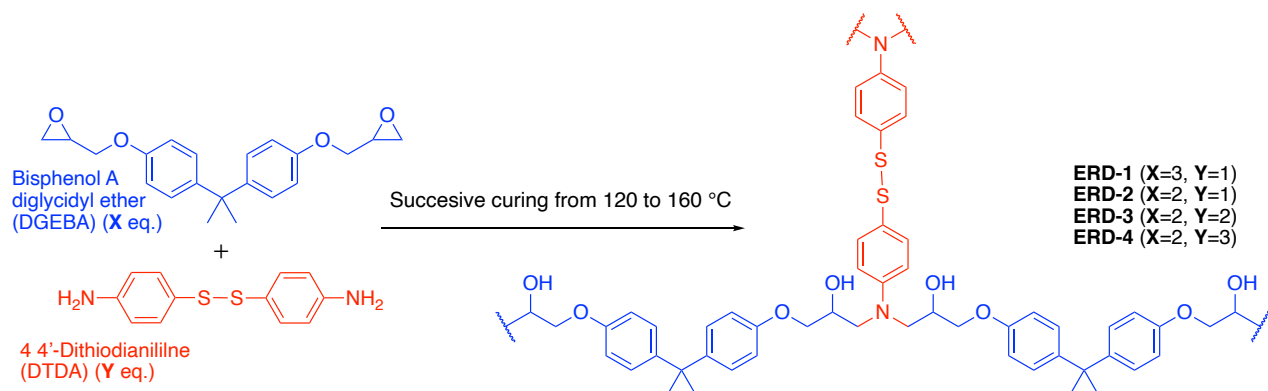


Figure 4.1 Synthesis and chemical structure of all epoxy networks in this work

Table 4.1 Formulation of all epoxy networks

Network	Epoxy resin (DGEBA)		Diamine hardener (DTDA)	
	mol	g	mol	g
ERD-1	3	5	1	1.22
ERD-2	2	5	1	1.83
ERD-3	2	5	2	3.65
ERD-4	2	5	3	5.48

4.1.2.2 Preparation of adhesive joints

Aluminum substrates (AA6061-T6) with dimensions of 100 (length) × 25 (width) × 2 (thickness) mm as shown in figure 3.3.(a) were prepared by mechanical surface polishing with 800 grit sandpaper, followed by ultrasonic cleaning in ethanol, hexane and acetone for 15 minutes in each solvent. Each substrate was subsequently immersed in an alkaline degreasing solution at 70 °C for 10 minutes (according to the ASTM D2651 standard procedure). Finally, substrates were rinsed with water at room temperature for 10 minutes and then dried at 70 °C as necessary to remove the residual water. In each trial, an epoxy monomer and amine hardener were combined in a glass vial and mixed at 90 °C for 30 min, then immediately applied on the overlapped area of treated metal substrates. The adhesive joint was held together using two clips. The overlapped area was fixed at 25 × 12.5 mm and the thickness of the adhesive was controlled within 100-150 micron (µm) by adding 1 wt.% glass beads to the polymer. Finally, the adhesive joints were cured in an oven under the same conditions as applied to the bulk samples. (120 °C for 2 hours, 140 °C for 2 hours, and 160 °C for 2 hours)

4.2 Characterization

Fourier transform near infrared (FT-nIR) spectra of the samples were performed in a JASCO FTIR 6100 instrument at the wavelength of 4000 - 7500 cm⁻¹. The disulfide-contained epoxy resin was detected directly. A spectrum of air was used as background.

Electron spin resonance (ESR) was obtained by JEC-FA100 spectrometer from Joel with temperature controller and data-collection system. 200 milligrams of solid samples were ground into powder by ball-milling for 60 minutes and placed into quartz testing tubes immediately. All spectra were recorded at 9.1 - 9.2 GHz of frequency and 1 mW microwave power. The g-value was calculated based on the equation: $h \nu = g \beta B$, where h is Planck's constant, ν is frequency, β is Bohr magneton, and B is magnetic field. The g-value of sulfur-centered radicals (thiyl radicals) is 2.04.

Swelling test was obtained by immersing pristine and recycled epoxy resin into toluene in light shielding bottle at room temperature for 72 hours. The weight before and after immersion were recorded. Finally, the swelling ratio was calculated according to the Equation 4.1

$$Q = (M_1 - M_2) / M_1 \quad (\text{Equation 4.1})$$

Q was swelling ration, M_1 and M_2 were the weight of epoxy resin before and after 72-hour immersion, respectively. All data presented in this experiment was the mean values of five measurements. Besides, the theoretical crosslinking density was calculated based on Flory-Rehner equation.

The glass transition temperature (T_g) was determined through differential scanning calorimetry (DSC) performing the equipment from Shimadzu DSC-60 plus with temperature controller under nitrogen flow. Temperature range was set up from 0 °C to 200 °C with heating and cooling rate 10 °C/min. Air was used as reference. T_g -value was obtained from second heating cycle.

The adhesion strength was evaluated through single lap shear tests using a Shimadzu autograph AG-X plus instrument with a crosshead speed of 1.0 mm/min. The reported values represent the averages of three samples along with the standard error.

4.3 Results and discussion

4.3.1 Mechanochromic effect

The cured bulk epoxy resin was polished by sandpaper to observe the mechanochromic effect of each formula, so that the change of color for ground epoxy powder remained on the surface of sandpaper could be easily observed. The time of mechanochromic behavior lasting was recorded by visual check and summarized in figure 4.2. After polishing the surface of brown bulk epoxy resin by sandpaper, the initial color of powder in the sandpaper was appeared as green. This change was due to the formation of thiyl radicals, originated from the mechanical scission of disulfide bonding. This was supported by electron spin resonance (ESR) (figure 4.3). As given in figure 4.3, the ESR spectrum of composition ERD-2 showed the detection of sulfur-centered radical (thiyl radical), indicated by the peak where g -value=2.04. After placing the sample at room temperature for specific time, the thiyl radicals would link to each other again, so that the green coloration disappeared and returned to yellow. The reconnection rate of such radicals would be variant depending on the crosslinking density and chain motion of whole polymer networks. In our case, the time from appearance of green coloration to turning back to yellow for ERD-1, ERD-2, and ERD-3 was 30 mins, 60 mins, and 5 mins, respectively; whereas, the color change almost could not be detected in ERD-4. Therefore, we suggested that the sample with longest duration of mechanochromic effect (in this case, ERD-2) possessed highest crosslinking density and lowest segmental mobility; on the other hand, the ERD-4 specimen would be expected to be the network with lowest crosslinking sites and highest chain motion.

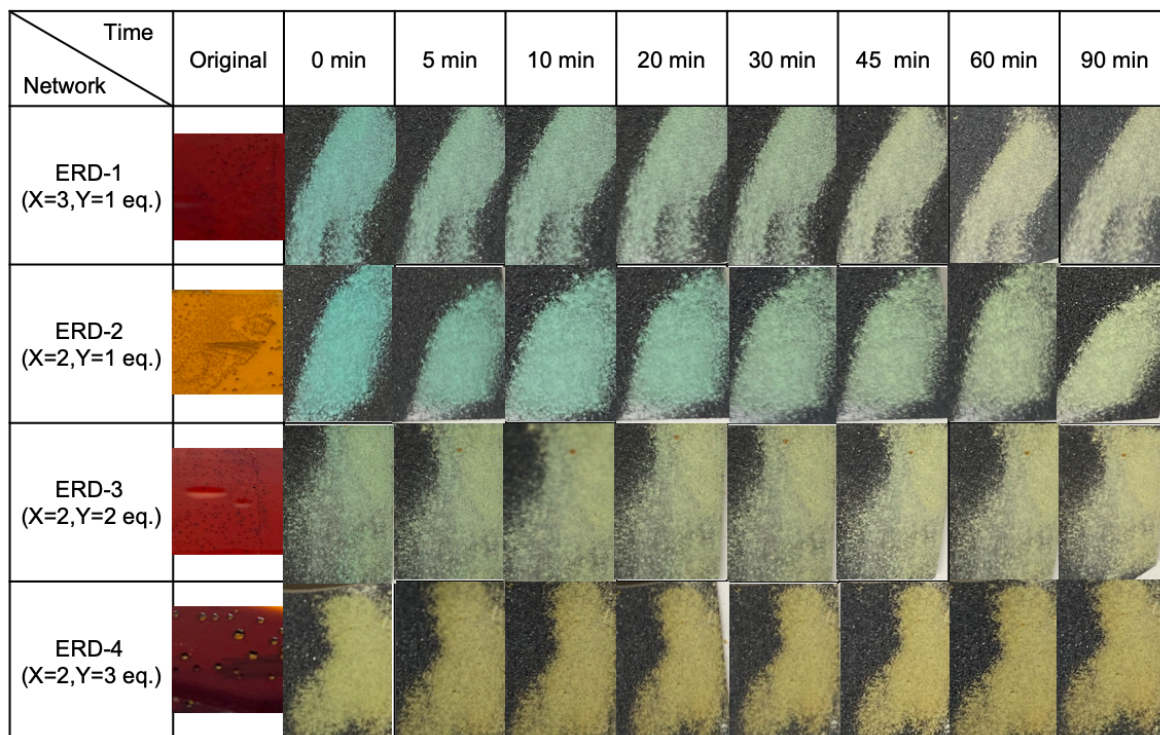


Figure 4.2 Time-dependent photographic sequence showing the mechanochromic performance for all epoxy networks in this work.

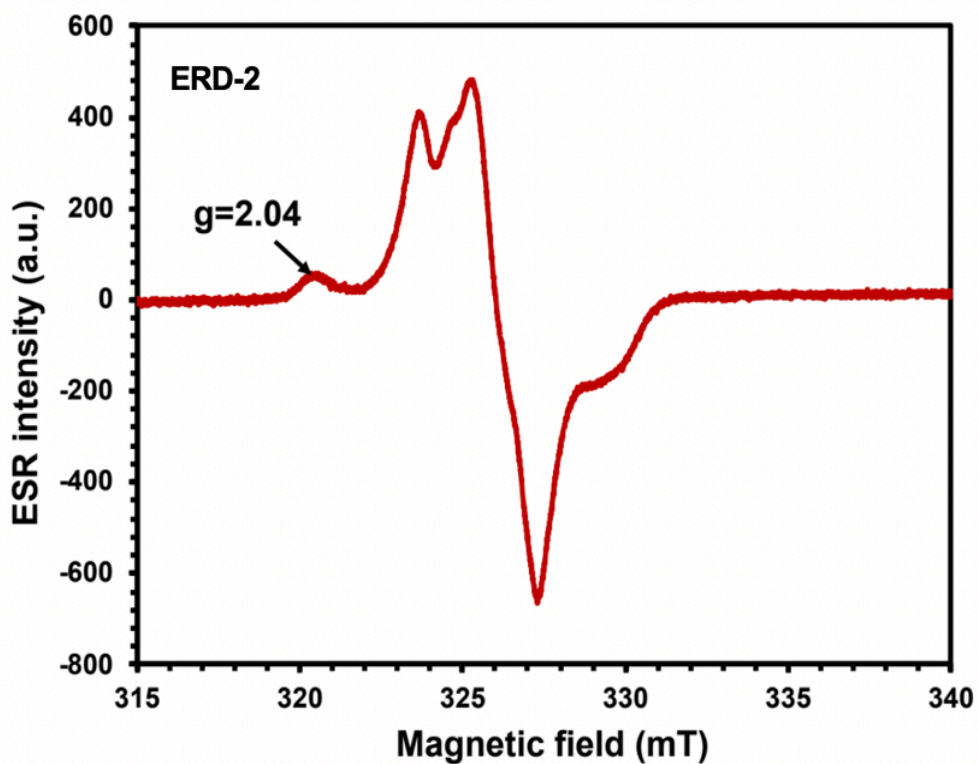


Figure 4.3 Electron spin resonance (ESR) spectrum for ERD-2. The sample was examined immediately after ball-milling into powder. The g-value of thiyl radical ($-S\cdot$) is 2.04.

4.3.2 Crosslinking density

In order to confirm this postulation, firstly, Fourier transform near-infrared spectroscopy (FT-nIR) was performed of all epoxy adhesives in this work. Figure 4.4 showed that the spectra of all compound were almost identical in the nIR region from 4000 cm^{-1} to 7500 cm^{-1} . The difference was that the combination band of N-H stretching and bending (ca. 5000-5100 cm^{-1}) for primary amine and the band of N-H stretching (ca. 6600-6800 cm^{-1}) for primary and secondary amine were only observable in formula ERD-3 and ERD-4, indicating the excess of unreacted diamine hardener. Also, the combination band of the second overtone of the epoxy ring stretching with the fundamental C-H stretching (ca. 4530 cm^{-1}) was detected in ERD-3 and ERD-4, suggesting the incomplete oxirane ring opening reaction. Therefore, since there were unreacted epoxide and amine group remained in the network structure of ERD-3 and ERD-4, we expected that the crosslinking density of ERD-3 and ERD-4 would be much lower compared to ERD-1 and ERD-2.¹⁴⁵

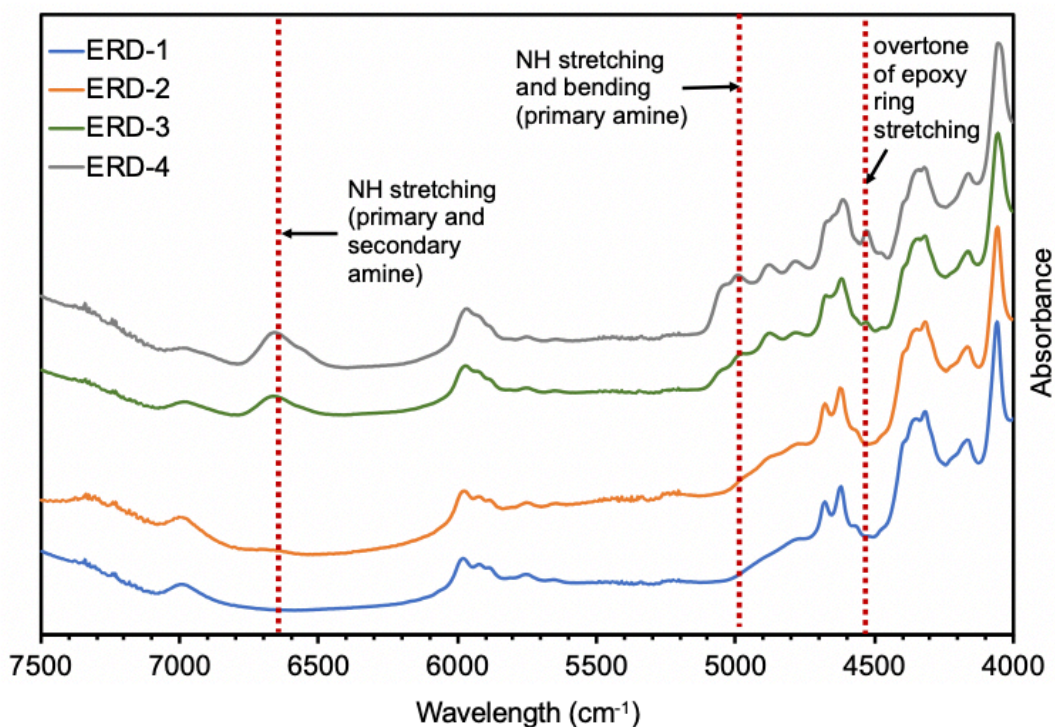


Figure 4.4 FT-nIR spectra for all epoxy networks at the wavelength from 4000 to 7500 cm^{-1}

To further assess the degree of crosslinking, swelling test was performed. All samples of epoxy adhesive were immersed into toluene for 72 hours at room temperature in the shielding of light. The swelling ratio after 72-hour immersion for ERD-1, ERD-2, ERD-3 and ERD-4 were 3.7%, 2.2%, 4.9%, and 6%, respectively, which calculated based on the absorbed amount of toluene (figure 4.5). The lower swelling ratio represented less toluene was penetrated into the swollen cross-linked epoxy network, indicating the higher crosslinking density of epoxy adhesive structure.

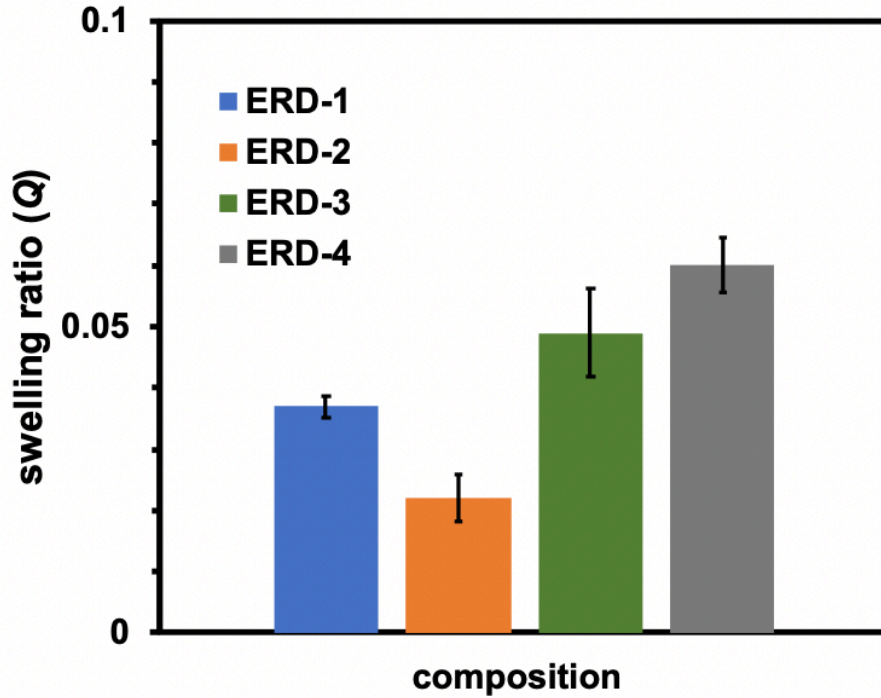


Figure 4.5 Swelling ratio (Q) for all epoxy networks in toluene at room temperature for 72 hours in swelling test

Therefore, we could calculate the theoretical crosslinking density of each formula based on Flory-Rehner equation as Equation 4.2.

$$\text{crosslinking density} = \ln[(1 - V_r) + V_r + \chi V_r^2] / 2 V_s (V_r / 2 - V_r^{1/3}) \quad (\text{Equation 4.2})$$

where V_r is the volume fraction of polymer in the swollen state at equilibrium, χ is the polymer-solvent interaction parameter, and V_s is the molar volume of solvent. V_r is calculated based on Equation 4.3.

$$V_r = M_1 \rho_s / [M_1 (\rho_s - \rho_r) + M_2 \rho_r] \quad (\text{Equation 4.3})$$

where M_1 is the weight of polymer before swelling, M_2 is the weight of polymer after swelling, ρ_s is the density of toluene (865 kg/m^3), ρ_r is the density of polymer (1200 kg/m^3). χ is calculated based on Equation 4.4.

$$\chi = \beta_1 + (V_s / RT) (\delta_s - \delta_p)^2 \quad (\text{Equation 4.4})$$

where β_1 is the lattice constant, usually about 0.34, R is the universal gas constant, T is the absolute temperature, δ_s and δ_p is solubility parameter for toluene ($8.9 \text{ cal}^{1/2}\text{cc}^{-3/2}$) and polymer ($13.0 \text{ cal}^{1/2}\text{cc}^{-3/2}$), respectively. V_s is calculated based on Equation 4.5.

$$V_s = M / \rho_s, \text{ (Equation 4.5)}$$

where M is the molecular weight of toluene (92.14 g/mol). As a result, the theoretical crosslinking density for ERD-1, ERD-2, ERD-3, and ERD-4 was 2478.9, 2582.5, 2400.6, and 2332.2 mol/m³, separately. These calculated results revealed that the rank of crosslinking density for all samples in this experiment from highest to lowest is ERD-2, ERD-1, ERD-3, and ERD-4.^{156,162,163}

4.3.3 Chain mobility

Generally, the segmental motion of high-crosslinking network would be relatively fixed and slow, leading to the less chain mobility and higher glass transition temperature (T_g). Differential scanning calorimetry (DSC) was the common experiment to determine the T_g -value. As seen in figure 4.6, the shift of the baseline occurred in DSC profile of ERD-1, ERD-2, ERD-3, and ERD-4 was located at 145 °C, 162 °C, 89 °C, and 51 °C, respectively, indicating the glass transition temperature of each formula. Consequently, the specimen ERD-2 with highest crosslinking density possessed highest T_g -value as assumption; whereas, T_g -value of ERD-4 was lowest, corresponding to its decreased crosslinking density. Based on this data, we confirmed that the network structure with higher crosslinking density exhibited less segmental movement of polymer chain, causing the higher T_g -value.

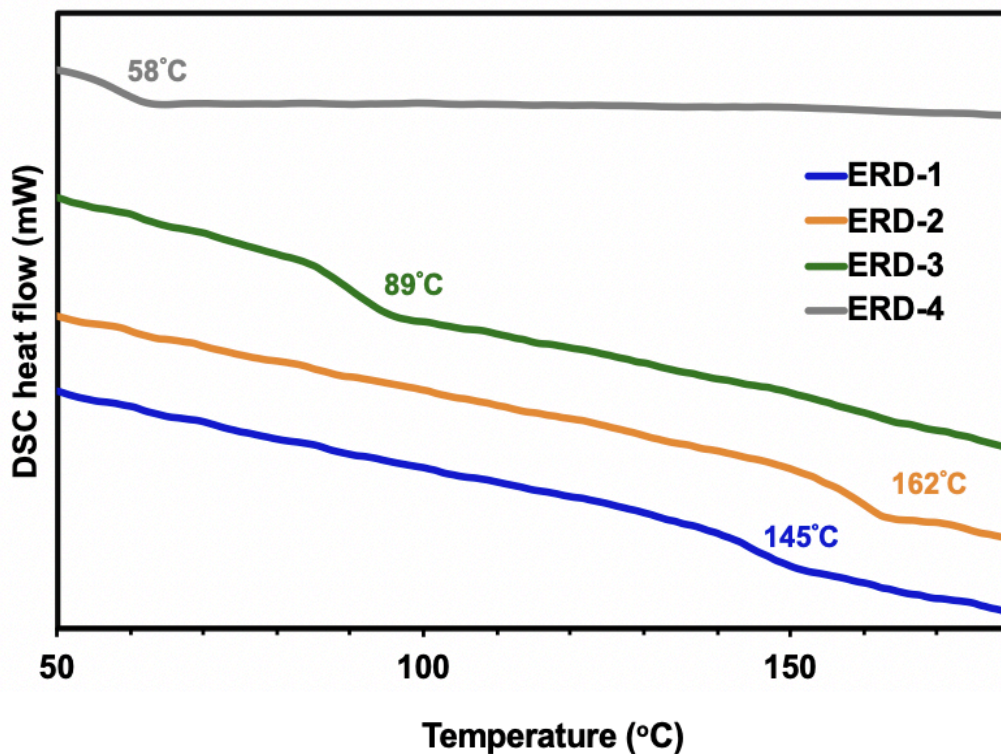


Figure 4.6 Differential scanning calorimetry (DSC) profiles and glass transition temperature (T_g) for all epoxy networks

4.3.4 Adhesion strength

Adhesion strength was determined by several factors during the manufacturing procedure of adhesive joint. Normally, the compact network structure and strong adhesion performance could be obtained in the adhesive network with increased crosslinking density and decreased segmental motion. Therefore, after confirming the crosslinking density and chain mobility through swelling test and DSC, the adhesion strength evaluation was determined by single lap shear test. According to the obtained data in figure 4.7, ERD-2 exhibited the most elevated adhesion strength (18.9 MPa); in comparison, ERD-4 showed poor adhesion performance (1.7 MPa). Besides, the adhesion strength would be declined with decreasing crosslinking density and T_g -value. This result indicated that the highest adhesion strength of disulfide-contained adhesive could be enhanced by increasing the crosslinking density and lowering the chain mobility, which was adjusted by the ratio between epoxy resin monomer and diamine crosslinker.

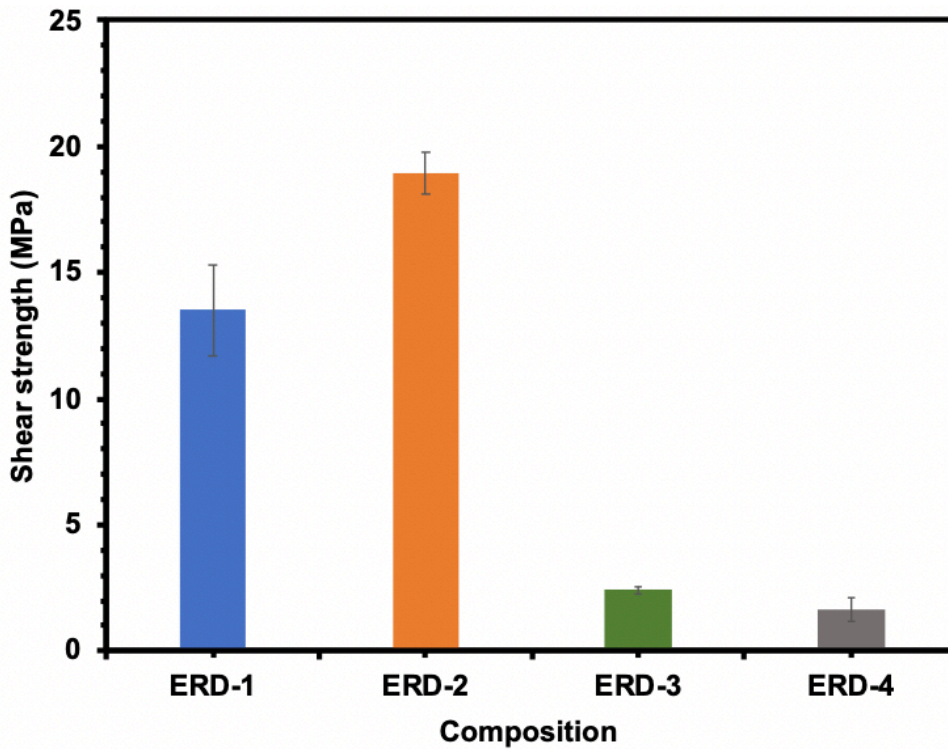


Figure 4.7 Adhesion strength based on single lap shear test for all epoxy networks

4.3.5 Correlation among each parameter

Based on these results, we plot the relation diagram among duration time of mechanochromic effect, crosslinking density, chain mobility, and adhesion strength as demonstrated in figure 4.8. The statistic R-square value for each figure was calculated to identify the relevance of each property. Generally, when the R-square value is over 0.9, the linear relationship between two variables was expected. First, the duration of mechanochromic behavior was defined as the lasting time of green coloration remained on the sandpaper by

visual check, which was directly related to the crosslinking density, since the connection time for thiyl radicals to disulfide bonds was longer in the case of high crosslinked network structure (figure 4.8.(a), R-square=0.9626). Then, the crosslinking density of the epoxy network, had an impact on both chain mobility and adhesion strength (figure 4.8.(b) and 4.8.(c), R-square=0.9293 and 0.9259, respectively). In general, the high crosslinked network with denser crosslinking networks had high T_g -value and adhesion shear strength since it was more difficult to proceed the segmental movement in response to heat and external stress. As a result, the lasting time of mechanochromic effect would be directly associated with adhesion strength (figure 4.8.(d), R-square=0.9592), which meant that adhesion strength could be speculated based on the time that the color of powder changed from green to yellow; namely, the duration of mechanochromic behavior sustained was the indicator to confirm both the crosslinking density, chain motion, and adhesion strength of disulfide-contained adhesive networks.

In summary, the duration of mechanochromism was highly related to the crosslinking density of polymer network. The longer lasting time of mechanochromic effect led to the dense crosslinking polymeric structure. Moreover, the crosslinking density played an important role on chain mobility and adhesion strength of epoxy network; therefore, through observing the duration of color change phenomenon, we could determine the adhesion strength and use this behavior as an indicator for pre-screening the low crosslinking networks, which prevented the failure of adhesive joint.

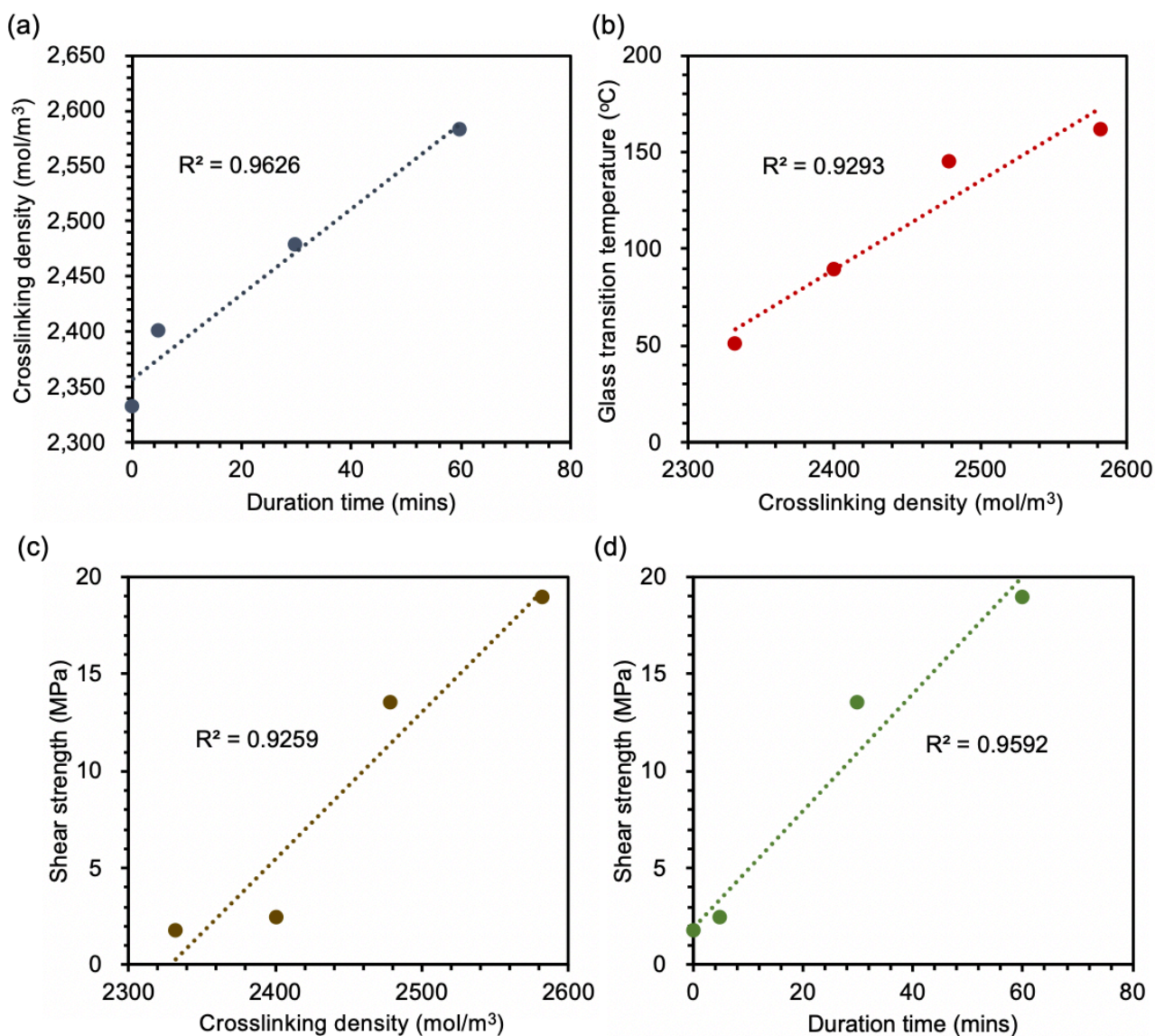


Figure 4.8 Correlation diagrams between (a) duration time of mechanochromic effect and crosslinking density (R-square=0.9626) (b) crosslinking density and glass transition temperature (T_g) (R-square=0.9293) (c) crosslinking density and shear strength of adhesive joint (R-square=0.9259) (d) duration time of mechanochromic effect and shear strength of adhesive joint (R-square=0.9592)

4.4 Conclusions

In conclusion, we provided the new determination method of crosslinking density and adhesion strength based on the mechanochromism of disulfide-contained epoxy resin. The green coloration appeared after applying the mechanical stress was attributed to the cleavage of disulfide bonding, followed by formation of thiyl radicals. After several hours, the color would be changed back to yellow because of the recombination of thiyl radicals. Consequently, longer reconnection time was required in the polymer networks with higher crosslinking density and lower chain mobility, that would exhibit longer duration of mechanochromic effect. Furthermore, this time-dependent color change behavior could be utilized in evaluation of adhesion strength because the crosslinking density and chain movement were critical determining factors for adhesion

performance. Based on the results presented in this work, we proved that the lasting time of mechanochromism was affected by the crosslinking density and segmental motion indeed; as a result, since crosslinking density has a direct influence on adhesion strength, the property of color change could also be utilized as an indicator to determine the adhesion performance. It is foreseen that such application in terms of crosslinking density and adhesion strength evaluation could help us to develop the more effective acceptance and error-proofing method of epoxy adhesive in practical industrial usage, providing the efficient approach to reduce the failure of adhesive joint.

CHAPTER V DECOMPOSITION AND RECYCLING

Epoxy resin is one of the most common polymeric materials, which has been used in wide ranges of applications, such as coating, paint, primer, adhesive, and composites. In general, epoxy resin exhibits excellent thermal, mechanical, and chemical stability due to its covalent crosslinked polymeric network. However, such the network structure results in thermosetting nature, leading to less recyclability and reworkability. Therefore, the epoxy resin and its composites are usually disposed by landfilling and incineration, which cause significant negative impacts on whole ecosystems. In particular, the epoxy resins used in our daily life is considered to be one of the sources of microplastics. Thus, developing the recyclable and reworkable thermoset epoxy resin to reduce the waste accumulation is highly needed.⁸⁰⁻⁸³

In order to solve this problem, dynamic covalent chemistry (DCC) was introduced into thermosetting epoxy network to satisfy this demand. Through the reversible and exchangeable bonds inside the networks, cleaving and rearrangement of the dynamic bonds via exchange reaction can be obtained under external stimuli. This dynamic property presents the new approach to decompose and recycle the crosslinked structure. Among all candidates, the system with exchangeable disulfide bonding has been applied in the rearrangeable, resettable, and removable thermosetting networks because of its excellent vitrimer characteristic. Therefore, the disulfide-contained epoxy resin would be the potential candidate to address this demand. Dynamic disulfide bonding played an important role not only as dynamic covalent bond, but also in decomposition and recycling due to the thiol-disulfide exchange reaction. Previously, some papers reported that the epoxy resin with disulfide bond could be easily degraded into thiol-contained compound, such as 2-mercaptoethanol (2-ME) with dimethylformamide (DMF) solution. In this case, the thiol bond in 2-ME would be reacted with the disulfide bond in epoxy network, leading to the decomposition of epoxy resin. However, the reworkability and recyclability of this strategy have never been demonstrated. Besides, 2-ME is considered as toxic chemical, which cause environmental contamination so that it may not be suitable for practical application in the viewpoint of green chemistry. Therefore, the eco-friendly alternative was necessary to reduce the environmental impact and accelerate the reuse of thermosetting epoxy resins.^{39,44,45}

Hence, we proposed an environmentally friendly reworking and recycling system of disulfide-contained epoxy resin, inspired by the drug metabolism in living organisms. In this work, we focused on glutathione (γ -glutamyl-cysteinyl-glycine), cysteine-containing tripeptide as a waterborne thiol-containing reductant. Glutathione is renowned as a natural antioxidant in organism, that has an antioxidant effect by reducing reactive oxygen species and peroxides using its own thiol group, and a detoxification effect by S-S bonding (glutathione conjugation) to the thiol group of cysteine residues of various poisons and drugs. We expected that glutathione enables us to mediate cleavages of the disulfide bonding in epoxy resin by thiol-disulfide exchange reaction. Consequently, disulfide-contained epoxy resin would be decomposed under the mediation of glutathione at room temperature in the advanced water/organic solvent binary system. The resulting liquid epoxy residue after decomposition was curable upon heating at 180 °C for 6 hours by oxidation of thiol bonding back to disulfide bonding. The obtained recycled solid bulk resin exhibited 90% of storage modulus compared to the virgin epoxy resin, and the value was almost identical even after several recycling cycles. Finally, we demonstrated the carbon fiber reinforced composites structure (CFRP) fabricated with disulfide-contained epoxy resin. The CFRP could be decomposed using glutathione aqueous solution, and then the carbon fibers

were successfully recovered without attachment of epoxy resin. It was further demonstrated that the decomposed liquid epoxy residue could be cured to form CFRP again or use in other application. We believed that this exploration will supply pioneering way for reusing and recycling the disulfide-contained epoxy networks and broadening relevant utilizations in the future.^{122,131,164–166}

5.1 Experimental

5.1.1 Materials

Diglycidyl ether of bisphenol A (DGEBA) (JER 825) with the epoxide equivalent weight of 170-180 g/mol was purchased from the Mitsubishi Chemical Corporation. As a diamine hardener, 4',4'-diaminodiphenylmethane (DDM) with an amine hydrogen equivalent weight of 49.6 g/mol and dithiodianiline (DTDA) with an amine hydrogen equivalent weight of 62.1 g/mol were purchased from the Tokyo Chemical Industry Co., Ltd.

Also, in order to synthesize the epoxy monomer with aromatic disulfide bonding (in this case, bis(4-glycidyoxyphenyl) disulfide (BGPDS)), bis(4-hydroxyphenyl) disulfide, epibromohydrin were purchased from the Tokyo Chemical Industry Co., Ltd. and anhydrous dimethylformamide (dehydrated DMF), hexane, chloroform, methanol, anhydrous potassium carbonate, anhydrous magnesium sulfate, and sodium chloride were purchased from Wako. Chemicals. On the other hand, glutathione (GSH) in the reduced form and tributylphosphine (TBP) were purchased from the Tokyo Chemical Industry Co., Ltd. to establish the dual-phase degradation and recycling system

5.1.2 Synthesis and preparation of samples

This section includes four parts, which are procedures used in establishing the small molecular model compound, synthesizing disulfide-contained epoxy monomers, curing epoxy-based resin, constructing the dual-phase degradation and recycling system in this study, and preparing the carbon fiber reinforced composites.

5.1.2.1 Small molecular model reaction

Solutions of glutathione in D₂O and 4,4'-dithiodianiline in CDCl₃ (0.25 M each), prepared separately, were mixed in 1:1 (v/v) ratio in an NMR tube covered with aluminum foil to shed the light. Besides, After the treatment of the sample at room temperature for 15 minutes, 30 minutes, 1 hour, 2 hours, and 4 hours, the composition of the two layers was monitored respectively by ¹H NMR.

5.1.2.2 Synthesis of disulfide-contained epoxy monomer

The mixture of bis(4-hydroxyphenyl) disulfide (10 g, 40.0 mmol), anhydrous potassium carbonate (55.28 g, 400 mmol), epibromohydrin (54.79 g, 400 mmol), and dehydrated dimethylformamide (200 mL) was heated at 60 °C and stirred overnight under nitrogen or argon atmosphere. The completion of the reaction was confirmed by thin layer chromatography (TLC), and solid substrates were removed from the reaction mixture by a suction filtration. Then, 250 mL of water was added into the reaction mixture, and the mixture was extracted by chloroform/hexane solution (2/3 v/v) for three times. The combined organic phase was washed

by water for three times and brine. The organic phase was dried by anhydrous magnesium sulfate and concentrated by rotary evaporation. The residue was re-crystallized from methanol to afford the product as a white solid (10.8 g, 29.8 mmol, 75 %). ¹H NMR (CDCl₃, 400 MHz): 7.40-7.36 (d, 4H, Ar-H), 6.87-6.84 (d, 4H, Ar-H), 4.25-4.20 (dd, 4H, OCH₂CH(O)CH₂), 3.96-3.90 (dd, 4H, OCH₂CH(O)CH₂), 3.37-3.32 (m, 2H, OCH₂CH(O)CH₂), 2.92-2.89 (dd, 4H, OCH₂CH(O)CH₂), 2.76-2.74 (dd, 4H, OCH₂CH(O)CH₂) as described previously in figure 3.1. ⁴¹

5.1.2.3 Synthesis of disulfide-contained epoxy resin networks (ERD)

Disulfide-contained epoxy resin networks (ERD) was prepared with bis(4-glycidyoxyphenyl) disulfide (BGPDS, A1) and 4,4'-dithiodianiline (DTDA, B1) as an epoxy monomer and diamine hardener, respectively. In order to clarify the effect of the amount of disulfide bonding on thiol-disulfide exchange reaction, diglycidyl ether of bisphenol A (DGEBA, A2) and diaminodiphenyl methane (DDM, B2) were employed as analogues of BGPDS and DTDA without disulfide bonding, respectively. The chemical reactivities of the aromatic disulfide in the epoxy monomer and amine hardener were assumed to be almost identical. ERD were prepared by combination of the epoxy monomer (either A1 or A2) and the diamine hardener (either B1 or B2). The detailed composition for each specimen was summarized in table 5.1. In pre-curing process, the mixture of epoxy monomer and diamine hardener was stirred at 90 °C for 30 mins in stoichiometric molar ratio (2: 1). The homogeneous mixture was transferred onto the Teflon mold, and successively cured at 120, 140 and 160 °C with two hours at each temperature. After cooling, ERD was obtained as a brown solid material. In this case, C25 without any disulfide bond was used as a control sample, whereas the others have some amount of disulfide bonds.

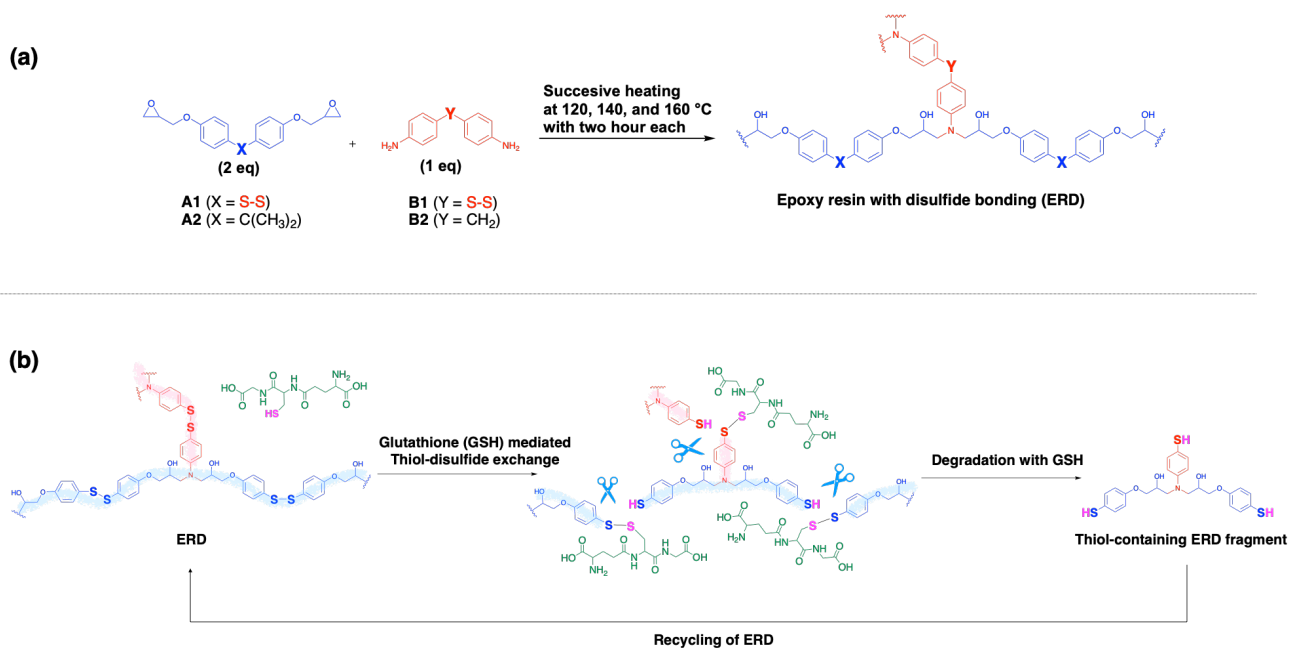


Figure 5.1 (a) Chemical structure of compounds used in this study, and (b) schematic representation of GSH mediated recycling system of ERD.

Table 5.1 All epoxy resin with disulfide bonding (ERD) used in this study.

		Molar ratio of diamine hardener (B1/B2)				
		100 / 0	75 / 25	50 / 50	25 / 75	0 / 100
Molar ratio of epoxy monomer (A1/A2)	100 / 0	C1	C2	C3	C4	C5
	75 / 25	C6	C7	C8	C9	C10
	50 / 50	C11	C12	C13	C14	C15
	25 / 75	C16	C17	C18	C19	C20
	0 / 100	C21	C22	C23	C24	C25

Table 5.2 Detail formulation of all epoxy networks (ERD) in this work

Network	epoxy monomer		diamine crosslinker	
	S-epoxy BGPDS (mol. ratio (g))	C-epoxy DGEBA (mol. ratio (g))	S-diamine DTDA (mol. ratio (g))	C-diamine DDM (mol. ratio (g))
C1	2 (3)	-	1 (1.029)	-
C2	2 (3)	-	0.75 (0.771)	0.25 (0.204)
C3	2 (3)	-	0.5 (0.516)	0.5 (0.411)
C4	2 (3)	-	0.25 (0.258)	0.75 (0.615)
C5	2 (3)	-	-	1 (0.822)
C6	1.5 (2.392)	0.5 (0.750)	1 (1.088)	-
C7	1.5 (2.392)	0.5 (0.750)	0.75 (0.818)	0.25 (0.218)
C8	1.5 (2.392)	0.5 (0.750)	0.5 (0.548)	0.5 (0.437)
C9	1.5 (2.392)	0.5 (0.750)	0.25 (0.274)	0.75 (0.656)
C10	1.5 (2.392)	0.5 (0.750)	-	1 (0.874)
C11	1 (1.590)	1 (1.500)	1 (1.095)	-
C12	1 (1.590)	1 (1.500)	0.75 (0.821)	0.25 (0.219)
C13	1 (1.590)	1 (1.500)	0.5 (0.548)	0.5 (0.437)
C14	1 (1.590)	1 (1.500)	0.25 (0.273)	0.75 (0.656)
C15	1 (1.590)	1 (1.500)	-	1 (0.873)
C16	0.5 (0.814)	1.5 (2.300)	1 (1.118)	-
C17	0.5 (0.814)	1.5 (2.300)	0.75 (0.840)	0.25 (0.223)
C18	0.5 (0.814)	1.5 (2.300)	0.5 (0.559)	0.5 (0.446)
C19	0.5 (0.814)	1.5 (2.300)	0.25 (0.281)	0.75 (0.669)
C20	0.5 (0.814)	1.5 (2.300)	-	1 (0.892)
C21	-	2 (3)	1 (1.095)	-
C22	-	2 (3)	0.75 (0.822)	0.25 (0.219)
C23	-	2 (3)	0.5 (0.546)	0.5 (0.438)
C24	-	2 (3)	0.25 (0.273)	0.75 (0.654)
C25	-	2 (3)	-	1 (0.873)

5.1.2.4 Synthesis of carbon fiber reinforced structure (CFRP)

The carbon fiber cloth was placed on aluminum plate covered with Teflon tape at first. Epoxy monomer BGPDS and amine hardener DTDA were prepared at a 2:1 molecular ratio in glass vial and mixed at 90 °C for 30 minutes. After mixing, the mixture was rapidly poured into aluminum plate where the fiber cloth was on. The other aluminum plate covered with Teflon tape was enclosed. Please note that the boundary of carbon fibers was established also by Teflon tape in case of outflow of epoxy resin at high temperature during curing. The sample and mold were cured in the oven at 120 °C for 2 hours, at 140 °C for 2 hours, and at 160 °C for 2 hours and finally cooled down to room temperature in the oven.

5.1.2.5 Preparation of peptide-assisted decomposition and recycling system

This new strategy could be separated into two stages, decomposition into solvent (in this case, was chloroform) by thiol-disulfide exchange reaction and recycling to epoxy-based network structure through reduction-oxidation reaction between thiol bonding and disulfide bonding.

All epoxy resin (ERD) was ground into powder by ball-milling for 30 minutes, and then placed into beaker. Chloroform and glutathione aqueous solution (20 mM) were added into at the ratio of 1:1 in volume. Additionally, tributylphosphine (0.1 eq.) was used as reaction accelerator.^{148,167} Please notice that the epoxy resin powder would be dispense in phase of chloroform solvent before mechanical stirring force applied. Degradation experiment was performed by rigorously stirring the mixed solution at room temperature. After that, suction filtration would be conducted to check whether the degradation was complete. Also, the dissolution of epoxy resin would be confirmed visually.

Recycling process was reached by following steps. First, dissolved epoxy resin (decomposed ERD) was settled into 300 ml flask. Then, organic solvent (chloroform) was removed by rotational evaporator. After that, the extracted epoxy resin liquid residue was washed by deionized water for three times. Finally, the cleaned liquid residue was transferred to Teflon mold immediately. In order to oxidize the decomposed ERD to original epoxy resin structure (ERD), heating to 180 °C for 6 hours was applied in this recycling technique.

5.2 Characterization

Fourier transform infrared (FTIR) spectra of the samples were performed in a JASCO FTIR 6100 instrument from potassium bromide (KBr) pellets. The uncured epoxy-diamine mixture was mixed with KBr powder to form the pellet. Besides, solid cured pristine epoxy resin (ERD) and the one after recycling (re-ERD) were ground into powder and then blended with KBr for pellet production; whereas, liquid degraded epoxy cluster (decomposed-ERD) was dropped on a KBr pellet with assistance of chloroform, and then the solvent would be removed by heating at 50 °C. Finally, the spectra for each compound were collected at the wavelength of 600 - 4500 cm^{-1} (m-IR) and 4000 - 7200 cm^{-1} (n-IR). A spectrum of blank KBr pellet was used as background.

¹H-Nuclear magnetic resonance spectroscopy (¹H-NMR) was observed at 25 °C by equipment from JEOL ECS-400 spectrometer at 400 MHz. ¹H-NMR spectra for CDCl₃ solution of degraded epoxy monomer and D₂O solution of glutathione, and reported in ppm δ (ppm) from internal tetramethylsilane signal.

Time-dependent absorbance-spectra was measured by equipment from JASCO V670. The samples with

different reaction times ranged from 10 minutes, 20 minutes, 30 minutes, 1 hour, 2 hours, 4 hours, and 8 hours were used in determination. All specimens were diluted to 0.03 wt%. Spectra were collected from 220-400 nm with an interval of 1 nm at scanning speed of 400 nm/min.

Dynamic mechanical analysis (DMA) was carried out by equipment from Netzsch DMA242E in tensile mode. The dimension of sample was 10 × 5 × 0.2 mm. Temperature range was from 25 °C to 200 °C with heating rate 3 °C /min. The oscillation frequency was kept at 1 Hz. Stress relaxation tests were carried out using the same equipment in the tensile mode at 130 °C allowing 30 extra minutes for thermal equilibration. To maintain straightness, a force of 0.006 N was applied to each sample. A strain of 1 % was applied and this deformation was maintained during the measurement process.

Swelling test was obtained by immersing pristine and recycled epoxy resin into toluene in light shielding bottle at room temperature for 72 hours. The weight before and after immersion were recorded. Finally, the swelling ratio was calculated according to the Equation 5.1

$$Q = (M_1 - M_2) / M_1 \quad (\text{Equation 5.1})$$

Q was swelling ratio, M_1 and M_2 were the weight of epoxy resin before and after 72-hour immersion, respectively. All data presented in this experiment was the mean values of five measurements.

5.3 Results and discussion

5.3.1 Reaction mechanism determination

The reaction mechanism was distinguished into three stages as discussed in following sections: curing of epoxy networks, degradation/decomposition of disulfide-contained epoxy networks, and recycling/reusing the decomposed epoxy monomers.

5.3.1.1 Curing

Disulfide-contained epoxy resin (ERD) synthesized by epoxy monomer and diamine crosslinker. In order to monitor curing process, Fourier transform near-infrared spectroscopy (FT-nIR) was performed. Figure 5.2 is a typical example of (a) uncured and (b) cured ERD with C1 combination. In the nIR region from 7200-4000 cm^{-1} , the well-defined bands related with the epoxy and primary amine were observable at the combination band of the second overtone of the epoxy ring with the fundamental C-H stretching (ca. 4530 cm^{-1}) and the combination band of NH stretching and bending (ca. 5000-5100 cm^{-1}); therefore, the epoxy monomer decreased after curing process, resulting in decrease of the band of the fundamental C-H stretching and the weak overtone of terminal CH_2 from ca. 4530 cm^{-1} and ca. 6060 cm^{-1} , respectively. The primary amine combination band at ca. 5000-5100 cm^{-1} also decreased. On the other hand, the band of O-H overtones at ca. 7000 cm^{-1} increased as a consequence of the oxirane ring opening reaction. This result indicated that the ring-opening reaction of epoxide group and diamine moieties was completed after heat-induced curing process, resulting in the crosslinked structure as conventional thermosetting resin, providing the excellent thermal and mechanical properties that could be applied in industrial structural application.

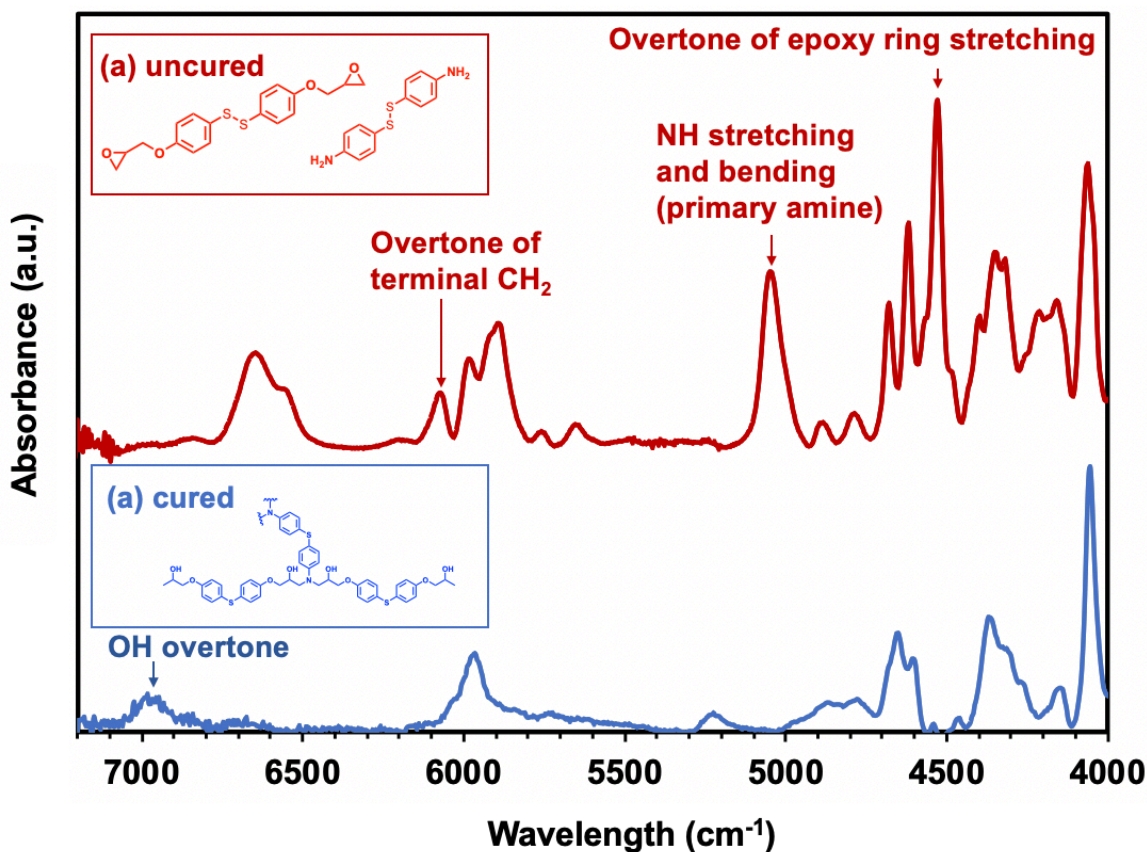


Figure 5.2 FT-nIR spectra of (a) uncured (red) and (b) cured (blue) EDR

5.3.1.2 Degradation/decomposition

Prior to the demonstration for degradation of disulfide-contained epoxy resin with glutathione (GSH) aqueous solution, we performed decomposition experiment using a disulfide-containing small molecule compound in a water/organic binary system. Herein, 4,4'-dithiodianiline (DTDA) was chosen as a model compound with disulfide containing molecule. DTDA and GSH was dissolved in deuterated chloroform (CDCl_3) (250 mM) and deuterated water (D_2O) (250 mM), respectively. The solution was controlled in 1:1 (v/v) ratio covered with aluminum foil to shed the light and avoid the interruption and unexpected reaction induced by UV-irradiation.

The reaction mixture was quantitatively evaluated with $^1\text{H-NMR}$ spectroscopy (figure 5.3). Figure 5.3.(a) and (b) show change in $^1\text{H-NMR}$ spectra of CDCl_3 and D_2O phase, respectively. In CDCl_3 phase, $^1\text{H-NMR}$ signals of an aromatic ring in DTDA (a) and (b) appeared at 6.55 and 7.22 ppm, and $^1\text{H-NMR}$ signal at 7.12 ppm was assigned as an aromatic ring of 4-aminobenzenethiol (4-ABT) (b'), which supposed to be a reduced form of DTDA (figure 5.3.(a)). In addition, no peak was detected in the range of 2-3 ppm, suggesting that the GSH and the exchange products with GSH did not exist in CDCl_3 phase. On the other hand, in D_2O phase, new $^1\text{H-NMR}$ signal (c') appeared at 3.12 ppm, suggesting formation of S-S bond between GSH and 4-ABT (figure 5.3.(b)). In addition, the $^1\text{H-NMR}$ peaks (d) and (e) of 4-ABT appeared at 7.12 and 7.3 ppm. Considering that DTDA and 4-ABT are immiscible to water phase, these signals were thought to originate from a water-

soluble reactant between GSH and 4-ABT (GSH-ABT).

Next, the time evolution of the composition in $\text{CDCl}_3 / \text{D}_2\text{O}$ was further evaluated. Figure 5.3.(c) showed a rate of change of DTDA and 4-aminobenzenthioi calculated from the peak areas of $^1\text{H-NMR}$ signal (b) and signal (b') in CDCl_3 , respectively. Consequently, DTDA was immediately decreased with time and reached equilibrium at 60 minutes. Correspondingly, 4-ABT began to generate immediately after stirring and reached equilibrium at 60 minutes in a symmetrical manner to DTDA. Similarly, figure 5.3.(d) presented the time evolution of decrease in GSH and increase in the water-soluble reactant of GSH and 4-ABT in D_2O phase. As in CDCl_3 phase, decrease in GSH and increase in the reactant of GSH-ABT tended to change symmetrically, reaching equilibrium in approximately 60 minutes. More importantly, the molar rate of increased and decreased compositions was kept at 30 mol% for both the CDCl_3 and D_2O phase based on equation 5.2 and 5.3 as follows.

$$X = \frac{I(b')}{\frac{I(b)}{2} + I(b')} \quad (\text{Equation 5.2})$$

where X was the conversion rate, while $I(b)$ and $I(b')$ were intensity of peak b and b'.

$$X = \frac{I(c')}{I(c) + I(c')} \quad (\text{Equation 5.3})$$

where X was the conversion rate, while $I(c)$ and $I(c')$ were intensity of peak c and c'.

From these results, the chemical reaction balance in each of CDCl_3 and D_2O phases was proposed in figure 5.4. Consequently, the thiol-disulfide exchange reaction between DTDA and GSH underwent at the interface of CDCl_3 and D_2O , resulting in generation of the water-soluble reactant of GSH and 4-ABT (GSH-ABT), and unreacted 4-ABT remained dissolved in CDCl_3 .

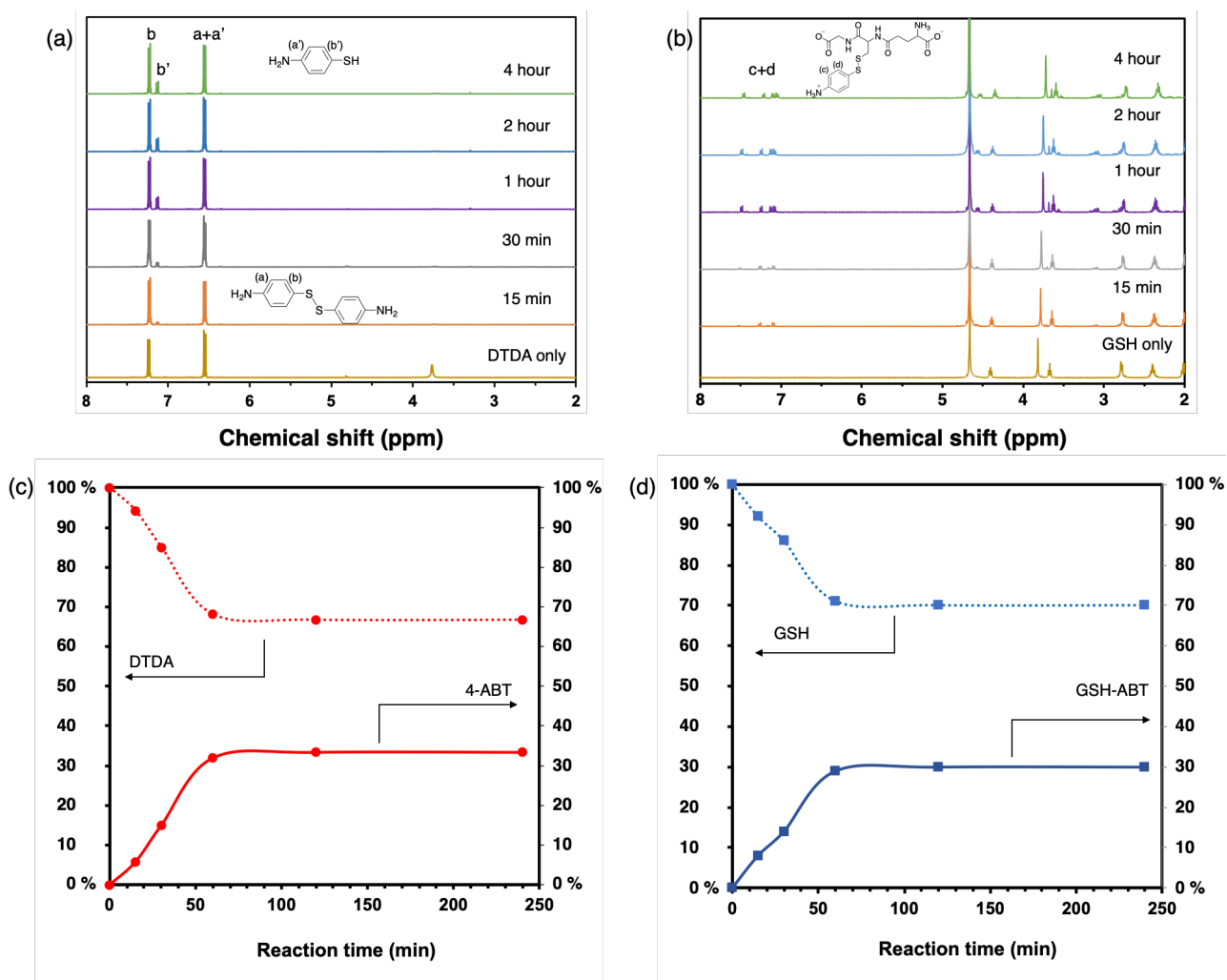


Figure 5.3 NMR spectra of (a) solvent phase and (b) water phase for GSH-assisted thiol-disulfide exchange reaction of model compounds at different reaction time. Time evolution of product by reaction of DTDA with GSH in (c) CDCl₃ and (d) D₂O. Amount of the product was monitored by ¹H-NMR at 7.22, 7.12, 2.8, and 3.12 ppm DTDA, 4-ABT, GSH, and GSH-ABT, respectively.

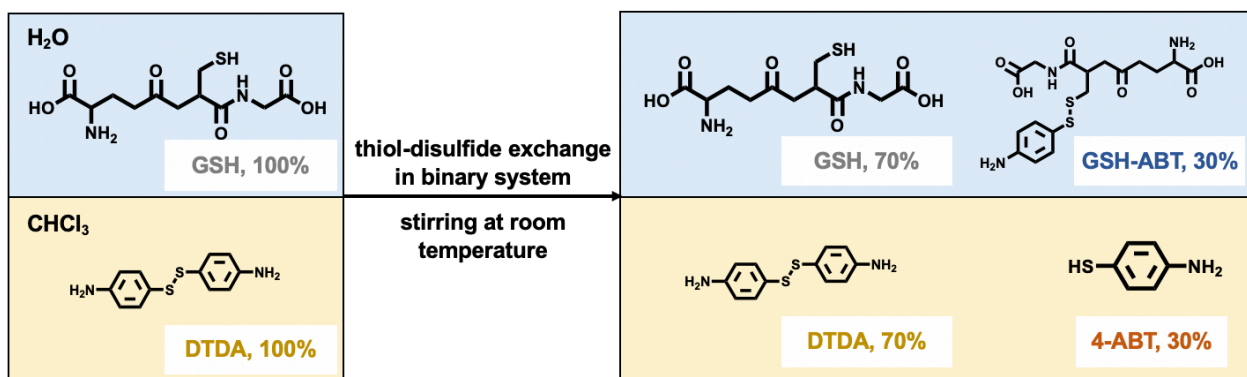


Figure 5.4 Chemical reaction balance for CDCl₃ (CHCl₃) and D₂O (H₂O) phases

After confirming the thiol-disulfide exchange reaction proceeds in $\text{CHCl}_3/\text{water}$ binary system with GSH mediation based on small molecular model compound, the disassembly test of disulfide-contained epoxy resin (ERD) was conducted with the same binary condition. Therefore, the small molecular compound dithiodianiline was replaced with epoxy resin powder to evaluate the practical degradation of disulfide-contained epoxy resin. First, in order to determine the concentration of glutathione aqueous solution that could provide most efficient equilibrium for dissolution of disulfide-contained epoxy resin applied in this decomposition system, the small amount of ERD-C1 epoxy resin powder (30 mg) was added into peptide-assisted degradation system to observe the relationship between concentration and decomposition time at room temperature. As revealed in figure 5.5, the correlation between the decomposition time needed and molar concentration of glutathione aqueous solution was obtained by changing the concentration at 1, 5, 10, 20, and 50 mM. The decomposition time would be significantly decreased from 9 to 6 hours when the concentration of glutathione water solution was enhanced from 1 to 5 mM, and then it seemed that the equilibrium of decomposition rate was finally reached in the molar concentration of 20 mM because the depolymerization times for 20 mM and 50 mM were identical; therefore, the concentration of glutathione solution was fixed at the 20 mM for this decomposition strategy not only to reduce the amount of glutathione used in this decomposition system, but also to ensure the optimized experimental dissolution rate.

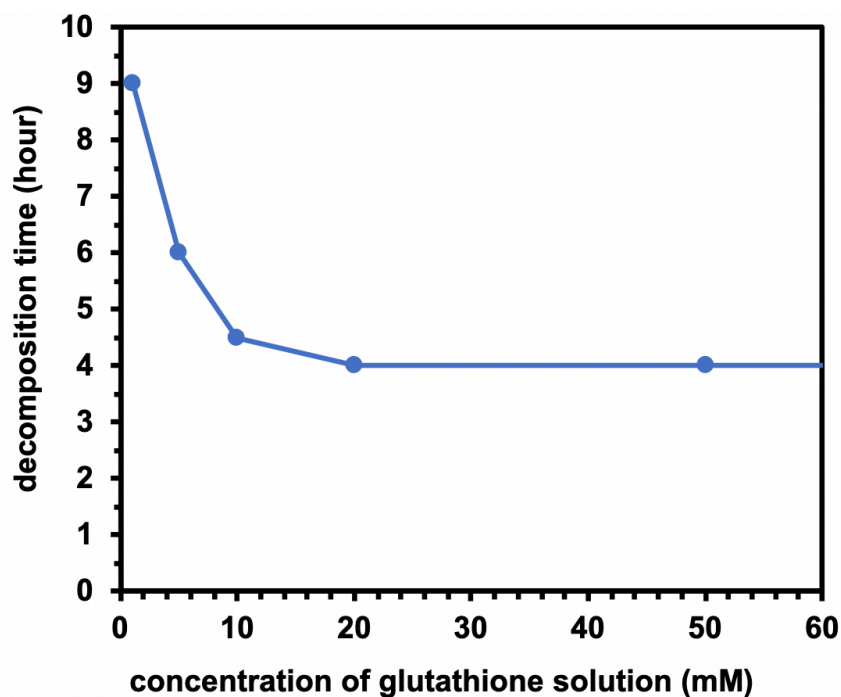


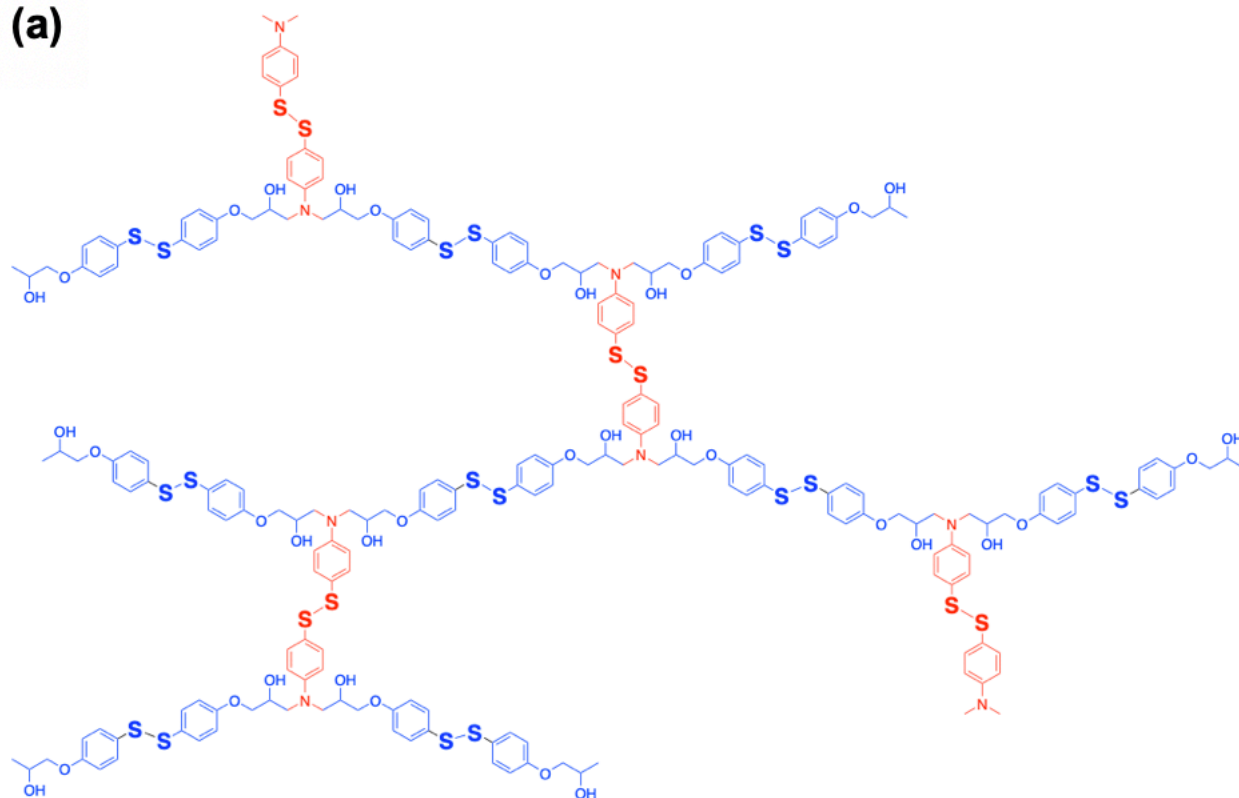
Figure 5.5 Relation between concentration of glutathione aqueous solution and decomposition time

Then, all ERDs (from C1 to C25) were ground by ball milling method and dispensed into the glutathione aqueous / chloroform binary decomposition system. After certain period of time, the results were divided into two types of features: (1) those in which the ERD was completely dissolved into CHCl_3 phase, resulting in a yellow chloroform solution, and (2) those in which precipitation occurred. The result of decomposition of ERDs was summarized in terms of composition ratio of the epoxy monomer (either A1 or A2) and the diamine hardener (either B1 or B2) as shown in table 5.3. Along with this, molar equivalents of disulfide bonds in each repeating unit of ERD by various combinations of BGPDS/ DGEBA and DTDA/ DDM in various proportions were summarized. In table 5.3, the compositions in which ERD was completely dissolved were marked in pink. It should be noted that the amine hardener (DTDA or DDM) can react with two equivalents of the epoxy monomer (BGPDS or DGEBA), which suggest that the disulfide bonds can be introduced up to three equivalents of the repeating units of ERD in the viewpoint of amine crosslinking sites as given in figure 5.6.(a). From completely dissolved parts, the viscous yellow liquid was obtained after removing CHCl_3 solvent under vacuum. Here, the solubility of ERD can be discussed in terms of the stoichiometric ratio of the disulfide group and the repeating units of ERD (table 5.3). ERD completely dissolved in CHCl_3 when the disulfide group was more than 1.5 equivalents to the repeating unit of ERD, in which ERD was decomposed into dimeric or monomeric units. On the other hand, If the stoichiometric ratio of the disulfide groups was less than 1.5, most of the repeating unit would be trimeric or higher units, resulting in precipitates. These results indicated that the density of disulfide bonding in epoxy network was the critical factors for decomposability.

Table 5.3 Photograph of the resultant of decomposed ERD in CHCl_3 / water binary system with GSH. Compositions in which ERD was completely dissolved were marked in pink.

S-S bonds/ C-C bonds (mole ratio)		molar ratio of B1 against ERD repeating unit (1 mol)				
		1 mol	0.75 mol	0.5 mol	0.25 mol	0 mol
molar ratio of A1 against ERD repeating unit (2 mol)	2 mol	C1 (3.0 mol)	C2 (2.75 mol)	C3 (2.5 mol)	C4 (2.25 mol)	C5 (2.0 mol)
		C6 (2.5 mol)	C7 (2.25 mol)	C8 (2.0 mol)	C9 (1.75 mol)	C10 (1.5 mol)
	1.5 mol	C11 (2.0 mol)	C12 (1.75 mol)	C13 (1.5 mol)	C14 (1.25 mol)	C15 (1.0 mol)
		C16 (1.5 mol)	C17 (1.25 mol)	C18 (1.0 mol)	C19 (0.75 mol)	C20 (0.5 mol)
	1 mol	C21 (1.0 mol)	C22 (0.75 mol)	C23 (0.5 mol)	C24 (0.25 mol)	C25 (0 mol)

(a)



(b)

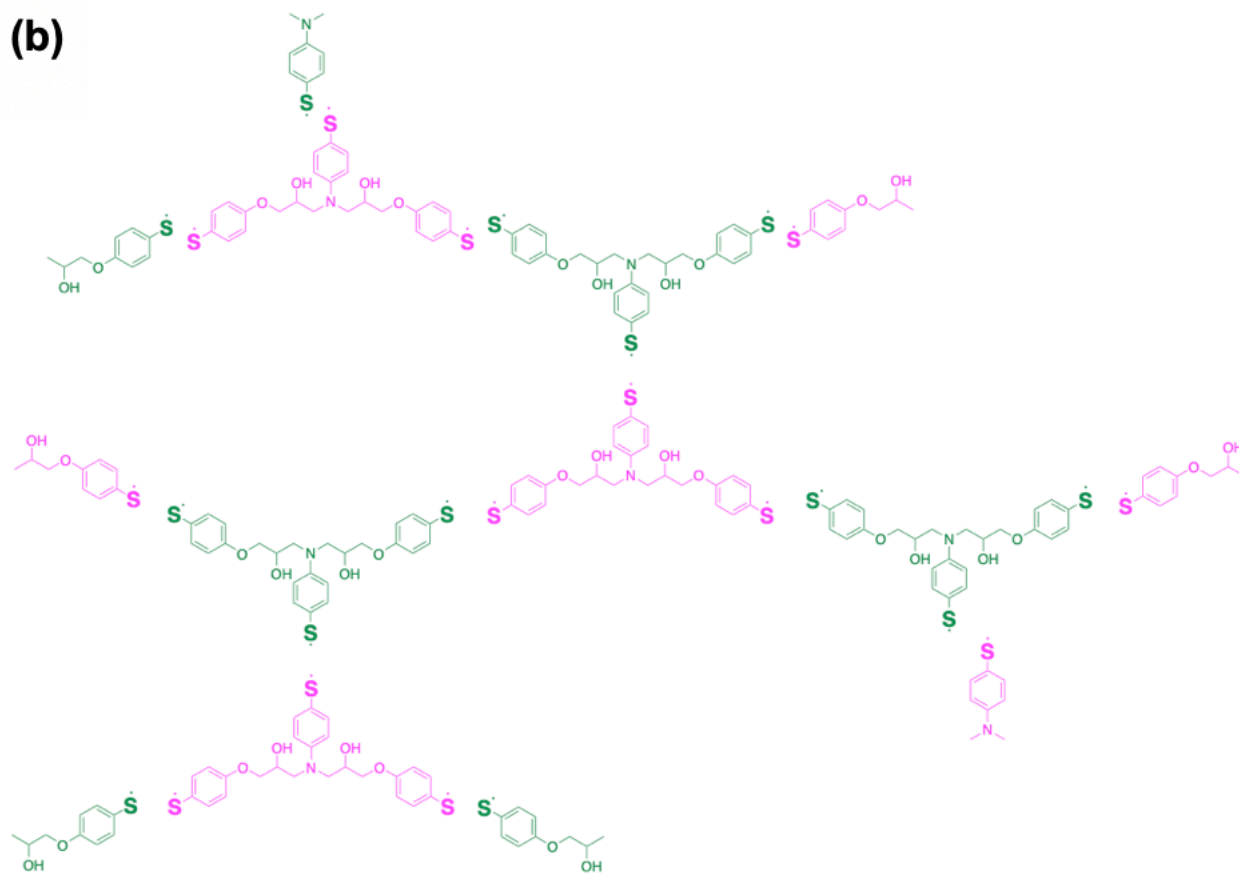


Figure 5.6 Schematic illustration of repeating unit of ERD with (a) cross-link point of amine bonding and (b) degradable disulfide bonding.

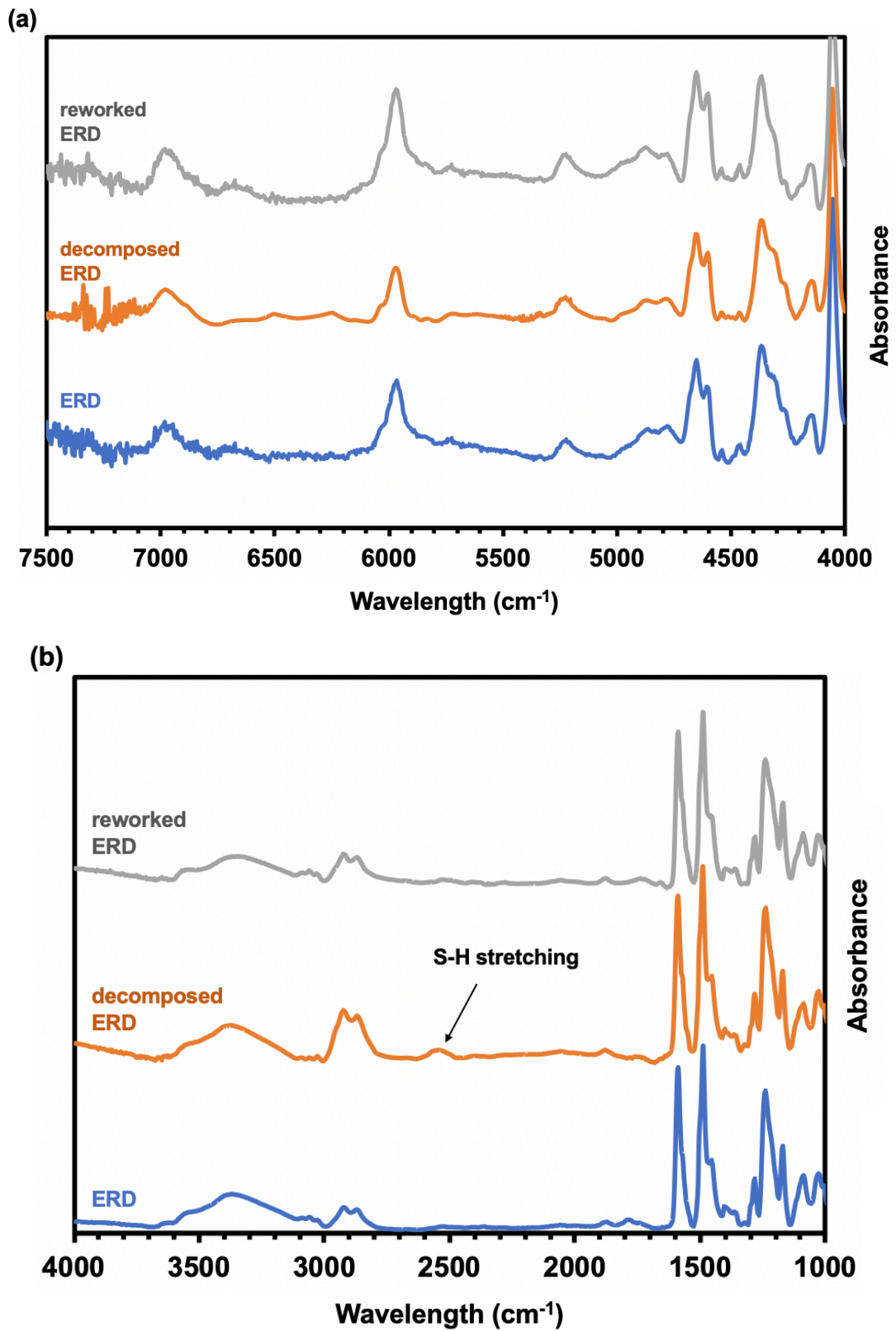


Figure 5.7 (a) FT-nIR and (b) FT-mIR spectra of ERD, decomposed ERD, and reworked ERD after curing.

In order to identify the chemical structure of these residues, FT-nIR spectroscopy was conducted. Figure 5.7 showed FT-IR spectrum of the decomposed soluble portion of ERD-C1 in CHCl_3 phase. The spectrum of this residue was almost identical to that of ERD in the nIR region as shown in Figure 5.7.(a) from 4000 cm^{-1} to 7200 cm^{-1} . This implied that the liquid residue remained the epoxy structure of ERD. On the other hand, a new thiol-derived absorption band appeared at 2550 cm^{-1} (Figure 5.7.(b)). This suggests that this fragment contains the thiol group by the reduction of the disulfide group of ERD, which was attributed to the thiol-disulfide exchange reaction from GSH. To further investigate degradation tendency of ERD, UV-vis spectra in CHCl_3 phase were measured at 254 nm with different interval time as presented in figure 5.8. When the suspension of ERD-C1 in CHCl_3 was mixed with GSH aqueous solution, UV absorption at 245 nm immediately increased and followed the saturation curve. After four hours, it reached a plateau region with a constant value, suggesting that ERD-C1 completely dissolved in CHCl_3 phase.

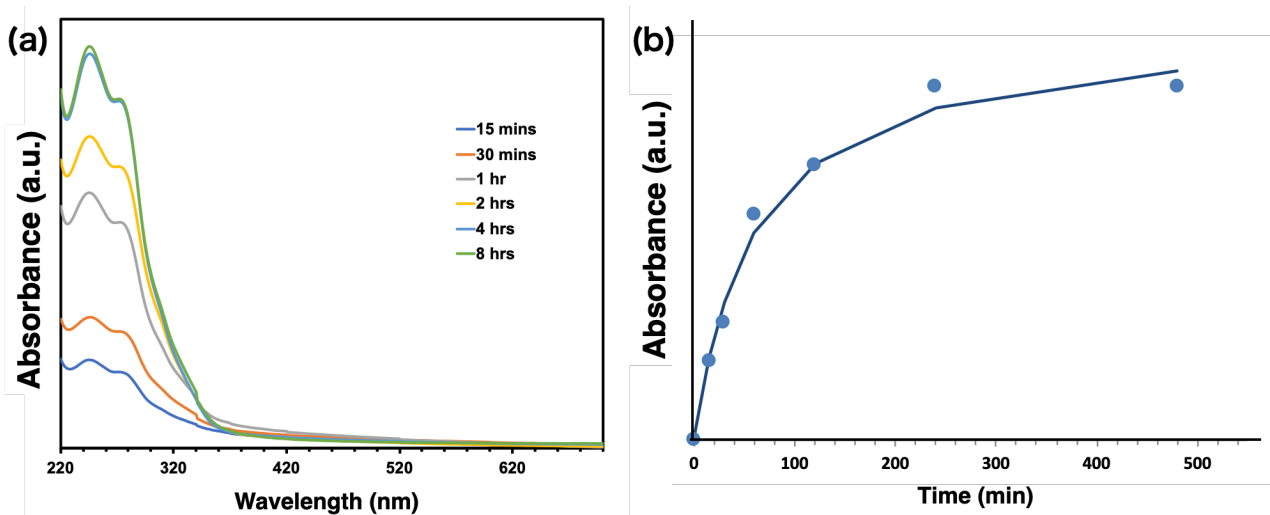


Figure 5.8 (a) Time-dependent UV-vis spectra for decomposed ERD in CHCl_3 phase, and (b) time course of UV spectra of decomposed ERD monitored at 254 nm.

5.3.1.3 Recycling

In general, amine-curing epoxy resins are regarded as network structures with amine bonds as cross-linking points, but in the case of ERD, it can also be regarded as dynamic covalent network polymers with disulfide bonds as the repeating units (Figure 5.6.(b)). Therefore, the recycling and reworking of epoxy resin network could be reached through the reconnection of thiol bonding to disulfide bonding by reduction-oxidation reaction.

As presented in figure 5.7, the FTIR spectra of pristine, degraded, and recycled epoxy resin was examined separately to compare the network structure of chemical bond and composition. First, in spectrum of pristine epoxy resin, no stretching peak of thiol-group located at 2550 cm^{-1} could be observed in this range, which indicated that the curing procedure without adding thiolate group would not cause the change of aromatic disulfide bonding. Even though the cleavage of disulfide bonding could be triggered at high temperature, the

reconnection of broken S-S bond would be occurred rapidly in this stage, so that there was no thiol bonding found. However, the S-S bonds would be attacked by thiolate groups of glutathione during degradation process in this new peptide-assisted system, and then was reduced to SH bonds, or was exchanged with glutathione. In this case, the band of SH stretching at 2550 cm^{-1} was observed for reduced epoxy residue in chloroform layer, which meant that decomposition was attained by transferring disulfide bonding to thiol bonding. And the disappearance of this peak after heating indicated that the SH bonds oxidized to S-S bonds through oxidation. Also, the spectrum of recycled resin was corresponded to the spectrum of original resin, which demonstrated that the recycling was carried out successfully.

5.3.2 Thermal and mechanical properties

Since the network structure of ERD was remained in decomposed ERD liquid residue as demonstrate in figure 5.6, it was assumed that the thermal and mechanical properties of recycled ERD would be kept as the original amine-cured epoxy resin even if ERD was degraded and regenerated by formation of disulfide bonds. In order to evaluate the thermal and mechanical property of disulfide-contained epoxy resin before and after recycling, the DSC and DMA was used in determination. The testing data were summarized as given in table 5.4. For mechanical property, the storage modulus maintained approximately 90-95% of initial value at room temperature after recovery as revealed in figure 5.9, which proved that high recycling efficiency of oxidation reaction in dual-phase system. This result presented that the new peptide-assisted dual-phase degradation and recycling system not only solved the problem in decomposition of wasted epoxy resin, but also provided the method to reuse the resin with superior mechanical property after oxidation of thiol groups. This evidence proved that the recycled epoxy resin may be able to be utilized in other application. However, the sharp decrease of glass transition temperature should be noticed. This deterioration may result from incomplete crosslinking, which cause less thermal stability.

The swelling test for pristine and recycled epoxy resin was also performed to confirm the crosslinking density before and after degradation and recycling. In figure 5.10, the swelling ratio after 72-hour immersion in toluene at room temperature for initial cured sample was around 3%, which explained the common high crosslinking density in epoxy networks that possessed excellent solvent resistant ability; in comparison, the swelling ratio for recycled epoxy resin was increased to 13% after first-time recycling, and then further enhanced to 16% in second round. This result proved that the crosslinking density after recycling could not be completely resumed to original structure, causing the lower glass transition temperature and slight decay of mechanical strength at room temperature but higher modulus in rubbery state.

The time-dependent relaxation examined by DMA was the other key characteristic for dynamic disulfide network to assess heat-induced malleability and ductility. Generally, the dynamic networks showed obvious relaxation behavior at sufficiently high temperature through reversible exchange reaction and chain mobility. As disclosed in figure 5.11, it showed the normalized stress relaxation of pristine and recycled epoxy resin at $130\text{ }^{\circ}\text{C}$. Based on Maxwell model equation, the relaxation time was defined as the time required to reach 37% of initial stress. Compared to the original networks (ESSE) that could not reach stress relaxation within 1.5 hours, the relaxation time of recycled network (re-ESSE) was 152 seconds at $130\text{ }^{\circ}\text{C}$, exhibiting more rapid stress release than original one. The result demonstrated that recycled network showed stress relaxation

above T_g as general dynamic network attributed to reformed exchangeable disulfide bonds because of oxidation reaction. Besides, due to relatively low T_g of recycled epoxy resin, the segmental chain motion could be activated in lower temperature, resulting in faster exchange reaction and then lead to stress release phenomenon with shorter relaxation time.

Table 5.4 Thermal and mechanical properties for ERD and reworked ERD characterized by dynamic mechanical analysis (DMA)

Networks	Glass transition temperature (T_g) (DSC) ($^{\circ}\text{C}$)	Storage modulus (E') (Glassy state) at 25 $^{\circ}\text{C}$ (GPa)	Storage modulus (E') (Rubbery state) (at $T_g + 30$ $^{\circ}\text{C}$) (MPa)
ERD	130.9	1.75	14.3
re-ERD (1st time)	82.7	1.54	49.9
re-ERD (2nd time)	81.7	1.68	26.8

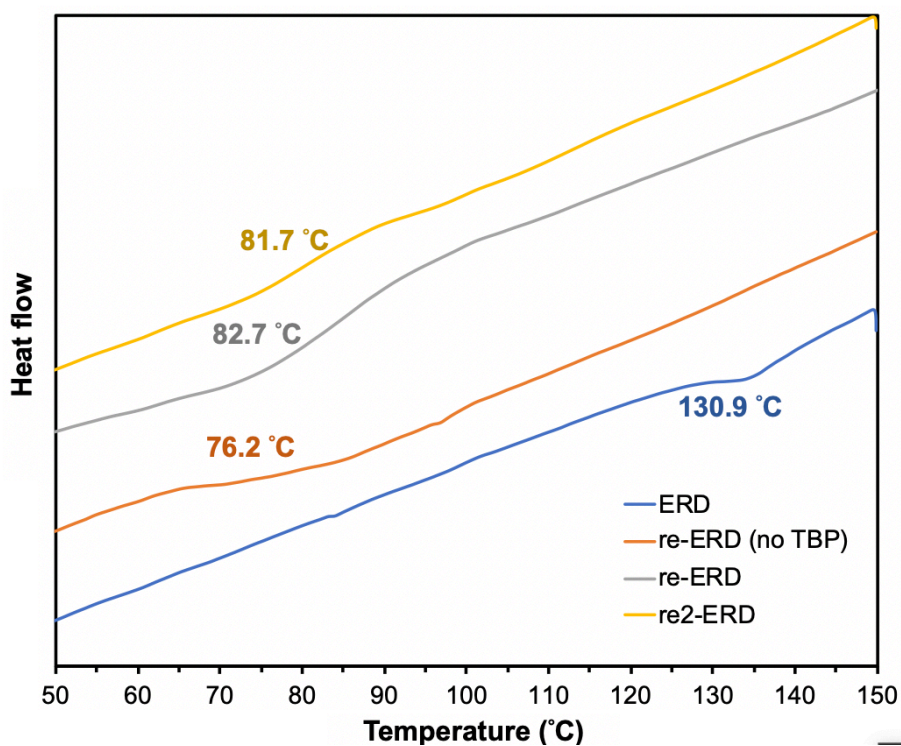


Figure 5.9 DSC curve for EDR, 1st-time reworked ERD, and 2nd-time reworked ERD

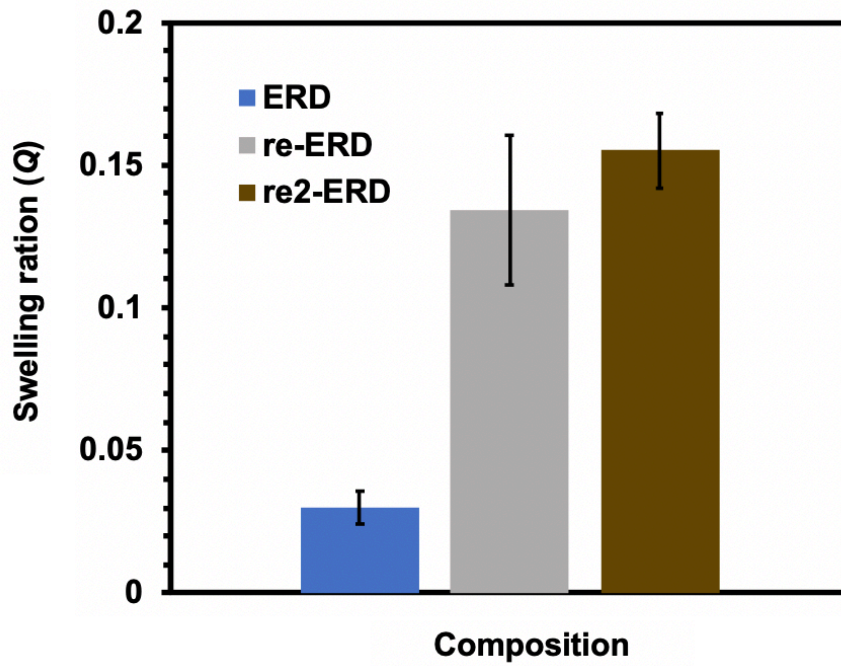


Figure 5.10 Swelling ratio (Q) for ERD, 1st-time reworked ERD, and 2nd-time reworked ERD in toluene at room temperature for 72 hours

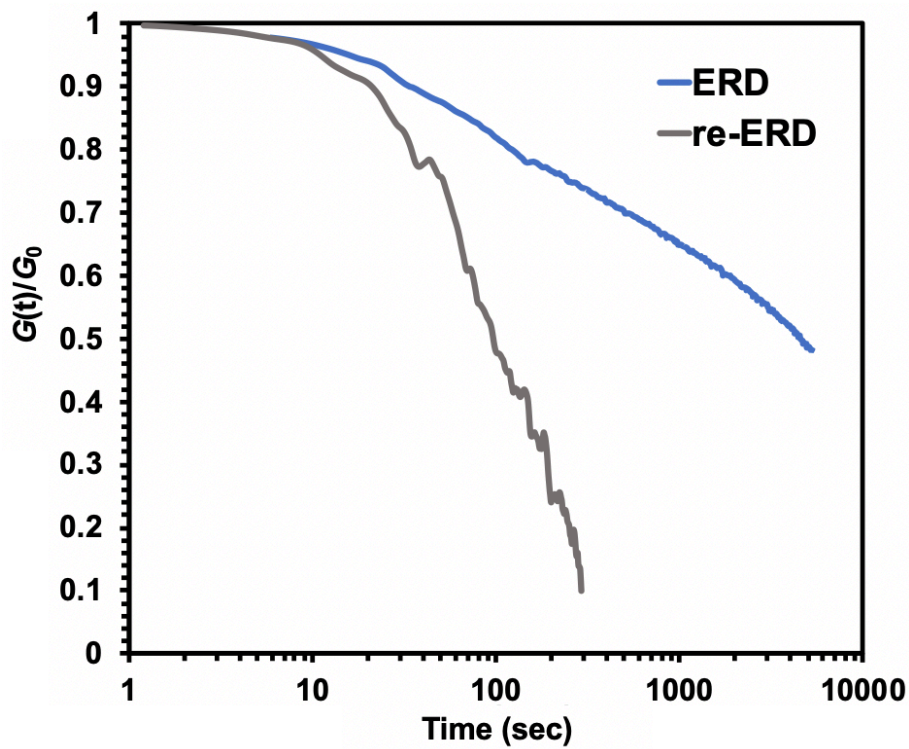


Figure 5.11 Stress relaxation for ERD and reworked ERD at 130 °C

5.3.3 Application for carbon fiber reinforced structure (CFRP)

Thus, once the new dual-phase degradation and recycling system was confirmed to be effective, its practical application was worthy being further discussed. Carbon fiber reinforced structure (CFRP) based on traditional thermoset resin is one of the most common high-performance structural materials in aerospace, automobile, and construction industry. However, the thermosetting crosslinked structure brought out the difficulty in decomposing and recycling, which caused serious environmental problem. In this study, we applied this new degradation technique on CFRP composite cured with disulfide-contained epoxy resin (ERD) matrix as illustrated in figure 5.12. The cured CFRP structure in figure 5.12.(a) was fixed by clip in dual-phase solution as given in figure 5.12.(b). By intensely stirring into one homogeneous mixture at ambient condition for 24 hours, the epoxy resin matrix ERD in CFRP was dissolved into solvent phase as shown in figure 5.12.(c). Figure 5.12.(d) revealed that the undamaged carbon fiber was completely recovered via washing by water and acetone and then drying at 100 °C after matrix dissolution. On the other hand, the decomposed epoxy monomer dissolved in chloroform solution was obtained as described in figure 5.12.(e) through solvent evaporation. The reduced monomer could be simply transferred to resin network via redox reaction by oxidizing thiol-group to sulfur-sulfur bonds. The re-cured network as figure 5.12.(f) was finally acquired. To our best knowledge, most degradation strategy used in epoxy-disulfide networks was irreversible, which meant that the recycling was restricted in fibers, fillers, and reinforcements but not resin. Through this advanced degradation system, the recycling of polymeric network could be reached since the reduced monomer and exchange product were divided into two parts, so that the degraded epoxy moieties could be reused as the starting material for new production of epoxy networks.

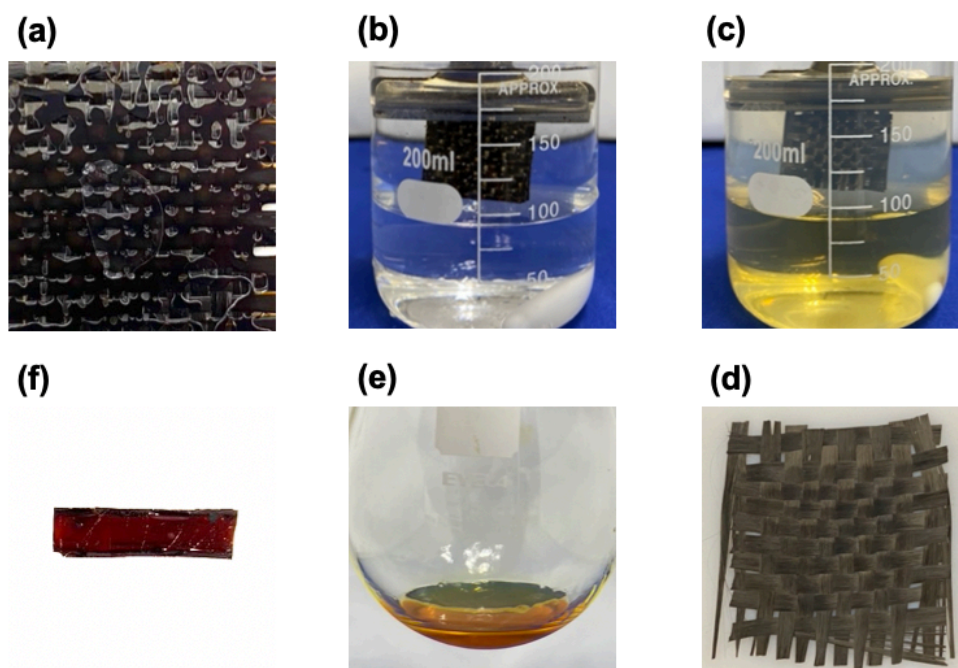


Figure 5.12 Demonstration of recycling procedure for carbon fiber reinforced composite (CFRP) (a) CFRP with ERD, (b) Decomposition test of CFRP-ERD with GSH, (c) after 24 hours, (d) recovered carbon fiber, (e) ERD residue recovered from CHCl_3 phase, and (f) reworked ERD cured at 180 °C for 6 hours.

5.4 Conclusion

In conclusion, the rebuildable and reformable epoxy resin with aromatic disulfide bonds through new degradation and recycling method was presented in this paper. By introducing the dynamic S-S bonds, we successfully obtained the resettable and recyclable thermosetting network structure. Also, establishing dual-phase solution contained the glutathione aqueous solution and chloroform provided the simpler method to decompose and reuse the epoxy resin. Dynamic disulfide bonds in epoxy resin could be broken, reduced, and exchanged with S-H bonds of glutathione through thiol-disulfide exchange reaction. Simultaneously, the peptide group in glutathione promoted the generation of hydrophilic exchange by-product, which would be automatically dispensed to aqueous solution. After degradation, the epoxy fragments were dissolved into chloroform, while exchange product would be distributed in water phase. This fact provided the pathway to separate the degraded epoxy monomer from mixture with by-product, which could be finally reused as reagent to epoxy resin network by redox reaction between thiol and disulfide bonding. Moreover, the bulk recycled resin with reconnected aromatic disulfide bonding maintained 90-95% of initial mechanical strength at room temperature, presenting the potential on different application. This decomposition and reworking technique could be practically applied in CFRP composite structure, so that the recycling could be derived both in fiber and resin matrix. These results would help us to broaden the applicability of degradable and recyclable epoxy-disulfide network in the future. This approach revealed a progressive and efficient decomposition and recycling method for epoxy-disulfide network, which expand the range of reusing both contents and matrix in composite structure.

CHAPTER VI SUMMARY AND PROSPECT

In this thesis, the repairable and recyclable epoxy resin networks with unique indicator functional could be obtained by introducing dynamic aromatic disulfide bonding into thermosetting structure. Different approaches were discussed based on three exchange reactions in disulfide bonding systems, which included: (1) reparability and adhesion strengthening effect through disulfide-disulfide exchange reaction and (2) crosslinking density and adhesion strength determination through mechanochromism of disulfide bonding (3) decomposition and recycling behavior through thiol-disulfide exchange reaction.

First, we prepared the epoxy resin networks with different content of aromatic disulfide bonding to evaluate the effect of amount of S-S bonds on thermal, mechanical, stress relaxation, and adhesion properties. The results indicated that the glass transition temperature (T_g) and decomposition temperature (T_d) were decreased with increasing the concentration of disulfide bonding due to less energetical stability than carbon-carbon bonds, while both mechanical and adhesion strength of the formula adding dynamic disulfide bonding would be comparable with traditional epoxy network. Also, the heat-induced stress relaxation could be only detected in the networks with adaptable bonds since the exchange reaction was triggered and then contributed to the release of stress. Higher density of disulfide bonding led to shorter relaxation time, causing lower topology freezing transition temperature (T_v) and activation energy (E_a). After determining the T_v -value, aromatic disulfide bonding was categorized into the case that dynamic covalent networks possessed higher T_g -value than T_v -value. Considering to this characteristic, there were two improvements that could be acquired when applied in adhesive joint, reprocessing and recovery at the temperature above T_g and T_v and tougher adhesion above T_v but below T_g . Through heating to the temperature above T_g and T_v , the dynamic epoxy networks could be transferred from thermosetting crosslinked solid to viscoelastic state due to fast reversible exchange reaction and high segmental motion. In our case, the adhesion performance of rebonded joint reached almost 95% of initial shear strength. On the other hand, at the temperature range between T_v and T_g (above T_g but below T_v), the unusual adhesion strengthening effect was detected because the accumulated internal stress in adhesive joint due to volume shrinkage during curing and cooling was released by relatively speedy cleavage and rearrangement of disulfide bonding above T_v ; simultaneously, the chain mobility was restricted for whole networks below T_g . Therefore, although reparability could be reached in most dynamic covalent systems, the adhesion improvement at elevated temperature before glass transition was only presented in the case owned lower T_v -value than T_g -value, such as disulfide bonding system.

Second, when the mechanical stress applied on disulfide-contained epoxy resin, the cleavage of disulfide bonding led to the generation of thiyl radicals, resulting in the green coloration in the broken area. This phenomenon was known as mechanochromic effect. As a result, we utilized the mechanochromism of disulfide bonding in the technique of crosslinking density and adhesion strength evaluation for disulfide-contained epoxy resin, since the color would be changed from green to yellow once the radical was recombined. In this study, the longer duration of mechanochromic effect was attributed to the higher crosslinking density and lower chain mobility, which meant that the color change would be remained in highly-crosslinked epoxy network structure. Since the crosslinking density had a critical impact on adhesion strength, we could determine the adhesion performance by observing the lasting time of mechanochromic behavior. Based on the collected data, the longer lasting time of mechanochromic performance indicated the tougher adhesion strength, which provided

the simple and direct identification method for low-crosslinked network structure and helped us to pre-screen the adhesive with weaker strength.

Finally, we proposed the new decomposition and recycling strategy for this disulfide-contained epoxy networks in the assistance of glutathione compound. The purpose of this research was to decompose the epoxy resin with eco-friendly chemical compound, and demonstrate the reworkability and recyclability of degraded epoxy residue back to epoxy resin network. This advanced water/chloroform binary solution system was composed of two immiscible layers, which were glutathione aqueous solution and chloroform solvent. In the stage of decomposition, the thiol bond in glutathione would be bound on the disulfide-contained epoxy resin, followed by the cleavage of disulfide bonding in epoxy resin through thiol-disulfide exchange reaction; therefore, the decomposed epoxy residue would be dissolved into chloroform phase. This decomposed compound could be reused as starting material to reform the new epoxy network through oxidizing the thiol bond back to disulfide bond by heating the epoxy residue at 180 °C for 6 hours. Also, the evaluation of FTIR and dynamic mechanical analysis proved that the recycled epoxy resin almost recovered back to pristine epoxy network structure and achieved the 90% of mechanical strength of virgin epoxy resin. Besides, the demonstration of degradation and reworking carbon fiber reinforced structure exhibited the practical application of this technique, which may help us to broaden the knowledge of degradable and recyclable epoxy network.

In conclusion, incorporating the disulfide bonding into epoxy networks offered us the more eco-friendly and economic choice. This study also presented the potential impact to develop the repairable and recyclable epoxy resin through dynamic covalent chemistry in practical structural application and worthy further exploration in the future.

REFERENCES

- (1) Europe, P.; EPRO. *Plastics - the Facts 2019*. **2019**.
- (2) Biron, M. Chapter 1 - Outline of the Actual Situation of Plastics Compared to Conventional Materials. In *Plastics Design Library*; Biron, M. B. T.-T. and T. C. (Third E., Ed.; William Andrew Publishing, 2018; pp 1–30. <https://doi.org/https://doi.org/10.1016/B978-0-08-102501-7.00001-1>.
- (3) Bruder, U. Chapter 1 - Polymers and Plastics; Bruder, U. B. T.-U. G. to P. (Second E., Ed.; Hanser, 2019; pp 1–6. <https://doi.org/https://doi.org/10.3139/9781569907351.001>.
- (4) Mallick, P. K. Chapter 1 - Overview. In *Woodhead Publishing in Materials*; Mallick Design and Manufacturing for Lightweight Vehicles (Second Edition), P. K. B. T.-M., Ed.; Woodhead Publishing, 2021; pp 1–36. <https://doi.org/https://doi.org/10.1016/B978-0-12-818712-8.00001-X>.
- (5) Pascault, J.-P.; Williams, R. J. J. General Concepts about Epoxy Polymers. *Epoxy Polymers*. January 13, 2010, pp 1–12. <https://doi.org/https://doi.org/10.1002/9783527628704.ch1>.
- (6) Drobny, J. G. 1 - Introduction. In *Plastics Design Library*; Drobny, J. G. B. T.-H. of T. E., Ed.; William Andrew Publishing: Norwich, NY, 2007; pp 1–8. <https://doi.org/https://doi.org/10.1016/B978-081551549-4.50002-5>.
- (7) Pascault, J.-P.; Williams, R. J. J. Chapter 1 - Overview of Thermosets: Present and Future. In *Thermosets*; Guo, Q. B. T.-T. (Second E., Ed.; Elsevier, 2018; pp 3–34. <https://doi.org/https://doi.org/10.1016/B978-0-08-101021-1.00001-0>.
- (8) Stokes, V. K. Introduction. *Introduction to Plastics Engineering*. May 11, 2020, p 1. <https://doi.org/https://doi.org/10.1002/9781119536550.part1>.
- (9) Ellis, B. Introduction to the Chemistry, Synthesis, Manufacture and Characterization of Epoxy Resins BT - Chemistry and Technology of Epoxy Resins; Ellis, B., Ed.; Springer Netherlands: Dordrecht, 1993; pp 1–36. https://doi.org/10.1007/978-94-011-2932-9_1.
- (10) Kloxin, C. J.; Scott, T. F.; Adzima, B. J.; Bowman, C. N. Covalent Adaptable Networks (CANs): A Unique Paradigm in Cross-Linked Polymers. *Macromolecules* **2010**, *43* (6), 2643–2653. <https://doi.org/10.1021/ma902596s>.
- (11) Kloxin, C. J.; Bowman, C. N. Covalent Adaptable Networks: Smart, Reconfigurable and Responsive Network Systems. *Chem. Soc. Rev.* **2013**, *42* (17), 7161–7173. <https://doi.org/10.1039/C3CS60046G>.
- (12) Jin, Y.; Yu, C.; Denman, R. J.; Zhang, W. Recent Advances in Dynamic Covalent Chemistry. *Chem. Soc. Rev.* **2013**, *42* (16), 6634–6654. <https://doi.org/10.1039/C3CS60044K>.
- (13) Scheutz, G. M.; Lessard, J. J.; Sims, M. B.; Sumerlin, B. S. Adaptable Crosslinks in Polymeric Materials: Resolving the Intersection of Thermoplastics and Thermosets. *J. Am. Chem. Soc.* **2019**, *141* (41), 16181–16196. <https://doi.org/10.1021/jacs.9b07922>.
- (14) Van Zee, N. J.; Nicolaÿ, R. Vitrimers: Permanently Crosslinked Polymers with Dynamic Network Topology. *Prog. Polym. Sci.* **2020**, *104*, 101233. <https://doi.org/10.1016/j.progpolymsci.2020.101233>.
- (15) Huang, S.; Kong, X.; Xiong, Y.; Zhang, X.; Chen, H.; Jiang, W.; Niu, Y.; Xu, W.; Ren, C. An Overview of Dynamic Covalent Bonds in Polymer Material and Their Applications. *Eur. Polym. J.* **2020**, *141* (September), 110094. <https://doi.org/10.1016/j.eurpolymj.2020.110094>.

- (16) Chakma, P.; Konkolewicz, D. Dynamic Covalent Bonds in Polymeric Materials. *Angew. Chemie - Int. Ed.* **2019**, *58* (29), 9682–9695. <https://doi.org/10.1002/anie.201813525>.
- (17) Krishnakumar, B.; Sanka, R. V. S. P.; Binder, W. H.; Parthasarthy, V.; Rana, S.; Karak, N. Vitrimers: Associative Dynamic Covalent Adaptive Networks in Thermoset Polymers. *Chem. Eng. J.* **2020**, *385* (July 2019), 123820. <https://doi.org/10.1016/j.cej.2019.123820>.
- (18) Schaufelberger, F.; Timmer, B. J. J.; Ramström, O. Principles of Dynamic Covalent Chemistry. *Dynamic Covalent Chemistry*. October 2, 2017, pp 1–30. <https://doi.org/https://doi.org/10.1002/9781119075738.ch1>.
- (19) Winne, J. M.; Leibler, L.; Du Prez, F. E. Dynamic Covalent Chemistry in Polymer Networks: A Mechanistic Perspective. *Polym. Chem.* **2019**, *10* (45), 6091–6108. <https://doi.org/10.1039/c9py01260e>.
- (20) Ninh, C.; Bettinger, C. J. Reconfigurable Biodegradable Shape-Memory Elastomers via Diels–Alder Coupling. *Biomacromolecules* **2013**, *14* (7), 2162–2170. <https://doi.org/10.1021/bm4002602>.
- (21) Zhang, G.; Zhao, Q.; Yang, L.; Zou, W.; Xi, X.; Xie, T. Exploring Dynamic Equilibrium of Diels–Alder Reaction for Solid State Plasticity in Remoldable Shape Memory Polymer Network. *ACS Macro Lett.* **2016**, *5* (7), 805–808. <https://doi.org/10.1021/acsmacrolett.6b00357>.
- (22) Das, S.; Samitsu, S.; Nakamura, Y.; Yamauchi, Y.; Payra, D.; Kato, K.; Naito, M. Thermo-Resettable Cross-Linked Polymers for Reusable/Removable Adhesives. *Polym. Chem.* **2018**, *9* (47), 5559–5565. <https://doi.org/10.1039/c8py01495g>.
- (23) Liu, C.; Park, E.; Jin, Y.; Liu, J.; Yu, Y.; Zhang, W.; Lei, S.; Hu, W. Surface-Confined Dynamic Covalent System Driven by Olefin Metathesis. *Angew. Chemie Int. Ed.* **2018**, *57* (7), 1869–1873. <https://doi.org/10.1002/anie.201711040>.
- (24) Lu, Y.-X.; Guan, Z. Olefin Metathesis for Effective Polymer Healing via Dynamic Exchange of Strong Carbon–Carbon Double Bonds. *J. Am. Chem. Soc.* **2012**, *134* (34), 14226–14231. <https://doi.org/10.1021/ja306287s>.
- (25) Memon, H.; Liu, H.; Rashid, M. A.; Chen, L.; Jiang, Q.; Zhang, L.; Wei, Y.; Liu, W.; Qiu, Y. Vanillin-Based Epoxy Vitrimer with High Performance and Closed-Loop Recyclability. *Macromolecules* **2020**, *53* (2), 621–630. <https://doi.org/10.1021/acs.macromol.9b02006>.
- (26) Zheng, P.; McCarthy, T. J. A Surprise from 1954: Siloxane Equilibration Is a Simple, Robust, and Obvious Polymer Self-Healing Mechanism. *J. Am. Chem. Soc.* **2012**, *134* (4), 2024–2027. <https://doi.org/10.1021/ja2113257>.
- (27) Rekondo, A.; Martin, R.; Ruiz De Luzuriaga, A.; Cabañero, G.; Grande, H. J.; Odriozola, I. Catalyst-Free Room-Temperature Self-Healing Elastomers Based on Aromatic Disulfide Metathesis. *Mater. Horizons* **2014**, *1* (2), 237–240. <https://doi.org/10.1039/c3mh00061c>.
- (28) Matxain, J. M.; Asua, J. M.; Ruy Pérez, F. Design of New Disulfide-Based Organic Compounds for the Improvement of Self-Healing Materials. *Phys. Chem. Chem. Phys.* **2016**, *18* (3), 1758–1770. <https://doi.org/10.1039/c5cp06660c>.
- (29) Chao, A.; Zhang, D. Investigation of Secondary Amine-Derived Aminal Bond Exchange toward the Development of Covalent Adaptable Networks. *Macromolecules* **2019**, *52* (2), 495–503.

<https://doi.org/10.1021/acs.macromol.8b02654>.

- (30) Denissen, W.; Rivero, G.; Nicolaÿ, R.; Leibler, L.; Winne, J. M.; Du Prez, F. E. Vinylogous Urethane Vitrimers. *Adv. Funct. Mater.* **2015**, *25* (16), 2451–2457. <https://doi.org/10.1002/adfm.201404553>.
- (31) Montarnal, D.; Capelot, M.; Tournilhac, F.; Leibler, L. Silica-like Malleable Materials from Permanent Organic Networks. *Science (80-.)*. **2011**, *334* (6058), 965–968. <https://doi.org/10.1126/science.1212648>.
- (32) Imbernon, L.; Oikonomou, E. K.; Norvez, S.; Leibler, L. Chemically Crosslinked yet Reprocessable Epoxidized Natural Rubber via Thermo-Activated Disulfide Rearrangements. *Polym. Chem.* **2015**, *6* (23), 4271–4278. <https://doi.org/10.1039/C5PY00459D>.
- (33) Matxain, J. M.; Asua, J. M.; Ruipérez, F. Design of New Disulfide-Based Organic Compounds for the Improvement of Self-Healing Materials. *Phys. Chem. Chem. Phys.* **2016**, *18* (3), 1758–1770. <https://doi.org/10.1039/c5cp06660c>.
- (34) Lei, Z. Q.; Xiang, H. P.; Yuan, Y. J.; Rong, M. Z.; Zhang, M. Q. Room-Temperature Self-Healable and Remoldable Cross-Linked Polymer Based on the Dynamic Exchange of Disulfide Bonds. *Chem. Mater.* **2014**, *26* (6), 2038–2046. <https://doi.org/10.1021/cm4040616>.
- (35) Johnson, L. M.; Ledet, E.; Huffman, N. D.; Swarner, S. L.; Shepherd, S. D.; Durham, P. G.; Rothrock, G. D. Controlled Degradation of Disulfide-Based Epoxy Thermosets for Extreme Environments. *Polymer (Guildf)*. **2015**, *64*, 84–92. <https://doi.org/10.1016/j.polymer.2015.03.020>.
- (36) Mandal, B.; Basu, B. Recent Advances in S-S Bond Formation. *RSC Adv.* **2014**, *4* (27), 13854–13881. <https://doi.org/10.1039/c3ra45997g>.
- (37) Ma, Z.; Wang, Y.; Zhu, J.; Yu, J.; Hu, Z. Bio-Based Epoxy Vitrimers: Reprocessability, Controllable Shape Memory, and Degradability. *J. Polym. Sci. Part A Polym. Chem.* **2017**, *55* (10), 1790–1799. <https://doi.org/10.1002/pola.28544>.
- (38) Johnson, L. M.; Ledet, E.; Huffman, N. D.; Swarner, S. L.; Shepherd, S. D.; Durham, P. G.; Rothrock, G. D. Controlled Degradation of Disulfide-Based Epoxy Thermosets for Extreme Environments. *Polymer (Guildf)*. **2015**, *64*, 84–92. <https://doi.org/https://doi.org/10.1016/j.polymer.2015.03.020>.
- (39) Ruiz De Luzuriaga, A.; Martin, R.; Markaide, N.; Rekondo, A.; Cabañero, G.; Rodríguez, J.; Odriozola, I. Epoxy Resin with Exchangeable Disulfide Crosslinks to Obtain Reprocessable, Repairable and Recyclable Fiber-Reinforced Thermoset Composites. *Mater. Horizons* **2016**, *3* (3), 241–247. <https://doi.org/10.1039/c6mh00029k>.
- (40) Ji, F.; Liu, X.; Sheng, D.; Yang, Y. Epoxy-Vitrimer Composites Based on Exchangeable Aromatic Disulfide Bonds: Reprocessability, Adhesive, Multi-Shape Memory Effect. *Polymer (Guildf)*. **2020**, *197* (April), 122514. <https://doi.org/10.1016/j.polymer.2020.122514>.
- (41) Takahashi, A.; Ohishi, T.; Goseki, R.; Otsuka, H. Degradable Epoxy Resins Prepared from Diepoxide Monomer with Dynamic Covalent Disulfide Linkage. *Polymer (Guildf)*. **2016**, *82*, 319–326. <https://doi.org/10.1016/j.polymer.2015.11.057>.
- (42) Black, S. P.; Sanders, J. K. M.; Stefankiewicz, A. R. Disulfide Exchange: Exposing Supramolecular Reactivity through Dynamic Covalent Chemistry. *Chem. Soc. Rev.* **2014**, *43* (6), 1861–1872. <https://doi.org/10.1039/c3cs60326a>.

- (43) Canadell, J.; Goossens, H.; Klumperman, B. Self-Healing Materials Based on Disulfide Links. *Macromolecules* **2011**, *44* (8), 2536–2541. <https://doi.org/10.1021/ma2001492>.
- (44) Zhou, F.; Guo, Z.; Wang, W.; Lei, X.; Zhang, B.; Zhang, H.; Zhang, Q. Preparation of Self-Healing, Recyclable Epoxy Resins and Low-Electrical Resistance Composites Based on Double-Disulfide Bond Exchange. *Compos. Sci. Technol.* **2018**, *167* (July), 79–85. <https://doi.org/10.1016/j.compscitech.2018.07.041>.
- (45) Si, H.; Zhou, L.; Wu, Y.; Song, L.; Kang, M.; Zhao, X.; Chen, M. Rapidly Reprocessable, Degradable Epoxy Vitrimer and Recyclable Carbon Fiber Reinforced Thermoset Composites Relied on High Contents of Exchangeable Aromatic Disulfide Crosslinks. *Compos. Part B Eng.* **2020**, *199* (July), 108278. <https://doi.org/10.1016/j.compositesb.2020.108278>.
- (46) Denissen, W.; Winne, J. M.; Du Prez, F. E. Vitrimers: Permanent Organic Networks with Glass-like Fluidity. *Chem. Sci.* **2016**, *7* (1), 30–38. <https://doi.org/10.1039/c5sc02223a>.
- (47) Chen, L.; Zhu, S.; Toendepi, I.; Jiang, Q.; Wei, Y.; Qiu, Y.; Liu, W. Reprocessable, Reworkable, and Mechanochromic Polyhexahydrotriazine Thermoset with Multiple Stimulus Responsiveness. *Polymers (Basel)*. **2020**, *12* (10), 1–13. <https://doi.org/10.3390/polym12102375>.
- (48) Ruiz De Luzuriaga, A.; Matxain, J. M.; Ruipérez, F.; Martin, R.; Asua, J. M.; Cabañero, G.; Odriozola, I. Transient Mechanochromism in Epoxy Vitrimer Composites Containing Aromatic Disulfide Crosslinks. *J. Mater. Chem. C* **2016**, *4* (26), 6220–6223. <https://doi.org/10.1039/c6tc02383e>.
- (49) Engels, T. 8 - Thermoset Adhesives: Epoxy Resins, Acrylates and Polyurethanes; Guo, Q. B. T.-T., Ed.; Woodhead Publishing, 2012; pp 228–253. <https://doi.org/https://doi.org/10.1533/9780857097637.2.228>.
- (50) Dodiuk, H.; Goodman, S. H. 1 - Introduction; Dodiuk, H., Goodman, S. H. B. T.-H. of T. P. (Third E., Eds.; William Andrew Publishing: Boston, 2014; pp 1–12. <https://doi.org/https://doi.org/10.1016/B978-1-4557-3107-7.00001-4>.
- (51) Dr Premamoy Ghosh, P. D. Addition Polymerization or Chain-Growth Polymerization; McGraw-Hill Education: New York, 2011.
- (52) Ravve, A. Introduction and Nomenclature BT - Principles of Polymer Chemistry; Ravve, A., Ed.; Springer New York: New York, NY, 2012; pp 1–15. https://doi.org/10.1007/978-1-4614-2212-9_1.
- (53) Dr Premamoy Ghosh, P. D. Condensation Polymerization or Step-Growth Polymerization; McGraw-Hill Education: New York, 2011.
- (54) Sun, Y.; Zhang, Z.; Moon, K.-S.; Wong, C. P. Glass Transition and Relaxation Behavior of Epoxy Nanocomposites. *J. Polym. Sci. Part B Polym. Phys.* **2004**, *42* (21), 3849–3858. <https://doi.org/https://doi.org/10.1002/polb.20251>.
- (55) Gardea, F.; Lagoudas, D. C. Characterization of Electrical and Thermal Properties of Carbon Nanotube/Epoxy Composites. *Compos. Part B Eng.* **2014**, *56*, 611–620. <https://doi.org/https://doi.org/10.1016/j.compositesb.2013.08.032>.
- (56) Tan, S. G.; Chow, W. S. Curing Characteristics and Thermal Properties of Epoxidized Soybean Oil Based Thermosetting Resin. *J. Am. Oil Chem. Soc.* **2011**, *88* (7), 915–923. <https://doi.org/10.1007/s11746-010-1748-x>.

- (57) Saleem, H.; Edathil, A.; Ncube, T.; Pokhrel, J.; Khoori, S.; Abraham, A.; Mittal, V. Mechanical and Thermal Properties of Thermoset–Graphene Nanocomposites. *Macromol. Mater. Eng.* **2016**, *301* (3), 231–259. <https://doi.org/https://doi.org/10.1002/mame.201500335>.
- (58) Vengatesan, M. R.; Varghese, A. M.; Mittal, V. Chapter 3 - Thermal Properties of Thermoset Polymers; Guo, Q. B. T.-T. (Second E., Ed.; Elsevier, 2018; pp 69–114. <https://doi.org/https://doi.org/10.1016/B978-0-08-101021-1.00003-4>.
- (59) Wetton, R. E.; Marsh, R. D. L.; Van-de-Velde, J. G. Theory and Application of Dynamic Mechanical Thermal Analysis. *Thermochim. Acta* **1991**, *175* (1), 1–11. [https://doi.org/https://doi.org/10.1016/0040-6031\(91\)80240-J](https://doi.org/https://doi.org/10.1016/0040-6031(91)80240-J).
- (60) Romo-Urbe, A. Dynamic Mechanical Thermal Analysis of Epoxy/Thermoplastic Blends BT - Handbook of Epoxy Blends; Parameswaranpillai, J., Hameed, N., Pionteck, J., Woo, E. M., Eds.; Springer International Publishing: Cham, 2017; pp 675–706. https://doi.org/10.1007/978-3-319-40043-3_23.
- (61) Akay, M. Aspects of Dynamic Mechanical Analysis in Polymeric Composites. *Compos. Sci. Technol.* **1993**, *47* (4), 419–423. [https://doi.org/https://doi.org/10.1016/0266-3538\(93\)90010-E](https://doi.org/https://doi.org/10.1016/0266-3538(93)90010-E).
- (62) Menard, K. P.; Menard, N. Dynamic Mechanical Analysis. *Encyclopedia of Analytical Chemistry*. September 15, 2017, pp 1–25. <https://doi.org/https://doi.org/10.1002/9780470027318.a2007.pub3>.
- (63) Mullins, M. J.; Liu, D.; Sue, H.-J. Chapter 2 - Mechanical Properties of Thermosets; Guo, Q. B. T.-T. (Second E., Ed.; Elsevier, 2018; pp 35–68. <https://doi.org/https://doi.org/10.1016/B978-0-08-101021-1.00002-2>.
- (64) Ebnesajjad, S.; Landrock, A. H. Chapter 1 - Introduction and Adhesion Theories. In *Adhesives Technology Handbook (Third Edition)*; Ebnesajjad, S., Landrock, A. H. B. T.-A. T. H. (Third E., Eds.; William Andrew Publishing: Boston, 2015; pp 1–18. <https://doi.org/https://doi.org/10.1016/B978-0-323-35595-7.00001-2>.
- (65) Shields, J. 1 - Introduction. In *Adhesives Handbook*; Shields, J. B. T.-A. H. (Third E., Ed.; Butterworth-Heinemann, 1984; pp 1–6. <https://doi.org/https://doi.org/10.1016/B978-0-408-01356-7.50006-9>.
- (66) da Silva, L. F. M.; Öchsner, A.; Adams, R. D. Introduction to Adhesive Bonding Technology BT - Handbook of Adhesion Technology; da Silva, L. F. M., Öchsner, A., Adams, R. D., Eds.; Springer Berlin Heidelberg: Berlin, Heidelberg, 2011; pp 1–7. https://doi.org/10.1007/978-3-642-01169-6_1.
- (67) Shields, J. 4 - Adhesive Materials and Properties; Shields, J. B. T.-A. H. (Third E., Ed.; Butterworth-Heinemann, 1984; pp 30–86. <https://doi.org/https://doi.org/10.1016/B978-0-408-01356-7.50009-4>.
- (68) Prolongo, S. G.; del Rosario, G.; Ureña, A. Comparative Study on the Adhesive Properties of Different Epoxy Resins. *Int. J. Adhes. Adhes.* **2006**, *26* (3), 125–132. <https://doi.org/https://doi.org/10.1016/j.ijadhadh.2005.02.004>.
- (69) Bascom, W. D.; Cottington, R. L. Effect of Temperature on the Adhesive Fracture Behavior of an Elastomer-Epoxy Resin. *J. Adhes.* **1976**, *7* (4), 333–346. <https://doi.org/10.1080/00218467608075063>.
- (70) Lapique, F.; Redford, K. Curing Effects on Viscosity and Mechanical Properties of a Commercial

- Epoxy Resin Adhesive. *Int. J. Adhes. Adhes.* **2002**, 22 (4), 337–346.
[https://doi.org/https://doi.org/10.1016/S0143-7496\(02\)00013-1](https://doi.org/https://doi.org/10.1016/S0143-7496(02)00013-1).
- (71) Pruksawan, S.; Samitsu, S.; Fujii, Y.; Torikai, N.; Naito, M. Toughening Effect of Rodlike Cellulose Nanocrystals in Epoxy Adhesive. *ACS Appl. Polym. Mater.* **2020**, 2 (3), 1234–1243.
<https://doi.org/10.1021/acsapm.9b01102>.
- (72) Pruksawan, S.; Samitsu, S.; Yokoyama, H.; Naito, M. Homogeneously Dispersed Polyrotaxane in Epoxy Adhesive and Its Improvement in the Fracture Toughness. *Macromolecules* **2019**, 52 (6), 2464–2475. <https://doi.org/10.1021/acs.macromol.8b02450>.
- (73) Pruksawan, S.; Lambard, G.; Samitsu, S.; Sodeyama, K.; Naito, M. Prediction and Optimization of Epoxy Adhesive Strength from a Small Dataset through Active Learning. *Sci. Technol. Adv. Mater.* **2019**, 20 (1), 1010–1021. <https://doi.org/10.1080/14686996.2019.1673670>.
- (74) Abbey, K. J. 2 - Advances in Epoxy Adhesives. In *Woodhead Publishing Series in Welding and Other Joining Technologies*; Dillard, D. A. B. T.-A. in S. A. B., Ed.; Woodhead Publishing, 2010; pp 20–34.
<https://doi.org/https://doi.org/10.1533/9781845698058.1.20>.
- (75) Jin, F.-L.; Li, X.; Park, S.-J. Synthesis and Application of Epoxy Resins: A Review. *J. Ind. Eng. Chem.* **2015**, 29, 1–11. <https://doi.org/10.1016/j.jiec.2015.03.026>.
- (76) Adams, R. D.; Coppendale, J.; Mallick, V.; Al-Hamdan, H. The Effect of Temperature on the Strength of Adhesive Joints. *Int. J. Adhes. Adhes.* **1992**, 12 (3), 185–190. [https://doi.org/10.1016/0143-7496\(92\)90052-W](https://doi.org/10.1016/0143-7496(92)90052-W).
- (77) da Silva, L. F. M.; Adams, R. D. Adhesive Joints at High and Low Temperatures Using Similar and Dissimilar Adherends and Dual Adhesives. *Int. J. Adhes. Adhes.* **2007**, 27 (3), 216–226.
<https://doi.org/10.1016/j.ijadhadh.2006.04.002>.
- (78) Grant, L. D. R.; Adams, R. D.; da Silva, L. F. M. Effect of the Temperature on the Strength of Adhesively Bonded Single Lap and T Joints for the Automotive Industry. *Int. J. Adhes. Adhes.* **2009**, 29 (5), 535–542. <https://doi.org/10.1016/j.ijadhadh.2009.01.002>.
- (79) Taynton, P.; Ni, H.; Zhu, C.; Yu, K.; Loob, S.; Jin, Y.; Qi, H. J.; Zhang, W. Repairable Woven Carbon Fiber Composites with Full Recyclability Enabled by Malleable Polyimine Networks. *Adv. Mater.* **2016**, 28 (15), 2904–2909. <https://doi.org/10.1002/adma.201505245>.
- (80) Ivleva, N. P.; Wiesheu, A. C.; Niessner, R. Microplastic in Aquatic Ecosystems. *Angew. Chemie Int. Ed.* **2017**, 56 (7), 1720–1739. <https://doi.org/https://doi.org/10.1002/anie.201606957>.
- (81) Rillig, M. C.; Lehmann, A. Microplastic in Terrestrial Ecosystems. *Science (80-.)*. **2020**, 368 (6498), 1430 LP – 1431. <https://doi.org/10.1126/science.abb5979>.
- (82) Rillig, M. C.; Ziersch, L.; Hempel, S. Microplastic Transport in Soil by Earthworms. *Sci. Rep.* **2017**, 7 (1), 1362. <https://doi.org/10.1038/s41598-017-01594-7>.
- (83) Lönnstedt, O. M.; Eklöv, P. Environmentally Relevant Concentrations of Microplastic Particles Influence Larval Fish Ecology. *Science (80-.)*. **2016**, 352 (6290), 1213 LP – 1216.
<https://doi.org/10.1126/science.aad8828>.
- (84) Yue, L.; Amirhosravi, M.; Gong, X.; Gray, T. G.; Manas-Zloczower, I. Recycling Epoxy by Vitrimization: Influence of an Initial Thermoset Chemical Structure. *ACS Sustain. Chem. Eng.* **2020**,

- 8 (33), 12706–12712. <https://doi.org/10.1021/acssuschemeng.0c04815>.
- (85) Kuang, X.; Zhou, Y.; Shi, Q.; Wang, T.; Qi, H. J. Recycling of Epoxy Thermoset and Composites via Good Solvent Assisted and Small Molecules Participated Exchange Reactions. *ACS Sustain. Chem. Eng.* **2018**, *6* (7), 9189–9197. <https://doi.org/10.1021/acssuschemeng.8b01538>.
- (86) Liu, Y.; Meng, L.; Huang, Y.; Du, J. Recycling of Carbon/Epoxy Composites. *J. Appl. Polym. Sci.* **2004**, *94* (5), 1912–1916. <https://doi.org/https://doi.org/10.1002/app.20990>.
- (87) Oliveux, G.; Dandy, L. O.; Leeke, G. A. Current Status of Recycling of Fibre Reinforced Polymers: Review of Technologies, Reuse and Resulting Properties. *Prog. Mater. Sci.* **2015**, *72*, 61–99. <https://doi.org/10.1016/j.pmatsci.2015.01.004>.
- (88) Pickering, S. J. Recycling Technologies for Thermoset Composite Materials—Current Status. *Compos. Part A Appl. Sci. Manuf.* **2006**, *37* (8), 1206–1215. <https://doi.org/https://doi.org/10.1016/j.compositesa.2005.05.030>.
- (89) Oliveux, G.; Dandy, L. O.; Leeke, G. A. Current Status of Recycling of Fibre Reinforced Polymers: Review of Technologies, Reuse and Resulting Properties. *Progress in Materials Science*. Elsevier Ltd July 1, 2015, pp 61–99. <https://doi.org/10.1016/j.pmatsci.2015.01.004>.
- (90) Wang, L.; Wong, C. P. Syntheses and Characterizations of Thermally Reworkable Epoxy Resins. Part I. *J. Polym. Sci. Part A Polym. Chem.* **1999**, *37* (15), 2991–3001. [https://doi.org/10.1002/\(SICI\)1099-0518\(19990801\)37:15<2991::AID-POLA32>3.0.CO;2-V](https://doi.org/10.1002/(SICI)1099-0518(19990801)37:15<2991::AID-POLA32>3.0.CO;2-V).
- (91) Musto, P. Two-Dimensional FTIR Spectroscopy Studies on the Thermal-Oxidative Degradation of Epoxy and Epoxy–Bis(Maleimide) Networks. *Macromolecules* **2003**, *36* (9), 3210–3221. <https://doi.org/10.1021/ma0214815>.
- (92) Rahimi, A.; García, J. M. Chemical Recycling of Waste Plastics for New Materials Production. *Nat. Rev. Chem.* **2017**, *1* (6), 46. <https://doi.org/10.1038/s41570-017-0046>.
- (93) Kuang, X.; Zhou, Y.; Shi, Q.; Wang, T.; Qi, H. J. Recycling of Epoxy Thermoset and Composites via Good Solvent Assisted and Small Molecules Participated Exchange Reactions. *ACS Sustain. Chem. Eng.* **2018**, *6* (7), 9189–9197. <https://doi.org/10.1021/acssuschemeng.8b01538>.
- (94) Wang, Y.; Cui, X.; Ge, H.; Yang, Y.; Wang, Y.; Zhang, C.; Li, J.; Deng, T.; Qin, Z.; Hou, X. Chemical Recycling of Carbon Fiber Reinforced Epoxy Resin Composites via Selective Cleavage of the Carbon-Nitrogen Bond. *ACS Sustain. Chem. Eng.* **2015**, *3* (12), 3332–3337. <https://doi.org/10.1021/acssuschemeng.5b00949>.
- (95) Lo, J. N.; Nutt, S. R.; Williams, T. J. Recycling Benzoxazine-Epoxy Composites via Catalytic Oxidation. *ACS Sustain. Chem. Eng.* **2018**, *6* (6), 7227–7231. <https://doi.org/10.1021/acssuschemeng.8b01790>.
- (96) Yue, L.; Amirhosravi, M.; Gong, X.; Gray, T. G.; Manas-Zloczower, I. Recycling Epoxy by Vitrimization: Influence of an Initial Thermoset Chemical Structure. *ACS Sustain. Chem. Eng.* **2020**, *8* (33), 12706–12712. <https://doi.org/10.1021/acssuschemeng.0c04815>.
- (97) Wang, B.; Ma, S.; Yan, S.; Zhu, J. Readily Recyclable Carbon Fiber Reinforced Composites Based on Degradable Thermosets: A Review. *Green Chem.* **2019**, *21* (21), 5781–5796. <https://doi.org/10.1039/C9GC01760G>.

- (98) Zou, W.; Dong, J.; Luo, Y.; Zhao, Q.; Xie, T. Dynamic Covalent Polymer Networks: From Old Chemistry to Modern Day Innovations. *Adv. Mater.* **2017**, *29* (14), 1606100. <https://doi.org/10.1002/adma.201606100>.
- (99) Scheutz, G. M.; Lessard, J. J.; Sims, M. B.; Sumerlin, B. S. Adaptable Crosslinks in Polymeric Materials: Resolving the Intersection of Thermoplastics and Thermosets. *J. Am. Chem. Soc.* **2019**, *141* (41), 16181–16196. <https://doi.org/10.1021/jacs.9b07922>.
- (100) Otera, J. Transesterification. *Chem. Rev.* **1993**, *93* (4), 1449–1470. <https://doi.org/10.1021/cr00020a004>.
- (101) Hendriks, B.; Waelkens, J.; Winne, J. M.; Du Prez, F. E. Poly(Thioether) Vitrimers via Transalkylation of Trialkylsulfonium Salts. *ACS Macro Lett.* **2017**, *6* (9), 930–934. <https://doi.org/10.1021/acsmacrolett.7b00494>.
- (102) Obadia, M. M.; Mudraboyina, B. P.; Serghei, A.; Montarnal, D.; Drockenmuller, E. Reprocessing and Recycling of Highly Cross-Linked Ion-Conducting Networks through Transalkylation Exchanges of C–N Bonds. *J. Am. Chem. Soc.* **2015**, *137* (18), 6078–6083. <https://doi.org/10.1021/jacs.5b02653>.
- (103) Konetski, D.; Mavila, S.; Wang, C.; Worrell, B.; Bowman, C. N. Production of Dynamic Lipid Bilayers Using the Reversible Thiol–Thioester Exchange Reaction. *Chem. Commun.* **2018**, *54* (58), 8108–8111. <https://doi.org/10.1039/C8CC03471K>.
- (104) Ghobril, C.; Charoen, K.; Rodriguez, E. K.; Nazarian, A.; Grinstaff, M. W. A Dendritic Thioester Hydrogel Based on Thiol–Thioester Exchange as a Dissolvable Sealant System for Wound Closure. *Angew. Chemie Int. Ed.* **2013**, *52* (52), 14070–14074. <https://doi.org/https://doi.org/10.1002/anie.201308007>.
- (105) Konieczynska, M. D.; Villa-Camacho, J. C.; Ghobril, C.; Perez-Viloria, M.; Tevis, K. M.; Blessing, W. A.; Nazarian, A.; Rodriguez, E. K.; Grinstaff, M. W. On-Demand Dissolution of a Dendritic Hydrogel-Based Dressing for Second-Degree Burn Wounds through Thiol–Thioester Exchange Reaction. *Angew. Chemie Int. Ed.* **2016**, *55* (34), 9984–9987. <https://doi.org/https://doi.org/10.1002/anie.201604827>.
- (106) Ochmann, M.; Hussain, A.; Von Ahnen, I.; Cordones, A. A.; Hong, K.; Lee, J. H.; Ma, R.; Adamczyk, K.; Kim, T. K.; Schoenlein, R. W.; Vendrell, O.; Huse, N. UV-Photochemistry of the Disulfide Bond: Evolution of Early Photoproducts from Picosecond X-Ray Absorption Spectroscopy at the Sulfur K-Edge. *J. Am. Chem. Soc.* **2018**, *140* (21), 6554–6561. <https://doi.org/10.1021/jacs.7b13455>.
- (107) Lei, Z. Q.; Xiang, H. P.; Yuan, Y. J.; Rong, M. Z.; Zhang, M. Q. Room-Temperature Self-Healable and Remoldable Cross-Linked Polymer Based on the Dynamic Exchange of Disulfide Bonds. *Chem. Mater.* **2014**, *26* (6), 2038–2046. <https://doi.org/10.1021/cm4040616>.
- (108) An, X.; Aguirresarobe, R. H.; Irusta, L.; Ruipérez, F.; Matxain, J. M.; Pan, X.; Aramburu, N.; Mecerreyes, D.; Sardon, H.; Zhu, J. Aromatic Diselenide Crosslinkers to Enhance the Reprocessability and Self-Healing of Polyurethane Thermosets. *Polym. Chem.* **2017**, *8* (23), 3641–3646. <https://doi.org/10.1039/C7PY00448F>.
- (109) Ji, S.; Cao, W.; Yu, Y.; Xu, H. Dynamic Diselenide Bonds: Exchange Reaction Induced by Visible Light without Catalysis. *Angew. Chemie Int. Ed.* **2014**, *53* (26), 6781–6785.

<https://doi.org/https://doi.org/10.1002/anie.201403442>.

- (110) Turkenburg, D. H.; van Bracht, H.; Funke, B.; Schmider, M.; Janke, D.; Fischer, H. R. Polyurethane Adhesives Containing Diels–Alder-Based Thermoreversible Bonds. *J. Appl. Polym. Sci.* **2017**, *134* (26), 44972–44982. <https://doi.org/10.1002/app.44972>.
- (111) Adzima, B. J.; Aguirre, H. A.; Kloxin, C. J.; Scott, T. F.; Bowman, C. N. Rheological and Chemical Analysis of Reverse Gelation in a Covalently Cross-Linked Diels–Alder Polymer Network. *Macromolecules* **2008**, *41* (23), 9112–9117. <https://doi.org/10.1021/ma801863d>.
- (112) Polyakov, V. A.; Nelen, M. I.; Nazarpak-Kandlousy, N.; Ryabov, A. D.; Eliseev, A. V. Imine Exchange in O-Aryl and O-Alkyl Oximes as a Base Reaction for Aqueous ‘Dynamic’ Combinatorial Libraries. A Kinetic and Thermodynamic Study. *J. Phys. Org. Chem.* **1999**, *12* (5), 357–363. [https://doi.org/https://doi.org/10.1002/\(SICI\)1099-1395\(199905\)12:5<357::AID-POC129>3.0.CO;2-Y](https://doi.org/https://doi.org/10.1002/(SICI)1099-1395(199905)12:5<357::AID-POC129>3.0.CO;2-Y).
- (113) Rowan, S. J.; Stoddart, J. F. Thermodynamic Synthesis of Rotaxanes by Imine Exchange. *Org. Lett.* **1999**, *1* (12), 1913–1916. <https://doi.org/10.1021/ol991047w>.
- (114) Ciaccia, M.; Di Stefano, S. Mechanisms of Imine Exchange Reactions in Organic Solvents. *Org. Biomol. Chem.* **2015**, *13* (3), 646–654. <https://doi.org/10.1039/C4OB02110J>.
- (115) Cash, J. J.; Kubo, T.; Dobbins, D. J.; Sumerlin, B. S. Maximizing the Symbiosis of Static and Dynamic Bonds in Self-Healing Boronic Ester Networks. *Polym. Chem.* **2018**, *9* (15), 2011–2020. <https://doi.org/10.1039/C8PY00123E>.
- (116) Cash, J. J.; Kubo, T.; Bapat, A. P.; Sumerlin, B. S. Room-Temperature Self-Healing Polymers Based on Dynamic-Covalent Boronic Esters. *Macromolecules* **2015**, *48* (7), 2098–2106. <https://doi.org/10.1021/acs.macromol.5b00210>.
- (117) Cromwell, O. R.; Chung, J.; Guan, Z. Malleable and Self-Healing Covalent Polymer Networks through Tunable Dynamic Boronic Ester Bonds. *J. Am. Chem. Soc.* **2015**, *137* (20), 6492–6495. <https://doi.org/10.1021/jacs.5b03551>.
- (118) Bowman, C. N.; Kloxin, C. J. Covalent Adaptable Networks: Reversible Bond Structures Incorporated in Polymer Networks. *Angew. Chemie Int. Ed.* **2012**, *51* (18), 4272–4274. <https://doi.org/10.1002/anie.201200708>.
- (119) Solid, L. D.; Hrubesh, L. W.; Chan, H. M.; Grenestedt, J. L.; Harmer, M. P.; Caram, H. S.; Roy, S. K.; Handbook, P. T.; Raton, B.; Ashby, M. F.; Jullien, R.; Scherer, G. W.; Nutt, S.; Nutt, S.; Nutt, S.; Lee, D. N.; Lee, Y. S.; Hsiao, H. L.; Chang, T. K.; Hartmann, B.; Dickrell, P. L.; Sawyer, W. G.; Ajayan, P. M.; Schuh, C. A.; Schlieff, T.; Fricke, J.; Kucheyev, S. O.; Hamza, A. V.; Baumann, T. F.; Fleck, N. A.; Ashby, M. F.; Ashby, M. F.; Fleck, N. A.; Fleck, N. A.; Ashby, M. F.; Attributes, H. H.; Roig, A.; Molins, E.; Martinez, E.; Esteve, J.; Hutchinson, J. W. Silica-Like Malleable Materials From. **2011**, No. November, 965–969.
- (120) Yang, Y.; Zhang, S.; Zhang, X.; Gao, L.; Wei, Y.; Ji, Y. Detecting Topology Freezing Transition Temperature of Vitrimers by AIE Luminogens. *Nat. Commun.* **2019**, *10* (1), 1–8. <https://doi.org/10.1038/s41467-019-11144-6>.
- (121) Kaiser, S.; Novak, P.; Giebler, M.; Gschwandl, M.; Novak, P.; Pilz, G.; Morak, M.; Schlögl, S. The Crucial Role of External Force in the Estimation of the Topology Freezing Transition Temperature of

- Vitrimers by Elongational Creep Measurements. *Polymer (Guildf)*. **2020**, *204*, 122804.
<https://doi.org/https://doi.org/10.1016/j.polymer.2020.122804>.
- (122) Bach, R. D.; Dmitrenko, O.; Thorpe, C. Mechanism of Thiolate-Disulfide Interchange Reactions in Biochemistry. *J. Org. Chem.* **2008**, *73* (1), 12–21. <https://doi.org/10.1021/jo702051f>.
- (123) Altuna, F. I.; Hoppe, C. E.; Williams, R. J. J. Shape Memory Epoxy Vitrimers Based on DGEBA Crosslinked with Dicarboxylic Acids and Their Blends with Citric Acid. *RSC Adv.* **2016**, *6* (91), 88647–88655. <https://doi.org/10.1039/C6RA18010H>.
- (124) Meng, F.; Saed, M. O.; Terentjev, E. M. Elasticity and Relaxation in Full and Partial Vitriimer Networks. *Macromolecules* **2019**, *52* (19), 7423–7429.
<https://doi.org/10.1021/acs.macromol.9b01123>.
- (125) Denissen, W.; Droesbeke, M.; Nicolaÿ, R.; Leibler, L.; Winne, J. M.; Du Prez, F. E. Chemical Control of the Viscoelastic Properties of Vinylogous Urethane Vitrimers. *Nat. Commun.* **2017**, *8* (1), 14857.
<https://doi.org/10.1038/ncomms14857>.
- (126) Chen, M.; Zhou, L.; Wu, Y.; Zhao, X.; Zhang, Y. Rapid Stress Relaxation and Moderate Temperature of Malleability Enabled by the Synergy of Disulfide Metathesis and Carboxylate Transesterification in Epoxy Vitrimers. *ACS Macro Lett.* **2019**, *8* (3), 255–260.
<https://doi.org/10.1021/acsmacrolett.9b00015>.
- (127) Liu, W.; Schmidt, D. F.; Reynaud, E. Catalyst Selection, Creep, and Stress Relaxation in High-Performance Epoxy Vitrimers. *Ind. Eng. Chem. Res.* **2017**, *56* (10), 2667–2672.
<https://doi.org/10.1021/acs.iecr.6b03829>.
- (128) Wang, S.; Ma, S.; Li, Q.; Xu, X.; Wang, B.; Huang, K.; liu, Y.; Zhu, J. Facile Preparation of Polyimine Vitrimers with Enhanced Creep Resistance and Thermal and Mechanical Properties via Metal Coordination. *Macromolecules* **2020**, *53* (8), 2919–2931.
<https://doi.org/10.1021/acs.macromol.0c00036>.
- (129) Li, L.; Chen, X.; Jin, K.; Torkelson, J. M. Vitrimers Designed Both To Strongly Suppress Creep and To Recover Original Cross-Link Density after Reprocessing: Quantitative Theory and Experiments. *Macromolecules* **2018**, *51* (15), 5537–5546. <https://doi.org/10.1021/acs.macromol.8b00922>.
- (130) Black, S. P.; Sanders, J. K. M.; Stefankiewicz, A. R. Disulfide Exchange: Exposing Supramolecular Reactivity through Dynamic Covalent Chemistry. *Chem. Soc. Rev.* **2014**, *43* (6), 1861–1872.
<https://doi.org/10.1039/C3CS60326A>.
- (131) Nagy, P. Kinetics and Mechanisms of Thiol-Disulfide Exchange Covering Direct Substitution and Thiol Oxidation-Mediated Pathways. *Antioxidants Redox Signal.* **2013**, *18* (13), 1623–1641.
<https://doi.org/10.1089/ars.2012.4973>.
- (132) Fava, A.; Iliceto, A.; Camera, E. Kinetics of the Thiol–Disulfide Exchange. *J. Am. Chem. Soc.* **1957**, *79* (4), 833–838. <https://doi.org/10.1021/ja01561a014>.
- (133) Fava, A.; Reichenbach, G.; Peron, U. Kinetics of the Thiol-Disulfide Exchange. II. Oxygen-Promoted Free-Radical Exchange between Aromatic Thiols and Disulfides. *J. Am. Chem. Soc.* **1967**, *89* (25), 6696–6700. <https://doi.org/10.1021/ja01001a052>.
- (134) Fernandes, P. A.; Ramos, M. J. Theoretical Insights into the Mechanism for Thiol/Disulfide Exchange.

- Chem. - A Eur. J.* **2004**, *10* (1), 257–266. <https://doi.org/10.1002/chem.200305343>.
- (135) Pleasants, J. C.; Guo, W.; Rabenstein, D. L. A Comparative Study of the Kinetics of Selenol/Diselenide and Thiol/Disulfide Exchange Reactions. *J. Am. Chem. Soc.* **1989**, *111* (17), 6553–6558. <https://doi.org/10.1021/ja00199a012>.
- (136) Gilbert, H. F. B. T.-M. in E. [2] Thiol/Disulfide Exchange Equilibria and Disulfidebond Stability. In *Biothiols Part A Monothiools and Dithiols, Protein Thiols, and Thiyl Radicals*; Academic Press, 1995; Vol. 251, pp 8–28. [https://doi.org/https://doi.org/10.1016/0076-6879\(95\)51107-5](https://doi.org/https://doi.org/10.1016/0076-6879(95)51107-5).
- (137) Sakai, H.; Aoki, D.; Seshimo, K.; Mayumi, K.; Nishitsuji, S.; Kurose, T.; Ito, H.; Otsuka, H. Visualization and Quantitative Evaluation of Toughening Polymer Networks by a Sacrificial Dynamic Cross-Linker with Mechanochromic Properties. *ACS Macro Lett.* **2020**, *9* (8), 1108–1113. <https://doi.org/10.1021/acsmacrolett.0c00321>.
- (138) Yamane, S.; Sagara, Y.; Mutai, T.; Araki, K.; Kato, T. Mechanochromic Luminescent Liquid Crystals Based on a Bianthryl Moiety. *J. Mater. Chem. C* **2013**, *1* (15), 2648–2656. <https://doi.org/10.1039/C3TC00861D>.
- (139) Calvino, C.; Neumann, L.; Weder, C.; Schrettl, S. Approaches to Polymeric Mechanochromic Materials. *J. Polym. Sci. Part A Polym. Chem.* **2017**, *55* (4), 640–652. <https://doi.org/https://doi.org/10.1002/pola.28445>.
- (140) Lee, J. P.; Hwang, H.; Chae, S.; Kim, J. M. A Reversibly Mechanochromic Conjugated Polymer. *Chem. Commun.* **2019**, *55* (63), 9395–9398. <https://doi.org/10.1039/c9cc03951a>.
- (141) Petrie, E. M. *Handbook of Adhesives and Sealants, Second Edition*, 2nd ed.; McGraw-Hill Education: New York, 2007.
- (142) Da Silva, L. F. M.; Adams, R. D.; Gibbs, M. Manufacture of Adhesive Joints and Bulk Specimens with High-Temperature Adhesives. *Int. J. Adhes. Adhes.* **2004**, *24* (1), 69–83. [https://doi.org/10.1016/S0143-7496\(03\)00101-5](https://doi.org/10.1016/S0143-7496(03)00101-5).
- (143) Andrews, E. H.; Kinloch, A. J.; Melville, H. W. Mechanics of Adhesive Failure. II. *Proc. R. Soc. London. A. Math. Phys. Sci.* **1973**, *332* (1590), 401–414. <https://doi.org/10.1098/rspa.1973.0033>.
- (144) Zosel, A. Adhesive Failure and Deformation Behaviour of Polymers. *J. Adhes.* **1989**, *30* (1–4), 135–149. <https://doi.org/10.1080/00218468908048202>.
- (145) González, M. G.; Cabanelas, J. C.; Baselga, J. Applications of FTIR on Epoxy Resins - Identification, Monitoring the Curing Process, Phase Separation and Water Uptake. *Infrared Spectrosc. - Mater. Sci. Eng. Technol.* **2012**, *2*. <https://doi.org/10.5772/36323>.
- (146) Hernández, B.; Pflüger, F.; López-Tobar, E.; Kruglik, S. G.; Garcia-Ramos, J. V; Sanchez-Cortes, S.; Ghomi, M. Disulfide Linkage Raman Markers: A Reconsideration Attempt. *J. Raman Spectrosc.* **2014**, *45* (8), 657–664. <https://doi.org/https://doi.org/10.1002/jrs.4521>.
- (147) Van Wart, H. E.; Lewis, A.; Scheraga, H. A.; Saeva, F. D. Disulfide Bond Dihedral Angles from Raman Spectroscopy. *Proc. Natl. Acad. Sci.* **1973**, *70* (9), 2619 LP – 2623. <https://doi.org/10.1073/pnas.70.9.2619>.
- (148) Nevejans, S.; Ballard, N.; Miranda, J. I.; Reck, B.; Asua, J. M. The Underlying Mechanisms for Self-Healing of Poly(Disulfide)S. *Phys. Chem. Chem. Phys.* **2016**, *18* (39), 27577–27583.

<https://doi.org/10.1039/c6cp04028d>.

- (149) Yang, X.; Guo, L.; Xu, X.; Shang, S.; Liu, H. A Fully Bio-Based Epoxy Vitrimer: Self-Healing, Triple-Shape Memory and Reprocessing Triggered by Dynamic Covalent Bond Exchange. *Mater. Des.* **2020**, *186*, 108248. <https://doi.org/https://doi.org/10.1016/j.matdes.2019.108248>.
- (150) Ding, Z.; Yuan, L.; Guan, Q.; Gu, A.; Liang, G. A Reconfiguring and Self-Healing Thermoset Epoxy/Chain-Extended Bismaleimide Resin System with Thermally Dynamic Covalent Bonds. *Polymer (Guildf)*. **2018**, *147*, 170–182. <https://doi.org/https://doi.org/10.1016/j.polymer.2018.06.008>.
- (151) Yu, Q.; Peng, X.; Wang, Y.; Geng, H.; Xu, A.; Zhang, X.; Xu, W.; Ye, D. Vanillin-Based Degradable Epoxy Vitrimers: Reprocessability and Mechanical Properties Study. *Eur. Polym. J.* **2019**, *117*, 55–63. <https://doi.org/https://doi.org/10.1016/j.eurpolymj.2019.04.053>.
- (152) Nishimura, Y.; Chung, J.; Muradyan, H.; Guan, Z. Silyl Ether as a Robust and Thermally Stable Dynamic Covalent Motif for Malleable Polymer Design. *J. Am. Chem. Soc.* **2017**, *139* (42), 14881–14884. <https://doi.org/10.1021/jacs.7b08826>.
- (153) Safranski, D. L.; Gall, K. Effect of Chemical Structure and Crosslinking Density on the Thermo-Mechanical Properties and Toughness of (Meth)Acrylate Shape Memory Polymer Networks. *Polymer (Guildf)*. **2008**, *49* (20), 4446–4455. <https://doi.org/https://doi.org/10.1016/j.polymer.2008.07.060>.
- (154) Vera-Graziano, R.; Hernandez-Sanchez, F.; Cauich-Rodriguez, J. V. Study of Crosslinking Density in Polydimethylsiloxane Networks by DSC. *J. Appl. Polym. Sci.* **1995**, *55* (9), 1317–1327. <https://doi.org/https://doi.org/10.1002/app.1995.070550905>.
- (155) Saleesung, T.; Reichert, D.; Saalwächter, K.; Sirisinha, C. Correlation of Crosslink Densities Using Solid State NMR and Conventional Techniques in Peroxide-Crosslinked EPDM Rubber. *Polymer (Guildf)*. **2015**, *56*, 309–317. <https://doi.org/https://doi.org/10.1016/j.polymer.2014.10.057>.
- (156) Chen, J.-S.; Ober, C. K.; Poliks, M. D.; Zhang, Y.; Wiesner, U.; Cohen, C. Controlled Degradation of Epoxy Networks: Analysis of Crosslink Density and Glass Transition Temperature Changes in Thermally Reworkable Thermosets. *Polymer (Guildf)*. **2004**, *45* (6), 1939–1950. <https://doi.org/https://doi.org/10.1016/j.polymer.2004.01.011>.
- (157) Fry, C. G.; Lind, A. C. Determination of Crosslink Density in Thermoset Polymers by Use of Solid-State Proton NMR Techniques. *Macromolecules* **1988**, *21* (5), 1292–1297. <https://doi.org/10.1021/ma00183a019>.
- (158) Aradhana, R.; Mohanty, S.; Nayak, S. K. High Performance Epoxy Nanocomposite Adhesive: Effect of Nanofillers on Adhesive Strength, Curing and Degradation Kinetics. *Int. J. Adhes. Adhes.* **2018**, *84*, 238–249. <https://doi.org/https://doi.org/10.1016/j.ijadhadh.2018.03.013>.
- (159) Jenkins, C. L.; Meredith, H. J.; Wilker, J. J. Molecular Weight Effects upon the Adhesive Bonding of a Mussel Mimetic Polymer. *ACS Appl. Mater. Interfaces* **2013**, *5* (11), 5091–5096. <https://doi.org/10.1021/am4009538>.
- (160) Galliano, A.; Bistac, S.; Schultz, J. Adhesion and Friction of PDMS Networks: Molecular Weight Effects. *J. Colloid Interface Sci.* **2003**, *265* (2), 372–379. [https://doi.org/https://doi.org/10.1016/S0021-9797\(03\)00458-2](https://doi.org/https://doi.org/10.1016/S0021-9797(03)00458-2).
- (161) Prolongo, S. G.; Ureña, A. Effect of Surface Pre-Treatment on the Adhesive Strength of Epoxy–

Aluminium Joints. *Int. J. Adhes. Adhes.* **2009**, 29 (1), 23–31.

<https://doi.org/https://doi.org/10.1016/j.ijadhadh.2008.01.001>.

- (162) Barikani, M.; Hepburn, C. Determination of Crosslink Density by Swelling in the Castable Polyurethane Elastomer Based on 1/4 - Cyclohexane Diisocyanate and Para-Phenylene Diisocyanate. *Iran. J. Polym. Sci. Technol.* **1992**, 1 (1), 1–5.
- (163) Chateauminois, A.; Sauvant, V.; Halary, J. L. Structure - Property Relationships as a Tool for the Formulation of High-Performance Epoxy-Amine Networks. *Polym. Int.* **2003**, 52 (4), 507–513. <https://doi.org/10.1002/pi.1074>.
- (164) Khorsand, B.; Lapointe, G.; Brett, C.; Oh, J. K. Intracellular Drug Delivery Nanocarriers of Glutathione-Responsive Degradable Block Copolymers Having Pendant Disulfide Linkages. *Biomacromolecules* **2013**, 14 (6), 2103–2111. <https://doi.org/10.1021/bm4004805>.
- (165) Abedinzadeh, Z.; Gardes-Albert, M.; Ferradini, C. Kinetic Study of the Oxidation Mechanism of Glutathione by Hydrogen Peroxide in Neutral Aqueous Medium. *Can. J. Chem.* **1989**, 67 (7), 1247–1255. <https://doi.org/10.1139/v89-190>.
- (166) Giustarini, D.; Galvagni, F.; Tesei, A.; Farolfi, A.; Zanoni, M.; Pignatta, S.; Milzani, A.; Marone, I. M.; Dalle-Donne, I.; Nassini, R.; Rossi, R. Glutathione, Glutathione Disulfide, and S-Glutathionylated Proteins in Cell Cultures. *Free Radic. Biol. Med.* **2015**, 89, 972–981. <https://doi.org/https://doi.org/10.1016/j.freeradbiomed.2015.10.410>.
- (167) Humphrey, R. E.; Potter, J. L. Reduction of Disulfides with Tributylphosphine. *Anal. Chem.* **1965**, 37 (1), 164–165. <https://doi.org/10.1021/ac60220a049>.

ACKNOWLEDGEMENTS

This thesis is based on my research work during doctoral program in materials science and engineering of pure and applied science department, jointed with the University of Tsukuba and the National Institute for Materials Science (NIMS). I would also like to acknowledge NIMS for providing the NIMS Graduate Research Assistantship during this period. I express the deepest appreciation to all people who have contributed to this thesis in multiple ways.

First, I would like to express my sincere gratitude and appreciation to my Ph.D. advisor Professor Dr. Masanobu Naito for his guidance and encouragement of my research and related experiments. I really cherish and respect his precious and continuous support from beginning until now. I would like to thank to Dr. Yasuyuki Nakamura and Dr. Takehiro Fujita (Data-driven polymer design group, NIMS) for discussion and instruction. Also, they provided the guides and techniques toward synthesis procedure, instrument performing, and results analysis. Furthermore, I would like to appreciate all thesis committee members: Professor Masayuki Takeuchi and Keitaro Sodeyama (Program in material science and engineering, University of Tsukuba) and Professor Yohei Yamamoto (Program in materials chemistry and bioscience, University of Tsukuba) for reviewing this thesis, advising the defense, and giving helpful suggestions.

I would like to extend my gratitude to Dr. Sadaki Samitsu (Data-driven polymer design group, NIMS) for his contribution in dynamic mechanical analysis and stress relaxation measurements. Besides, I am thankful for his advice to explain the data and interpret the results. I would like to appreciate to Dr. Kazuaki Kato (Data-driven polymer design group, NIMS) for instrumental support of hot-pressing machine. I would like to thank Kotaro Doi (Corrosion property group, NIMS) for instrumental and technical support of Raman spectroscopy. I would like to acknowledge Professor Kohsaku Kawakami (Program in material science and engineering, University of Tsukuba) for instrumental support and useful instruction of the thermogravimetric analysis. I would like to thank Dr. Hiroyo Segawa (Electroceramics group, NIMS) for instrumental support and kind instruction of the electron spin resonance analysis. I am grateful to Dr. Sandip Das (Data-driven polymer design group, NIMS) for advice and discussion in the beginning of research. I would like to thank Dr. Mizuki Tenjimbayashi, Dr. Debabrata Payra, Dr. Siqian Wang, Dr. Sirawit Pruksawan, Ms. Junko Takaishi, Mr. Chen Xian Ng, Ms. Xiao Di Fan, Mr. Wei-Hsun Hu, and Ms. Yoko Hyakutake (Data-driven polymer design group, NIMS) for their support in various experiments. I would also like to acknowledge all members of Data-driven polymer design group at NIMS.

Besides research activities, I would like to thank Ms. Mami Kamisaka, Ms. Rei Sugiyama, and Ms. Nao Nakamura (Data-driven polymer design group, NIMS) for supporting the administrative affairs during this period in Japan. I express my sincere thanks to my colleagues and friends, Mr. Sirawit Pruksawan, Mr. Chen Xian Ng, Ms. Xiao Di Fan, Mr. Wei-Hsun Hu (Data-driven polymer design group, NIMS), Ms. Ya-Ling Chang and Mr. Da-De Chen (High strength materials group, NIMS) for their assistance and support in daily life. I would like to acknowledge my ex-instructor Professor Shiow-Kang Yen and Professor Ko-Wei Lin (Department of material engineering, National Chung Hsing University) and Ms. Shu-Yen Liu (Taichung Municipal Taichung Girls Senior High School) for their constant encouragement. I would like to appreciate my supervisors and colleagues in company, Mr. Pao-Hua Ho, Mr. Hsien-Tang Lin, Mr. Pi-Chung Lee, Ms. Hsuan-Hsuan Lin, Ms. Li-Rong Hsu, Ms. Mei-Chi Wang, and Mr. Kuan-Chieh Huang (Aerospace Industrial Development Corporation)

for support and encouragement. I express my gratitude to my friends, Ms. Yi-Hsiu Chen, Ms. Yin-Lien Chen, Ms. Yi-Chen Lin, Ms. Yu-Hsuan Lin, Ms. Sz-Mei Wang, and Ms. Ya-Chu Yang for valuable companion and concern wherever I am.

Last but definitely not the least, I must thank my mother, my father, my sister, my grandma, and other family members in Taiwan for supporting and inspiring me all the time no matter who I am. This thesis cannot be completed without them.